

Search for new physics at LHC

N.V.Krasnikov and V.A.Matveev

INR RAS, Moscow 117312

September 2003

Abstract

We review the search for new physics to be performed at the Large Hadron Collider(LHC). Namely, we review the expectations for the Higgs boson, supersymmetry and exotica detection at LHC. We also describe the main parameters of the CMS and ATLAS detectors.

1 Introduction

The SM (Standard Model) [1] which describes within an unprecedented scale of energies and distances the strong and electroweak interactions of elementary particles relays on a few basic principles - the renormalizability, the gauge invariance and the spontaneous breaking of the underlying gauge symmetry. The principle of the renormalizability [2] which is considered often as something beyond the limits of experimental test is one of the most important (if not the major) ingredients of the quantum field theory. The SM gauge group $SU_c(3) \otimes SU_L(2) \otimes U(1)$ is spontaneously broken to $SU_c(3) \otimes U_{em}(1)$ by the existence of scalar field with nonzero vacuum expectation value, leading to massive vector bosons - the W^\pm and Z - which mediate the weak interactions; the photon remains massless. One physical degree of freedom remains in the scalar sector, a neutral scalar boson (Higgs boson) H , which is the last nondiscovered particle of the SM. It should be noted that the existence of the Higgs boson is direct consequence of the renormalizability of the SM model. The $SU_c(3)$ gauge group describes the strong interactions (quantum chromodynamics or QCD). The eight vector gluons carry colour charges and are selfinteracting. Due to the property of asymptotic freedom the effective QCD coupling constant α_s is small for large momentum transfers that allows to calculate reliably deep inelastic cross sections. The fundamental fermions in the SM are leptons and quarks; the left-handed states are doublets under $SU_L(2)$ gauge group, while the right-handed states are singlets. There are three generations of fermions, each generation identical except for mass.

Despite the apparent striking success of the SM, there are a lot of reasons why it is not the ultimate theory. In the SM the neutrinos are massless and hence there are no neutrino oscillations. However there is strong evidence for neutrino oscillations [3] coming from measurements of neutrinos produced in the atmosphere and from a deficit in the flux of electron neutrinos from sun. It is easy to extend the SM to include neutrino masses, however the natural explanation of small neutrino masses is rather untrivial and probably it requires qualitatively new physics. In the SM an elementary Higgs field generates masses

for the W , Z and fermions. For the SM to be consistent the Higgs boson mass should be relatively light $M_H \leq 1 \text{ TeV}$. The tree-level Higgs boson mass receives quadratically divergent corrections at quantum level: $\delta M_H^2 \sim \Lambda^2$, where Λ is some ultraviolet cutoff. The natural ultraviolet cutoff in particle physics is usually assumed to be the Planck scale $M_{PL} \sim 10^{19} \text{ GeV}$ or grand unification scale $M_{GUT} \sim 10^{16} \text{ GeV}$. Hence the natural scale for the Higgs boson mass is $O(\Lambda)$. To explain the smallness of the Higgs boson mass some delicate cancellation is required that is rather untrivial “fine tuning” or gauge hierarchy problem. At present the supersymmetric solution [4], [5] of the gauge hierarchy problem is the most fashionable one. It predicts that the masses of supersymmetric particles have to be lighter than $O(1) \text{ TeV}$. Other possible explanation is based on models with “technicolour” [6]. Also we can’t exclude the possibility that the natural scale of the nature is $\Lambda \sim O(1) \text{ TeV}$. At any rate all solutions of the gauge hierarchy problem predict the existence of new physics at TeV scale¹. Other untrivial problem is that the SM can’t predict the fermion masses, which vary over at least five orders of magnitude (fermion problem).

The scientific programme at the LHC (Large Hadron Collider) [7] which will be the biggest particle accelerator complex ever built in the world consists in many goals. Among them there are two supergoals:

- a. Higgs boson discovery,
- b. supersymmetry discovery.

LHC [7] will accelerate mainly two proton beams with the total energy $\sqrt{s} = 14 \text{ TeV}$. At low luminosity stage (first two-three years of the operation) the luminosity is planned to be $L_{low} = 10^{33} \text{ cm}^{-2} \text{ s}^{-1}$ with total luminosity $L_t = 10 \text{ fb}^{-1}$ per year. At high luminosity stage the luminosity is planned to be $L_{high} = 10^{34} \text{ cm}^{-2} \text{ s}^{-1}$ with total luminosity $L_t =$

¹There is crucial difference between the Higgs boson prediction and the prediction of new physics at TeV scale. Really, electroweak models without Higgs boson are nonrenormalizable ones and we simply can’t make quantitative radiative calculations for such models. The SM with small Higgs boson mass is consistent renormalizable quantum field theory, however within the SM we can’t explain naturally the smallness of the Higgs boson mass (the smallness of electroweak scale) in comparison with Planck scale.

100 fb^{-1} per year. Also the LHC will accelerate heavy ions, for example, Pb-Pb ions at 1150 TeV in the centre of mass and luminosity up to $10^{27} \text{ cm}^{-2}\text{s}^{-1}$. Bunches of protons will intersect at four points where detectors are placed. There are planned to be two big detectors at the LHC: the CMS (Compact Muon Solenoid) [8] and ATLAS (A Toroidal LHC Apparatus) [9]. Two other detectors are ALICE detector [10], to be used for the study of heavy ions, and LHC-B [11], the detector for the study of B-physics.

The LHC will start to work in 2007 year. There are a lot of lines for the research at the LHC [12]:

- a. the search for Higgs boson,
- b. the search for supersymmetry,
- c. the search for new physics beyond the MSSM (Minimal Supersymmetric Model) and the SM,
- d. B-physics,
- e. heavy ion physics,
- f. top quark physics,
- g. standard physics (QCD, electroweak interactions).

In this paper we briefly review the search for new physics to be performed at the LHC. Namely, we review the expectations for the Higgs boson, the supersymmetry and exotica (new physics beyond the SM and the MSSM) detection. We also describe the main parameters of the CMS [8] and ATLAS [9] detectors. The organisation of the paper is the following. In section 2 we describe the main parameters of the CMS and ATLAS detectors. In section 3 we review the search for standard Higgs boson to be done at LHC. In section 4 the expectations for supersymmetry detection are discussed. Section 5 is devoted to the review of the search for new physics beyond the SM and the MSSM to be done at the LHC. Section 6 contains concluding remarks.

2 CMS and ATLAS detectors

One of the most important tasks for the LHC is the quest for the origin of the spontaneous symmetry breaking mechanism in the electroweak sector of the SM. The Higgs boson [13] search is therefore used as a first benchmark for the detector optimisation for both the CMS and ATLAS. For the SM Higgs boson, the detector has to be sensitive to the following processes in order to cover the full mass range above the LEP limit $M_H \geq 114.4 \text{ GeV}$ [17] on the SM Higgs boson mass:

1. $H \rightarrow \gamma\gamma$ for the mass range $114 \text{ GeV} \leq m_H \leq 150 \text{ GeV}$,
2. $H \rightarrow b\bar{b}$ from $WH, ZH, t\bar{t}H$ using $l^\pm (l^\pm = e^\pm \text{ or } \mu^\pm)$ - tag and b-tagging,
3. $H \rightarrow ZZ^* \rightarrow 4l^\pm$ for the mass range $130 \text{ GeV} \leq m_H \leq 2m_Z$,
4. $H \rightarrow ZZ \rightarrow 4l^\pm, 2l^\pm 2\nu$ for the mass range $m_H \geq 2m_Z$.

The second supergoal of the LHC project is the supersymmetry discovery [5], i.e. the detection of superparticles. Here the main signature are the missing transverse energy events which are the consequence of undetected lightest stable supersymmetric particle (LSP) predicted in supersymmetric models with R-parity conservation. Therefore it is necessary to set stringent requirements for the hermeticity and E_T^{miss} capability of the detector. Also the search for new physics different from supersymmetry (new gauge bosons W' and Z' , additional dimensions etc.) requires high resolution lepton measurements and charge identification even in the p_T range of a few TeV. Other possible signature of new physics - compositeness can be provided by very high p_T jet measurements. Also an important task of the LHC is the study of b- and t-physics.

Therefore the basic design considerations for both the ATLAS and CMS are the following:

1. very good electromagnetic calorimetry for electron and photon identifications and measurements,
2. good hermetic jet and missing E_T -calorimetry,
3. efficient tracking at high luminosity for lepton momentum measurements, for b-quark tagging, and for enhanced electron and photon identification, as well as tau and

heavy-flavour vertexing and reconstruction capability of some B decay final states at low luminosity,

4. stand-alone, precision, muon-momentum measurement up to highest luminosity, and very low- p_T trigger capability at lower luminosity,
5. large acceptance in η ($\eta \equiv -\ln(\tan(\frac{\theta}{2}))$) coverage.

2.1 CMS detector

The CMS detector [8] consists of inner detector(tracker), electromagnetic calorimeter, hadron calorimeter and muon spectrometer. A schematic view of the CMS detector is shown in Fig.1.

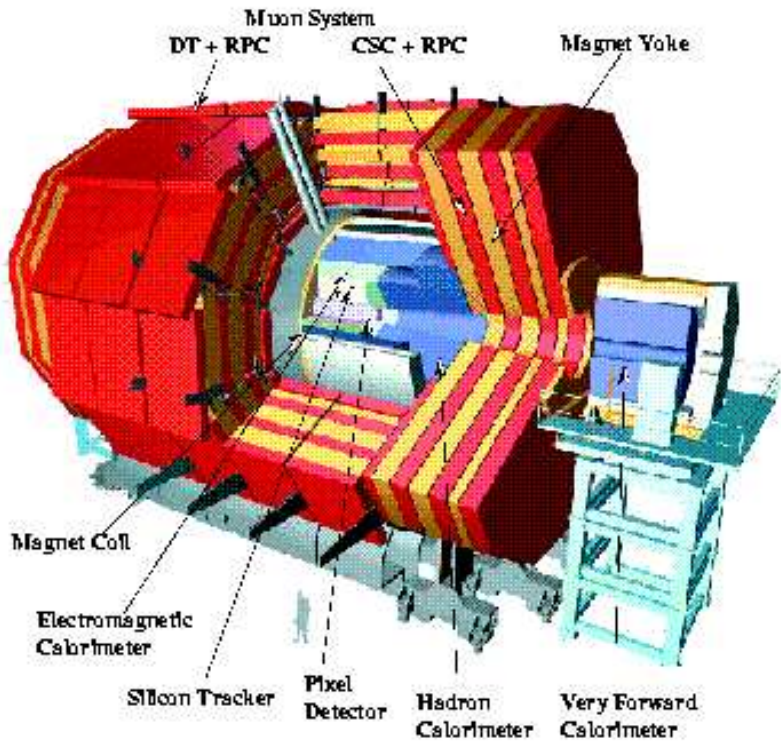


Figure 1: *Perspective view of the CMS detector*

The CMS tracking system is contained in a 4 Tesla superconducting coil which provides the magnetic field for charged particle tracking. The tracking system uses silikon pixels and silikon strip detectors. The expected momentum resolution in the central rapidity

region is $\frac{\delta p_T}{p_T} = 0.01$ for $p_T = 100 \text{ GeV}$ and it is 5 times worse for $p_T = 1 \text{ TeV}$.

The CMS has a precision electromagnetic calorimeter based on lead tungstate ($PbWO_4$) crystals, covering $|\eta| < 3$ (with trigger coverage $|\eta| < 2.6$). The energy resolution at low luminosity is assumed to be

$$\frac{\Delta E}{E} = \frac{0.03}{\sqrt{E}} \oplus 0.005. \quad (1)$$

Estimates [8] give the following di-photon mass resolution for $H \rightarrow \gamma\gamma$ channel ($m_H = 100 \text{ GeV}$):

$$\delta m_{\gamma\gamma} = 475 \text{ MeV} \text{ (low luminosity } L = 10^{33} \text{ cm}^{-2}\text{s}^{-1}\text{)},$$

$$\delta m_{\gamma\gamma} = 775 \text{ MeV} \text{ (high luminosity } L = 10^{34} \text{ cm}^{-2}\text{s}^{-1}\text{)}.$$

The hadron calorimeter surrounds the electromagnetic calorimeter and acts in conjunction with it to measure the energies and directions of particle jets, and to provide hermetic coverage for measurement the transverse energy. The pseudorapidity range ($|\eta| \leq 3$) is covered by the barrel and endcap hadron calorimeters which sit inside the 4 *Tesla* magnetic field of CMS solenoid. The assumed energy resolution for jets is $\Delta E/E = 1.1/\sqrt{E} \oplus 0.05$. The pseudorapidity range ($3.0 \leq \eta \leq 5.0$) is covered by a separate very forward calorimeter. The expected energy resolution for jets in the very forward calorimeter is :

$$\frac{\sigma_E}{E} = \frac{1.8}{\sqrt{E}} \oplus 0.1. \quad (2)$$

At the LHC the effective detection of muons from Higgs bosons, W , Z and $t\bar{t}$ decays requires coverage over a large rapidity interval. Muons from pp collisions are expected to provide clean signatures for a wide range of new physics processes. Many of these processes are expected to be rare and will require the highest luminosity. The goal of the muon detector is to identify these muons and to provide a precision measurement of their momenta from a few *GeV* to a few *TeV*. The barrel detector covers the region $|\eta| \leq 1.3$. The endcap detector covers the region $1.3 \leq |\eta| \leq 2.4$. For $0 \leq |\eta| \leq 2$ the transverse momentum resolution after matching with tracker is $0.015 - 0.05$ for $p_T = 100 \text{ GeV}$ and $0.05 - 0.2$ for $p_T = 1 \text{ TeV}$.

2.2 ATLAS detector

The design of the ATLAS detector [9] is similar to the CMS detector. It also consists of inner detector (tracker), electromagnetic calorimeter, hadron calorimeter and the muon spectrometer. A schematic view of the ATLAS detector is shown in Fig.2.

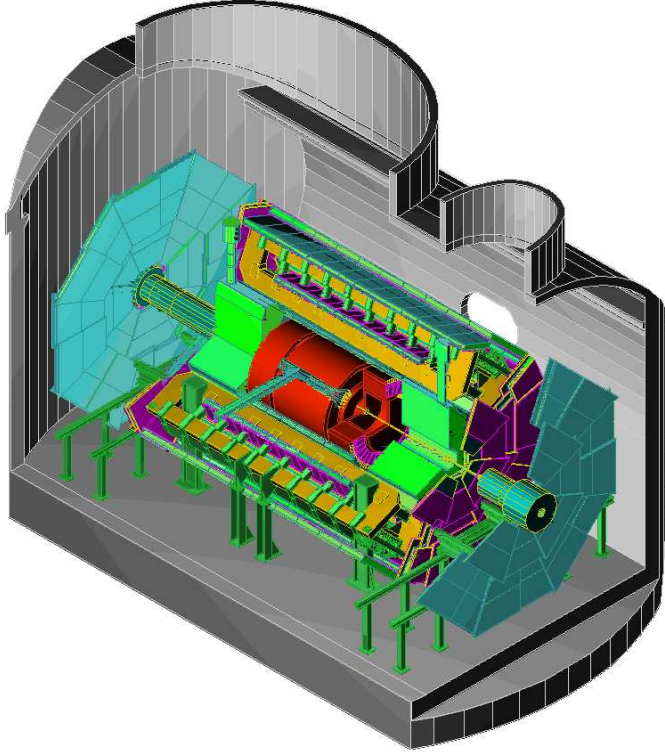


Figure 2: *Three-dimensional view of the ATLAS detector*

The ATLAS inner detector consists of silikon pixels, silicon strip detectors and a transition radiation detector. The charged track resolution is assumed to be $\Delta p_T/p_T = 0.2$ at $p_T = 500 \text{ GeV}$.

The lead-liquid argon electromagnetic calorimeter covers $|\eta| < 3$ with trigger coverage $|\eta| < 2.5$. The expected energy resolution is of $\frac{\Delta E}{E} = \frac{0.1}{\sqrt{E}} \oplus 0.007$ for $|\eta| \leq 2.5$. Diphoton mass resolution is estimated to be 1.4 GeV for the Higgs boson mass $m_H = 100 \text{ GeV}$ for $L = 10^{34} \text{ cm}^{-2} \text{s}^{-1}$.

The hadronic calorimeter uses scintillator tiles in the barrel ($|\eta| < 1.5$) and liquid argon in the endcaps ($1.5 < |\eta| < 3$). Jet energy resolution is of $\frac{\Delta E}{E} = \frac{0.5}{\sqrt{E}} \oplus 0.03$. Forward calorimeter covers the region $3 \leq |\eta| \leq 5$ with a resolution better than $\Delta E/E = \frac{1}{\sqrt{E}} \oplus$

0.1. The muon system measures muon trajectories and the resulting muon momentum resolution is estimated to be $\frac{\Delta p_T}{p_T} = 0.02(p_T = 100 \text{ GeV})$, $\frac{\Delta p_T}{p_T} = 0.08(p_T = 1 \text{ TeV})$ for $|\eta| \leq 2.2$.

3 Search for standard Higgs boson at the LHC

3.1 The Lagrangian of the Standard Model

The standard model is the renormalizable model of strong and electroweak interactions. It has the gauge group $SU_c(3) \otimes SU_L(2) \otimes U(1)$ and the minimal Higgs structure consisting of one complex doublet of scalar particles. The spontaneous electroweak symmetry breaking $SU_c(3) \otimes SU_L(2) \otimes U(1) \rightarrow SU_c(3) \otimes U(1)$ due to nonzero vacuum expectation value of the Higgs doublet provides the simplest realization of the Higgs mechanism [13] which generates masses for W^\pm , Z gauge bosons and masses to quarks and leptons. In this approach, the Goldstone bosons are generated by dynamics of elementary scalar fields and precisely one neutral Higgs scalar (the Higgs boson) remains in the physical spectrum. The Lagrangian of the SM model consists of several pieces [15]:

$$L_{WS} = L_{YM} + L_{HYM} + L_{SH} + L_f + L_{Yuk}. \quad (3)$$

Here L_{YM} is the Yang-Mills Lagrangian without matter fields

$$L_{YM} = -\frac{1}{4}F_{\mu\nu}^i(W)F_i^{\mu\nu}(W) - \frac{1}{4}F^{\mu\nu}(W^0)F_{\mu\nu}(W^0) - \frac{1}{4}F_{\mu\nu}^a(G)F_a^{\mu\nu}(G), \quad (4)$$

where $F_{\mu\nu}^i(W)$, $F_{\mu\nu}^a(G)$, $F_{\mu\nu}(W^0)$ are given by

$$F_{\mu\nu}^i(W) = \partial_\mu W_\nu^i - \partial_\nu W_\mu^i + g_2 \epsilon^{ijk} W_\mu^j W_\nu^k, \quad (5)$$

$$F_{\mu\nu}(W^0) = \partial_\mu W_\nu^0 - \partial_\nu W_\mu^0, \quad (6)$$

$$F_{\mu\nu}^a(G) = \partial_\mu G_\nu^a - \partial_\nu G_\mu^a + g_s f^{abc} G_\mu^b G_\nu^c, \quad (7)$$

and W_μ^i , W_μ^0 are the $SU_L(2) \otimes U(1)$ gauge fields, G_μ^a are the gluon fields, ϵ^{ijk} , f^{abc} are the structure constants of the $SU(2)$ and $SU(3)$ gauge groups. The Lagrangian L_{HYM}

describes the Higgs doublet interaction with $SU_L(2) \otimes U(1)$ gauge fields

$$L_{HYM} = (D_{L\mu}H)^+(D_L^\mu H), \quad (8)$$

where covariant derivatives are given by

$$D_{L\mu} = \partial_\mu - ig_1 \frac{Y}{2} W_\mu^0 - ig_2 \frac{\sigma^i}{2} W_\mu^i, \quad (9)$$

$$D_{R\mu} = \partial_\mu - ig_1 \frac{Y}{2} W_\mu^0, \quad (10)$$

$$D_{L\mu}^q = \partial_\mu - ig_1 \frac{Y}{2} W_\mu^0 - ig_2 \frac{\sigma^i}{2} W_\mu^i - ig_s t^a G_\mu^a, \quad (11)$$

$$D_{R\mu}^q = \partial_\mu - ig_1 \frac{Y}{2} W_\mu^0 - ig_s t^a G_\mu^a. \quad (12)$$

Here g_1 is the $U(1)$ gauge coupling constant, Y is the hypercharge determined by the relation $Q = \frac{\sigma_3}{2} + \frac{Y}{2}$, σ^i are Pauli matrices, t^a are $SU(3)$ matrices in the fundamental representation, $H = \begin{pmatrix} H_1 \\ H_2 \end{pmatrix}$ is the Higgs $SU(2)$ doublet with $Y = 1$. The Lagrangian L_{SH} describing Higgs doublet self-interaction has the form

$$L_{SH} = -V_0(H) = M^2 H^+ H - \frac{\lambda}{2} (H^+ H)^2, \quad (13)$$

where $H^+ H = \sum_i H_i^* H_i$ and λ is the Higgs self-coupling constant. Lagrangian L_f describes the interaction of fermions with gauge fields. Fermions constitute only doublets and singlets in $SU_L(2) \otimes U(1)$

$$R_1 = e_R, \quad R_2 = \mu_R, \quad R_3 = \tau_R, \quad (14)$$

$$L_1 = \begin{pmatrix} \nu \\ e \end{pmatrix}_L \quad L_2 = \begin{pmatrix} \nu' \\ \mu \end{pmatrix}_L \quad L_3 = \begin{pmatrix} \nu'' \\ \tau \end{pmatrix}_L \quad (15)$$

$$R_{qIu} = (q_{Iu})_R, \quad (q_{1u} = u, \quad q_{2u} = c, \quad q_{3u} = t), \quad (16)$$

$$R_{qid} = (q_{id})_R, \quad (q_{1d} = d, \quad q_{2d} = s, \quad q_{3d} = b), \quad (17)$$

$$L_{qI} = \begin{pmatrix} q_{Iu} \\ V_{Ii}^{-1} q_{id} \end{pmatrix}_L, \quad (18)$$

where L and R denote left- and right-handed components of the spinors respectively,

$$\psi_{R,L} = \frac{1 \pm \gamma_5}{2} \psi \quad (19)$$

and V_{iI} is the Kobayashi-Maskawa matrix. The neutrinos are assumed to be left-handed and massless. The Lagrangian L_f has the form

$$L_f = \sum_{k=1}^3 [i\bar{L}_k \hat{D}_L L_k + i\bar{R}_k \hat{D}_R R_k + i\bar{L}_{qk} \hat{D}_L^q L_{qk} + i\bar{R}_{qku} \hat{D}_R^q R_{qku} + i\bar{R}_{qkd} \hat{D}_R^q R_{qkd}], \quad (20)$$

where $\hat{D}_L = \gamma^\mu D_{L\mu}$, $\hat{D}_R = \gamma^\mu D_{R\mu}$, $\hat{D}_L^q = \gamma^\mu D_{L\mu}^q$, $\hat{D}_R^q = \gamma^\mu D_{R\mu}^q$. The Lagrangian L_{Yuk} generates fermion mass terms. Supposing the neutrinos to be massless, the Yukawa interaction of the fermions with Higgs doublet has the form

$$L_{Yuk} = - \sum_{k=1}^3 [h_{lk} \bar{L}_k H R_k + h_{dk} \bar{L}_{dk} H R_{dk} + h_{uk} \bar{L}_{uk} (i\sigma^2 H^*) R_{uk}] + h.c.. \quad (21)$$

The potential term $V_0(H) = -M^2 H^+ H + \frac{\lambda}{2} (H^+ H)^2$ for $M^2 > 0$ gives rise to the spontaneous symmetry breaking. The doublet H acquires the nonzero vacuum expectation value

$$\langle H \rangle = \begin{pmatrix} 0 \\ \frac{v}{\sqrt{2}} \end{pmatrix}, \quad (22)$$

where $v = 246$ GeV. In the unitary gauge unphysical Goldstone massless fields are absent and the Higgs doublet scalar field depends on the single physical scalar field $H(x)$ (Higgs field):

$$H(x) = \begin{pmatrix} 0 \\ \frac{v}{\sqrt{2}} + \frac{H(x)}{\sqrt{2}} \end{pmatrix}. \quad (23)$$

Due to spontaneous gauge symmetry breaking gauge fields except photon field acquire masses. Diagonalization of mass matrix gives

$$W_\mu^\pm = \frac{1}{\sqrt{2}} (W_\mu^1 \mp W_\mu^2), \quad M_W = \frac{1}{2} g_2 v, \quad (24)$$

$$Z_\mu = \frac{1}{\sqrt{g_2^2 + g_1^2}} (g_2 W_\mu^3 - g_1 W_\mu^0), \quad M_Z = \frac{1}{2} \sqrt{g_2^2 + g_1^2} v, \quad (25)$$

$$A_\mu = \frac{1}{\sqrt{g_2^2 + g_1^2}} (g_1 W_\mu^3 + g_2 W_\mu^0), \quad M_A = 0, \quad (26)$$

where W_μ^\pm , Z_μ are charged and neutral electroweak bosons, A_μ is photon. It is convenient to introduce rotation angle θ_W between (W^3, W^0) and (Z, A) which is called Weinberg angle

$$\sin \theta_W \equiv \frac{g_1}{\sqrt{g_1^2 + g_2^2}}. \quad (27)$$

Experimentally $\sin^2 \theta_W \approx 0.23$ [16]. The formula for the electric charge e has the form

$$e = \frac{g_2 g_1}{\sqrt{g_2^2 + g_1^2}}. \quad (28)$$

At the tree level the Higgs boson mass is determined by the formula

$$m_H = \sqrt{2}M = \sqrt{\lambda}v. \quad (29)$$

The Lagrangian L_{Yuk} is responsible for the fermion masses generation. In the unitary gauge the Lagrangian L_{HYM} takes the form

$$L_{HYM} = \frac{1}{2} \partial^\mu H \partial_\mu H + M_W^2 (1 + \frac{H}{v})^2 W_\mu^+ W^\mu + \frac{1}{2} M_Z^2 (1 + \frac{H}{v})^2 Z^\mu Z_\mu. \quad (30)$$

The Yukawa Lagrangian in the unitary gauge can be written in the form

$$L_{Yuk} = - \sum_i m_{\psi_i} (1 + \frac{H}{v}) \bar{\psi}_i \psi_i. \quad (31)$$

3.2 Higgs boson mass bounds

The current lower limit on the SM Higgs boson mass from LEP experiments is $m_H \geq 114.4 \text{ GeV}$ at 95% C.L. [17]. Analysis of high-precision measurements of electroweak observables leads to indirect upper bound [18] $m_H \leq 193 \text{ GeV}$ at 95% C.L. on the Higgs boson mass, so within the SM the Higgs boson should be relatively light.

It is possible to derive bounds on the Higgs boson mass from the requirement of the absence of the Landau pole singularity for the effective Higgs self-coupling constant [19] and from the vacuum stability requirement [20]. The idea of the derivation of the bound resulting from the requirement of the absence of Landau pole singularity is the following [19]. Suppose the SM is valid up to scale Λ . From the requirement of the absence of Landau pole singularity for the effective Higgs self-coupling constant $\bar{\lambda}(E)$ for $E \leq \Lambda$ one can obtain an upper bound on the Higgs boson mass. For $\Lambda = (10^3; 10^4; 10^6; 10^8; 10^{12}; 10^{14}) \text{ GeV}$ and $m_t^{pole} = 175 \text{ GeV}$ one can find [12] an upper bound on the Higgs boson mass $m_H \leq (400; 300; 240; 200; 180; 170; 160) \text{ GeV}$ respectively. The vacuum stability bound [20] comes from the requirement that the electroweak minimum of the effective potential is

the deepest one for $|H| \leq \Lambda$. For $|H| \gg v$ the mass terms in the effective potential are negligible compared to the self-interaction term and the vacuum stability requirement means that the effective Higgs self-interaction coupling constant $\bar{\lambda}(\mu)$ is nonnegative, $\bar{\lambda}(\mu) \geq 0$, for $\mu \leq \Lambda$. For $\Lambda = (10^3; 10^4; 10^6; 10^8; 10^{12}; 10^{14}) \text{ GeV}$ and $m_t^{pole} = 175 \text{ GeV}$ one can find [12] lower bound on the Higgs boson mass $m_H \geq (78; 101; 121; 129; 136; 137) \text{ GeV}$ respectively. In the MSSM the radiative corrections can increase the mass of lightest Higgs boson [21] up to 135 GeV ($m_H \leq 135 \text{ GeV}$) [22]. As it has been mentioned in refs.[23] by the measurement of the Higgs boson mass it is possible to distinguish between the SM and the MSSM or at least to estimate the scale Λ where we can expect deviations from the SM predictions.

3.3 Higgs boson decays

The tree-level Higgs boson couplings to gauge bosons and fermions can be deduced from the Lagrangians (30, 31). Of these, the HW^+W^- , HZZ and $H\bar{\psi}\psi$ are the most important for the phenomenology. The partial decay width into fermion-antifermion pair is [15]

$$\Gamma(H \rightarrow \psi\bar{\psi}) = \frac{G_F m_\psi^2 m_H N_c}{4\pi\sqrt{2}} \left(1 - \frac{4m_\psi^2}{m_H^2}\right)^{\frac{3}{2}}, \quad (32)$$

where N_c is the number of fermion colours. For $m_H \leq 2m_W$ Higgs boson decays mainly with (≈ 90 percent) probability into b quark-antiquark pair and with ≈ 7 percent probability into τ lepton-antilepton pair. An account of higher order QCD corrections can be effectively taken into account in the formula (32) for the Higgs boson decay width into b quark-antiquark pair by the replacement of pole b-quark mass in formula (32) by the effective b-quark mass $\bar{m}_b(m_H)$. Remember that the relation between the perturbative quark pole mass m_Q and the \bar{MS} running quark mass $\bar{m}_Q(m_Q)$ has the form [24]

$$m_Q = \left(1 + \frac{4}{3} \frac{\alpha_s(m_Q)}{\pi} + K_Q \left(\frac{\alpha_s(m_Q)}{\pi}\right)^2\right) \bar{m}_Q(m_Q), \quad (33)$$

where numerically $K_t \approx 10.9$, $K_b \approx 12.4$ and $K_c \approx 13.4$.

Higgs boson with $m_H \geq 2M_W$ will decay into pairs of gauge bosons with the partial

widths

$$\Gamma(H \rightarrow W^+W^-) = \frac{G_F m_H^3}{32\pi\sqrt{2}} (4 - 4a_w + 3a_w^2) (1 - a_w)^{\frac{1}{2}}, \quad (34)$$

$$\Gamma(H \rightarrow Z^0Z^0) = \frac{G_F m_H^3}{64\pi\sqrt{2}} (4 - 4a_Z + 3a_Z^2) (1 - a_Z)^{\frac{1}{2}}, \quad (35)$$

where $a_W = \frac{4M_W^2}{m_H^2}$ and $a_Z = \frac{4M_Z^2}{m_H^2}$. In the heavy Higgs mass regime ($2m_Z \leq m_H \leq 800$ GeV), the Higgs boson decays dominantly into gauge bosons. For example, for $m_H \gg 2m_Z$ one can find that

$$\Gamma(H \rightarrow W^+W^-) = 2\Gamma(H \rightarrow ZZ) \simeq \frac{G_F m_H^3}{8\pi\sqrt{2}}. \quad (36)$$

The m_H^3 behaviour is a consequence of the longitudinal polarisation states of the W and Z . As m_H gets large, so does the coupling of H to the Goldstone bosons which have been eaten by the W and Z . However, the Higgs boson decay width to a pair of heavy quarks growth only linearly in the Higgs boson mass. Thus, for the Higgs masses sufficiently above $2m_Z$, the total Higgs boson width is well approximated by ignoring the Higgs boson decay to $t\bar{t}$ and including only the two gauge boson modes. For heavy Higgs boson mass one can find that

$$\Gamma_{total}(H) \simeq 0.48 \text{ TeV} \left(\frac{m_H}{1 \text{ TeV}} \right)^3. \quad (37)$$

Below threshold the decays into off-shell gauge particles are important. The decay width into single off-shell gauge boson has the form [26]

$$\Gamma(H \rightarrow VV^*) = \delta_V \frac{3G_F^2 M_V^4 m_H}{16\pi^3} R\left(\frac{M_V^2}{m_H^2}\right), \quad (38)$$

where $\delta_W = 1$, $\delta_Z = \frac{7}{12} - \frac{10}{9} \sin^2 \theta_W \frac{40}{27} \sin^4 \theta_W$ and

$$R(x) = 3 \frac{1 - 8x + 20x^2}{\sqrt{4x - 1} \arccos(\frac{3x-1}{2x^{3/2}})} - \frac{1 - x}{2x} (2 - 13x + 47x^2) - \frac{3}{2} (1 - 6x + 4x^2) \log(x), \quad (39)$$

$x = \frac{M_V^2}{m_H^2}$. For Higgs boson mass slightly larger than the corresponding gauge boson mass the decay widths into pairs of off-shell gauge bosons play important role. The corresponding formulae can be found in ref. [26].

It should be noted that there are a number of important Higgs couplings which are absent at tree level but appear at one-loop level. Among them the couplings of the Higgs boson to two gluons and two photons are extremely important for the Higgs boson

searches at supercolliders. One-loop induced Higgs coupling to two gluons is due to t-quark exchange in the loop [27] and it leads to an effective Lagrangian

$$L_{Hgg}^{eff} = \frac{8g_2\alpha_s}{24\pi m_W} HG_{\mu\nu}^a G^{a\mu\nu}. \quad (40)$$

for the interaction of the Higgs boson with gluons. At lowest order the partial decay width is given by [26]

$$\Gamma_{LO}(H \rightarrow gg) = \frac{G_F^2 \alpha_s^2 m_H^3}{36\sqrt{2}\pi^3} \left| \sum_Q A_Q^H(\tau_Q) \right|^2, \quad (41)$$

$$A_Q^H(\tau) = \frac{3}{2}\tau[1 + (1 - \tau)f(\tau)], \quad (42)$$

$$f(\tau) = \text{argsin}^2\left(\frac{1}{\sqrt{\tau}}\right), \tau \geq 1, \quad (43)$$

$$f(\tau) = -\frac{1}{4}[\log\left(\frac{1 + \sqrt{1 - \tau}}{1 - \sqrt{1 - \tau}}\right) - i\pi]^2, \tau < 1 \quad (44)$$

The parameter $\tau_Q = \frac{4m_Q^2}{m_H^2}$ is defined by the pole mass M_Q of the heavy quark in the loop. For large quark mass $A_Q^H(\tau_Q) \rightarrow 1$. It appears that QCD radiative corrections are very large [28] : the decay width is shifted by about (60 -70) percent upwards in the most interesting mass region $100 \text{ GeV} \leq m_H \leq 500 \text{ GeV}$. Three loop QCD corrections have been calculated in the limit of a heavy top quark. They are positive and increase the full next leading order expression by 10 percent [29].

Also very important is the one-loop induced Higgs boson coupling to two photons due to W- and t-quark exchanges in the loop (see Fig.3). The partial decay width can be written in the form [26]

$$\Gamma(H \rightarrow \gamma\gamma) = \frac{G_F \alpha^2 m_H^3}{128\sqrt{2}\pi^3} \left| \sum_f N_{cf} e_f^2 A_f^H(\tau_f) + A_W^H(\tau_W) \right|^2, \quad (45)$$

where

$$A_f^H(\tau) = 2\tau[1 + (1 - \tau)f(\tau)], \quad (46)$$

$$A_W^H(\tau) = -[2 + 3\tau + 3\tau(2 - \tau)f(\tau)], \quad (47)$$

$\tau_i = \frac{4M_i^2}{m_H^2}$, $i = f, W$ and the function $f(\tau)$ is determined by the formulae (43,44). The W-loop gives the dominant contribution in the intermediate Higgs boson mass range. The branching ratios and decay width of the SM Higgs boson are presented in Fig.4.

3.4 Higgs boson production at the LHC

Typical processes that can be exploited to produce Higgs bosons at the LHC are [25], [26]:

gluon fusion: $gg \rightarrow H$ (Fig.5),

WW, ZZ fusion: $W^+W^-, ZZ \rightarrow H$ (Fig.6),

Higgs-strahlung off W, Z : $q\bar{q}W, Z \rightarrow W, Z + H$ (Fig7),

Higgs bremsstrahlung off top: $q\bar{q}, gg \rightarrow t\bar{t} + H$ (Fig.8) .

Gluon fusion plays a dominant role throughout the entire Higgs boson mass range of the SM whereas the WW/ZZ fusion process becomes increasingly important with Higgs boson mass rising. The last two reactions are important only for light Higgs boson masses.

The gluon-fusion mechanism [27]

$$pp \rightarrow gg \rightarrow H \quad (48)$$

is the dominant production mechanism of the Higgs boson at the LHC for Higgs boson mass up to 1 TeV. The gluon coupling to the Higgs boson in the SM is mediated by triangular loop of top quark. The corresponding form factor approaches a non-zero value for large loop-quark masses. At lowest order the partonic cross section can be expressed by the gluonic width of the Higgs boson

$$\hat{\sigma}_{LO}(gg \rightarrow H) = \sigma_0 m_H^2 \delta(\hat{s} - m_H^2), \quad (49)$$

$$\sigma_0 = \frac{\pi^2}{8m_H^2} \Gamma_{LO}(H \rightarrow gg) \left| \sum_Q A_Q^H(\tau_Q) \right|^2, \quad (50)$$

where $\tau_Q = \frac{4M_Q^2}{m_H^2}$, \hat{s} denotes the partonic system of mass energy squared and the form factor $A_Q^H(\tau_Q)$ is determined by the formulae (42-44). In the narrow-width approximation hadronic cross section can be written in the form

$$\sigma_{LO}(pp \rightarrow H) = \sigma_0 \tau_H \frac{dL^{gg}}{d\tau_H}, \quad (51)$$

where $\frac{dL^{gg}}{d\tau_H}$ denotes gg luminosity of the pp collider with $\tau_H = \frac{m_H^2}{s}$. The QCD corrections to the gluon fusion process are essential [26], [28], [29]. They stabilise the theoretical

predictions for the cross section when the renormalization and factorisation scales are varied. Moreover, they are large and positive, thus increasing the production cross section for Higgs bosons.

The theoretical prediction for the Higgs boson production cross section is presented in Fig.9. The cross section decreases with increasing of the Higgs boson mass mainly due to the decrease of gg partonic luminosity for large invariant masses.

The second important process for the Higgs boson production at the LHC is vector-boson fusion, ZZ , $W^+W^- \rightarrow H$. For large Higgs boson mass this mechanism becomes competitive to gluon fusion; for intermediate masses the cross section is smaller by about an order of magnitude. The corresponding formulae for the cross section can be found in refs.[30].

Higgs-strahlung $q\bar{q} \rightarrow V^* \rightarrow VH$ ($V = W, Z$) is a very important process for the search of light Higgs boson at the LHC. Though the cross section is smaller than for gluon fusion, leptonic decays of electroweak vector bosons are extremely useful to filter Higgs boson signal from huge background. The corresponding formulae for the cross section are contained in ref.[31].

The process $gg, q\bar{q} \rightarrow t\bar{t}H$ is relevant for small Higgs boson masses. The analytical expression for the parton cross section is quite involved [32]. Note that Higgs boson bremsstrahlung off top quarks is an interesting process for measurements of the fundamental $Ht\bar{t}$ Yukawa coupling. The cross section $\sigma(pp \rightarrow t\bar{t}H + \dots)$ is directly proportional to the square of this coupling constant.

One can say that three classes of processes can be distinguished. The gluon fusion of Higgs boson is an universal process, dominant over the entire Higgs boson mass range. Higgs-strahlung of electroweak W, Z bosons or top quarks is important for light Higgs boson. The WW/ZZ fusion channel, by contrast, becomes rather important in the upper part of the Higgs boson mass. An overview of the production cross section for the Higgs boson at the LHC is presented in Fig.9.

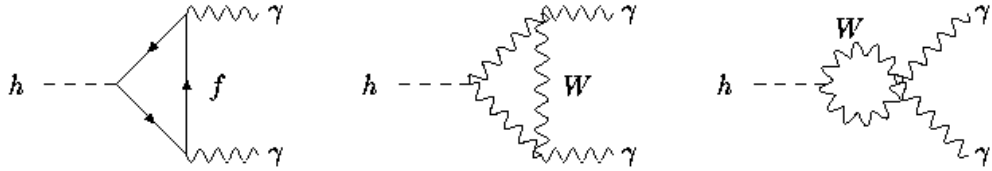


Figure 3: One loop diagrams contributing to $h \rightarrow \gamma\gamma$

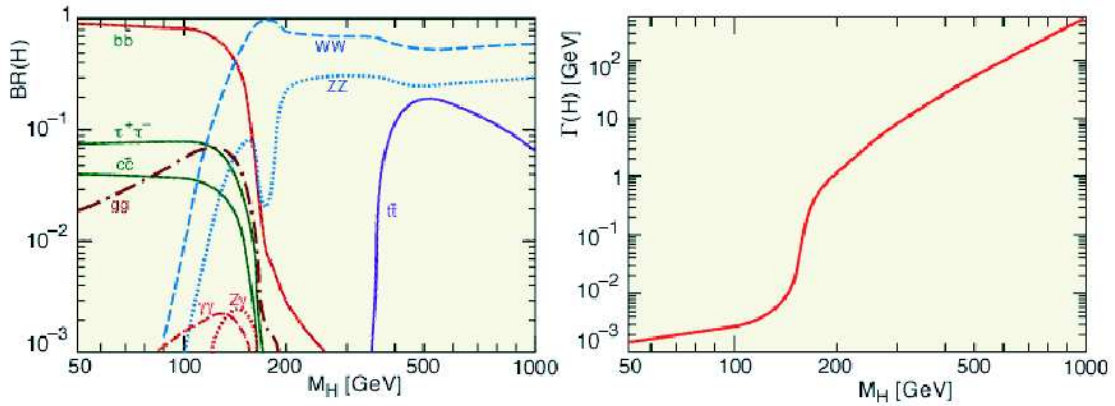


Figure 4: Branching ratios and decay width of the SM Higgs boson

3.5 $H \rightarrow \gamma\gamma$

One of the most important reactions for the search for Higgs boson at LHC is

$$pp \rightarrow (H \rightarrow \gamma\gamma) + \dots, \quad (52)$$

which is the most promising one [33] for the search for Higgs boson in the most interesting region $100 \text{ GeV} \leq m_H \leq 150 \text{ GeV}$. The signal significance $S = \frac{N_S}{\sqrt{N_B}}$ is estimated to be 6.6(9) for $m_H = 110(130) \text{ GeV}$ for low luminosity $L_{low,t} = 30 \text{ fb}^{-1}$ and 10(13) for $m_H = 110(130) \text{ GeV}$ and for high luminosity $L_{high,t} = 100 \text{ fb}^{-1}$ [8]. The general conclusion is that at 5σ level CMS detector will be able to discover Higgs boson ² for

²It should be noted that more appropriate characteristic for future experiments [38] is the probability of the discovery, i.e. the probability that future experiment will measure the number of events N_{ev} such that the probability that standard physics reproduces N_{ev} is less than $5.7 \cdot 10^{-7}$ (5σ). For instance,

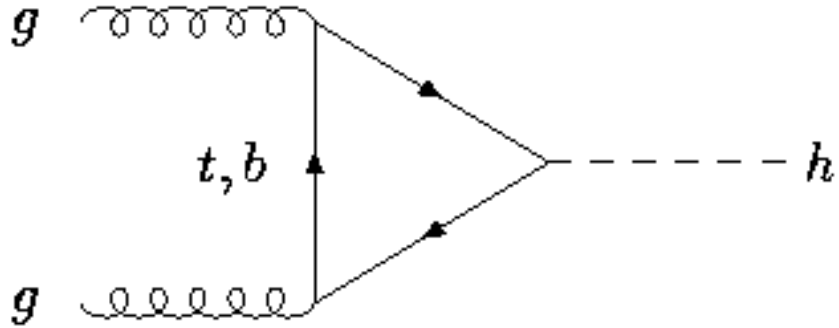


Figure 5: *Diagram contributing to the production of the Higgs boson in gluon-gluon collisions*

$95 \text{ GeV} \leq m_H \leq 145 \text{ GeV}$ at low luminosity and at high luminosity the corresponding Higgs boson mass discovery interval is $85 \text{ GeV} \leq m_H \leq 150 \text{ GeV}$ (see Fig.10). The similar estimates have been made for the ATLAS detector [37] and they coincide with the CMS estimates (in terms of signal significances) up to 30% [37].

3.6 $H \rightarrow \gamma\gamma$ in association with high E_T jets.

The idea to look for Higgs boson signal associated with a high p_t jet in the final state was considered in ref.[39], where the matrix elements of signal subprocesses $gg \rightarrow g + H$, $gq \rightarrow q + H$ and $q\bar{q} \rightarrow g + H$ have been calculated in the leading order α_s^3 . For the Higgs boson mass $100 \text{ GeV} \leq M_H \leq 150 \text{ GeV}$ and for an integrated luminosity 10 fb^{-1} this channel has dozens of signal events with a number of background events only by factor 2-3 higher [39]. The significance $N_S/\sqrt{N_B} \sim 4, 5$ and 4 for $M_H = 100, 120$ and 140 GeV respectively indicating good prospects for discovery of the light Higgs boson at low luminosity. These results also imply that at high luminosity phase with year for the standard Higgs boson search with $m_H = 110 \text{ GeV}$ and for $L = 30 \text{ fb}^{-1}(20 \text{ fb}^{-1})$ the standard significance is $6.6(5.4)$. At the language of the probabilities it means [38] that the CMS will discover at $\geq 5\sigma$ the Higgs boson with the probability 96(73) percent.

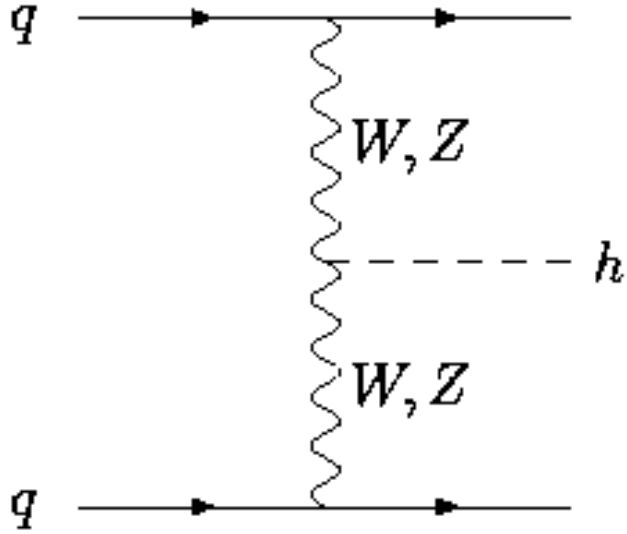


Figure 6: *Diagram contributing to $qq \rightarrow qqV^*V^* \rightarrow qqh$*

luminosity 100 fb^{-1} LHC will give hundred of events with high p_t associated with hard jet with the signal significance ~ 15 .

3.7 $H \rightarrow WW^* \rightarrow l^+\nu l^-\bar{\nu}$

The signature $pp \rightarrow H \rightarrow WW^* \rightarrow l^+\nu l^-\bar{\nu}$ [40] provides the Higgs boson discovery for the Higgs boson mass region between 155 GeV and 180 GeV at the LHC. Especially important is that the signature $H \rightarrow WW^* \rightarrow l^+\nu l^-\bar{\nu}$ allows to discover Higgs boson in the mass region around 170 GeV where the branching ratio for $H \rightarrow 4l$ is small and the use of four lepton signature for the Higgs boson discovery does not help at least for low luminosity. This signature does not require extraordinary detector performance and only requires a relatively low integrated luminosity of about 5 fb^{-1} . The results of the analysis [40] demonstrate that this signature provides not only the Higgs boson discovery channel for a mass range between $(155 - 180) \text{ GeV}$ with $S/B \geq 0.35$ but also helps to establish a LHC Higgs boson signal for masses between $(120 - 500) \text{ GeV}$. Simulations [41] based on PYTHIA to generate events and CMSCIM calorimeter simulation for the jet veto confirm

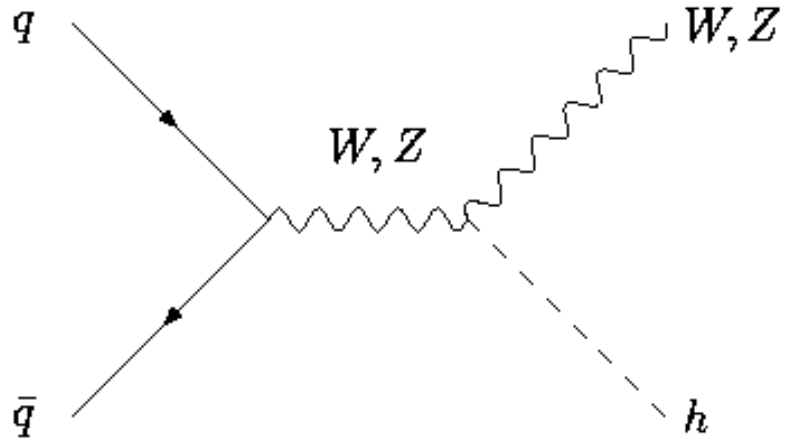


Figure 7: *Diagram contributing to $q\bar{q} \rightarrow V^* \rightarrow Vh$*

qualitatively the results of ref.[40].

3.8 $pp \rightarrow H + 2$ forward jets

The weak boson fusion channels $qq \rightarrow qqH$ lead to energetic jets in the forward and backward directions, and the absence of colour exchange in the hard process [42],[43],[44] that allows to obtain a large reduction of backgrounds from $t\bar{t}$, QCD jets, W- and Z-production and compensate the smallness of the Higgs weak boson fusion cross section

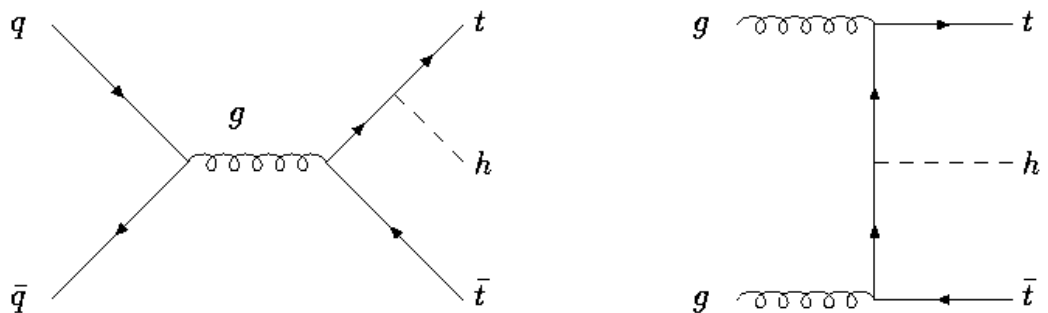


Figure 8: *Diagrams contributing to $q\bar{q}/gg \rightarrow ht\bar{t}$*

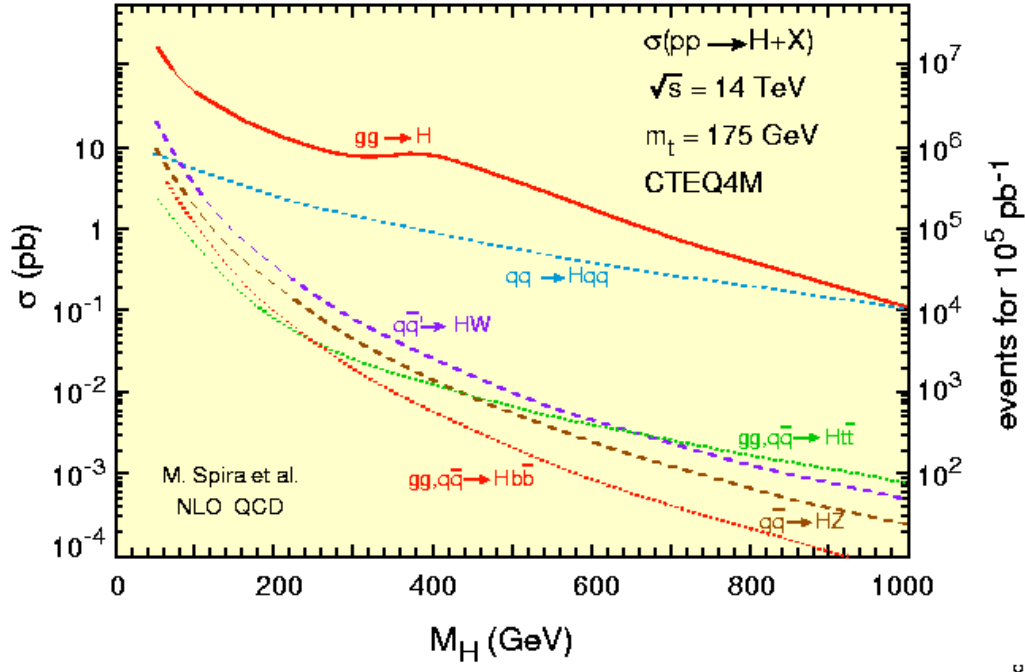


Figure 9: *Higgs boson production cross sections at the LHC for the various production mechanisms as a function of the Higgs boson mass*

compared to inclusive $gg \rightarrow H$. Note that the process of Higgs boson production in the weak boson fusion with forward jet tagging has been considered first for the channels $H \rightarrow ZZ \rightarrow 4l, 2l2\nu$ in ref.[45]. The reaction $pp \rightarrow (H \rightarrow \gamma\gamma) + 2$ forward jets has been investigated at parton level in ref.[42] and at fast CMS detector simulation level in ref.[46]. The main conclusion of ref.[46] is that the significance $S = \frac{N_S}{\sqrt{N_B}} = 5$ is reached at the luminosities $(25 - 35) \text{ fb}^{-1}$ for $m_H = 115 - 145 \text{ GeV}$. Additional advantage of this signature is that the ratio of signal to background $S/B \sim 1$ in comparison with $S/B \sim 1/15$ for inclusive $pp \rightarrow (H \rightarrow \gamma\gamma) + \dots$ reaction.

The signature $H \rightarrow W^{(*)}W \rightarrow e^\pm \mu^\mp p_T^{miss}$ in weak boson fusion mechanism with forward jet tagging has been investigated in ref.[43]. The spin correlations, leading to small opening angles between two charged leptons, are used to suppress the backgrounds. This mode provides the Higgs boson discovery for $m_H \geq 120 \text{ GeV}$.

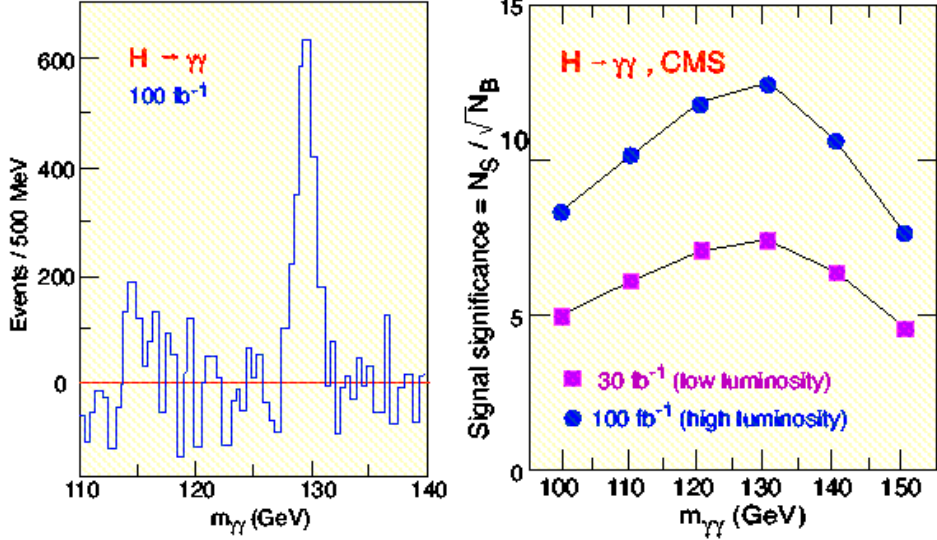


Figure 10: *Mass peak and signal significance for $H \rightarrow \gamma\gamma$*

3.9 $H \rightarrow ZZ^*(ZZ) \rightarrow 4$ leptons

The channel $H \rightarrow ZZ^* \rightarrow 4l$ is the most promising one to observe Higgs boson in the mass range $130 \text{ GeV} - 180 \text{ GeV}$. Below $2M_Z$ the event rate is small and the background reduction more difficult, as one of the Z s is off mass shell. In this mass region the width of the Higgs boson is small $\Gamma_H < 1 \text{ GeV}$, and the observed width is entirely determined by the instrumental mass resolution. The significance of the signal is proportional to the square root of the four-lepton mass resolution ($S = N_S / \sqrt{N_B}$ and $N_{S,B} \sim \sigma_{4l}$), so the lepton energy/momentum resolution is of decisive importance ³. The comparison of the CMS and ATLAS discovery potentials with $H \rightarrow ZZ^* \rightarrow 4$ leptons based on the analyses presented in the two Technical Proposals has been performed in ref.[48]. The main conclusion of the ref.[48] is that in terms of significances ATLAS and CMS discovery potentials coincide up to 20%. For the region $130 \text{ GeV} \leq m_H \leq 180 \text{ GeV}$ and for $L_t = 100 \text{ fb}^{-1}$ CMS detector [33] will discover the Higgs boson with $\geq 5\sigma$ signal significance except narrow mass region around 170 GeV where $\sigma \times Br$ has a minimum

³Typical Higgs boson mass resolutions in this mass range are: $\sigma_{4\mu} \approx 1 \text{ GeV}$, $\sigma_{4e} \approx 1.5 \text{ GeV}$ (CMS) [8] and $\sigma_{4\mu} \approx 1.6 \text{ GeV}$, $\sigma_{4e} \approx 1.6 \text{ GeV}$ (ATLAS) [9].

due to the opening of the $H \rightarrow WW$ channel and drop of the $H \rightarrow ZZ^*$ branching ratio just below the ZZ threshold.

For $180 \text{ GeV} \leq m_H \leq 600 \text{ GeV}$, the four-lepton signature is considered to be the most reliable one for the Higgs boson discovery at LHC, since the expected signal rates are large and the background is small. The main background to the $H \rightarrow ZZ \rightarrow 4l^\pm$ process is the irreducible ZZ production from $q\bar{q} \rightarrow ZZ$ and $gg \rightarrow ZZ$. The $t\bar{t}$ and $Zb\bar{b}$ backgrounds are small and reducible by a Z -mass cut. The use of this signature allows to detect the Higgs boson at $\geq 5\sigma$ level up to $m_H \approx 400 \text{ GeV}$ at 10 fb^{-1} and up to $m_H \approx 650 \text{ GeV}$ at 100 fb^{-1} [33].

3.10 $WH(t\bar{t}H) \rightarrow \gamma\gamma + \text{lepton} + \dots$

The $WH \rightarrow l\gamma\gamma + X$ and $t\bar{t}H \rightarrow l\gamma\gamma + X$ final states are other promising signature for the Higgs boson search. The production cross section is smaller than the inclusive $H \rightarrow \gamma\gamma$ by a factor ≈ 30 . However the isolated hard lepton from the W and t decays allows to obtain a strong background reduction and to indicate the primary vertex at any luminosity. The main conclusion [39] is that for an integrated luminosity 165 fb^{-1} in both channels $pp \rightarrow WH$ and $pp \rightarrow t\bar{t}H$ in the two-photon invariant mass interval $M_H - 1 \text{ GeV} \leq M_{\gamma\gamma} \leq M_H + 1 \text{ GeV}$ there are ~ 100 signal for $M_H = 120 \text{ GeV}$ and ~ 20 irreducible background events if the photon transverse momentum cuts are 20 GeV . Only in the high luminosity phase the use of this signature allows to make an important cross-checking if the Higgs boson signal has shown up before in $pp \rightarrow H + \dots \rightarrow \gamma\gamma + \dots$ classical signature.

3.11 $t\bar{t}H \rightarrow t\bar{t}b\bar{b}$

The large $H \rightarrow b\bar{b}$ branching ratio for $m_H \leq 130 \text{ GeV}$ can be used in the associated production channel $t\bar{t}H$. To extract the Higgs signal in $t\bar{t}H \rightarrow l^\pm \nu q\bar{q}b\bar{b}b\bar{b}$ channel requires tagging of up to 4 jets, reconstruction of the Higgs boson mass from two b-jets and the reconstruction of the associated leptonic and hadronic top. The main conclusion [33] is

that this channel allows to discover light Higgs boson ($m_H \leq 120 \text{ GeV}$).

3.12 $H \rightarrow WW \rightarrow ll\nu\nu$, $H \rightarrow WW \rightarrow l\nu jj$ and $H \rightarrow ZZ \rightarrow lljj$.

The channel $H \rightarrow ll\nu\nu$ has a six times larger branching than $H \rightarrow 4l^\pm$. The main background comes from ZZ , ZW , $t\bar{t}$ and $Z + jets$. The conclusion [8], [37] is that using this mode it would be possible to discover Higgs boson in the interval $400 \text{ GeV} \leq m_H \leq (800 - 900) \text{ GeV}$ for $L_t = 100 \text{ fb}^{-1}$.

The channels $H \rightarrow WW \rightarrow l\nu jj$ and $H \rightarrow ZZ \rightarrow lljj$ are important for $m_H \approx 1 \text{ TeV}$ region, where the large $W, Z \rightarrow q\bar{q}$ branching ratios are used. Two hard jets from hadronic decays of W/Z plus one or two high p_T leptons from W/Z decays are required. The backgrounds are: $Z + jets$, $W + jets$, ZW , WW , $t\bar{t}$. For $m_H \approx 1 \text{ TeV}$ the Higgs boson is very broad ($\Gamma_H \approx 0.5 \text{ TeV}$) and WW/ZZ fusion mechanism gives about 50 percent of the total cross section, therefore the forward region signature is essential. The main conclusion [8], [37] is that the use of the decays $H \rightarrow WW \rightarrow l\nu jj$ and $H \rightarrow ZZ \rightarrow lljj$ allows to discover the heavy Higgs boson with a mass up to 1 TeV for $L_t = 100 \text{ fb}^{-1}$.

3.13 Investigation of the Higgs boson properties

For the most interesting Higgs boson mass region $114.4 \text{ GeV} \leq m_H \leq 193 \text{ GeV}$ the $H \rightarrow \gamma\gamma$ and $H \rightarrow ZZ/ZZ^* \rightarrow 4l^\pm$ channels provide a precision in mass determination better than 10^{-3} [33], [36], [37]. Direct measurement of the SM Higgs boson width is possible only for $m_H \geq 200 \text{ GeV}$ where the natural width exceeds the experimental mass resolution $\sim 1 \text{ GeV}$. Precision at the $O(10^{-2})$ level is expected from $H \rightarrow ZZ^* \rightarrow 4l^\pm$.

The use of weak boson channels and $H \rightarrow WW^*$, $H \rightarrow \gamma\gamma$ decays allows to extract information on the HWW coupling. The ratio of the Higgs boson decay widths Γ_W/Γ_Z can be measured in the direct Higgs boson production using $\sigma_H \times BR(H \rightarrow WW^*)/\sigma_H \times BR(H \rightarrow ZZ^*) = \Gamma_W/\Gamma_Z$. The simultaneous use of the channels $H \rightarrow \gamma\gamma$ and $H \rightarrow ZZ^*$ allows to determine $\sigma_H \times BR(H \rightarrow \gamma\gamma)/\sigma_H \times BR(H \rightarrow ZZ^*) = \Gamma(H \rightarrow \gamma\gamma)/\Gamma(H \rightarrow ZZ^*)$. Precision of better than 20 percent is expected for these measurements

with 300 fb^{-1} [33], [36].

3.14 Summary

LHC will be able to discover the SM Higgs boson from the lower LEP2 limit $m_H \geq 114.4 \text{ GeV}$ up to $m_H = 1 \text{ TeV}$ value (see Figs.11-13) where the Higgs boson is very broad $\Gamma_H \approx 0.5 \text{ TeV}$ and it is no longer sensible to consider it as an elementary particle. The most reliable signatures for the LHC Higgs boson search are:

1. $H \rightarrow \gamma\gamma$,
2. $H \rightarrow ZZ^*, ZZ \rightarrow 4l^\pm$,
3. $H \rightarrow WW^* \rightarrow l^+\nu l^-\nu$,
4. $H \rightarrow ZZ, WW \rightarrow ll\nu\nu, lljj, l\nu jj$.

The simultaneous use of different channels allows to extract the ratio of the Higgs boson decay widths.

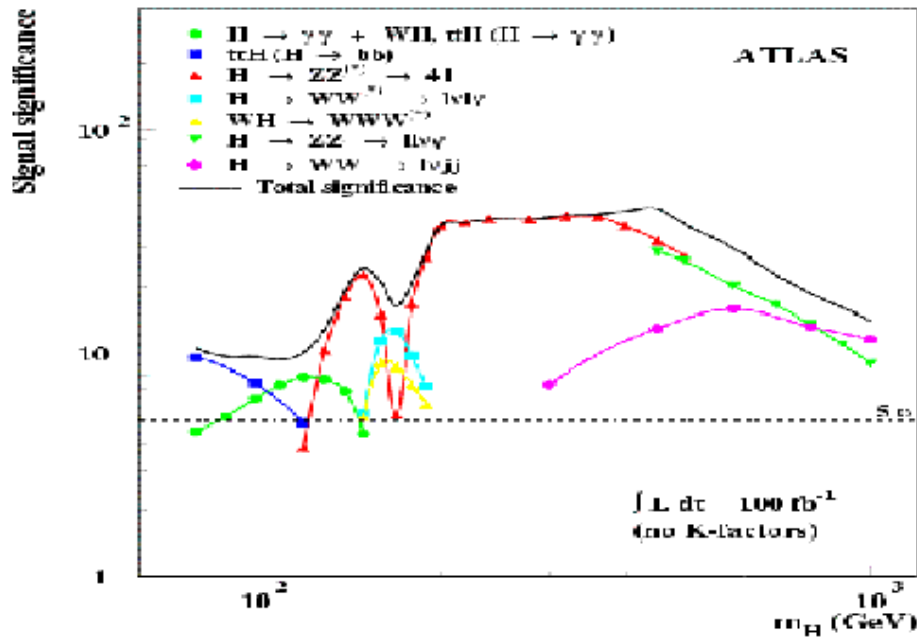


Figure 11: The discovery reach of the SM Higgs boson for 100 fb^{-1} in ATLAS

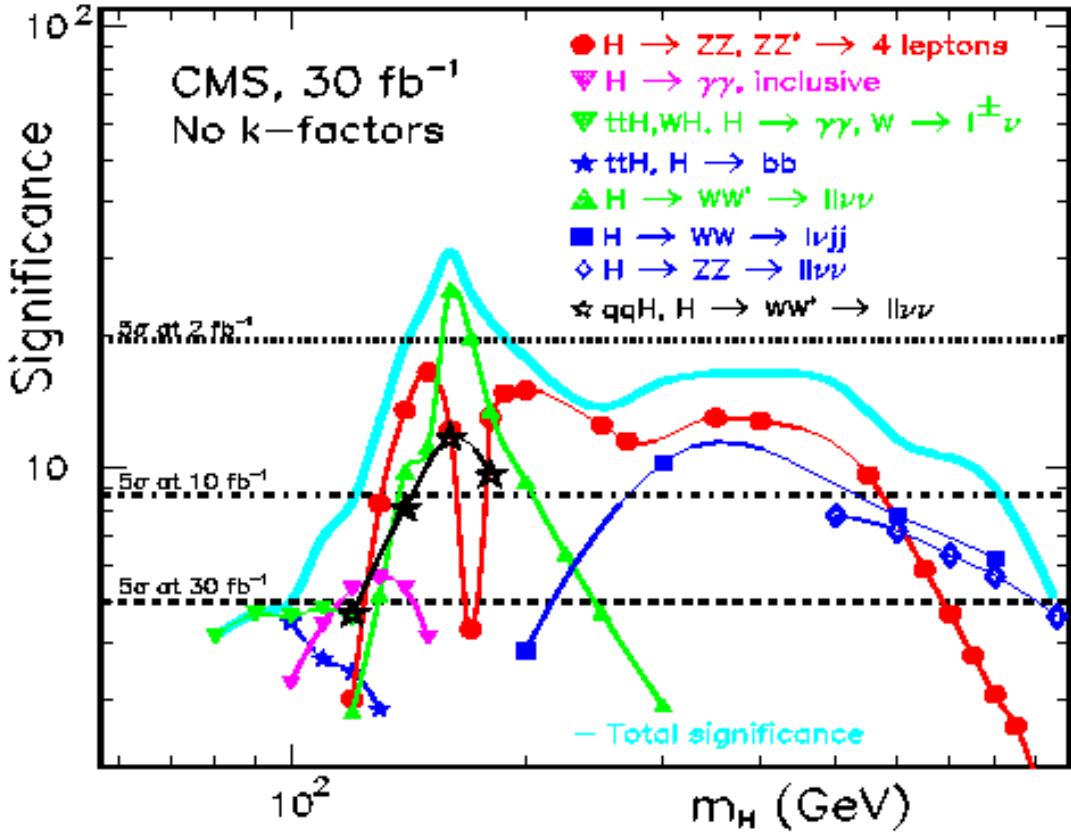


Figure 12: *The discovery reach of the SM Higgs boson in the CMS for 30 fb^{-1}*

4 Supersymmetry search within MSSM

4.1 The MSSM model

Supersymmetry (SUSY) is a new type of symmetry that relates bosons and fermions [4], [5]. Locally supersymmetric theories necessarily incorporate gravity [50]. SUSY is also an essential ingredient of superstring theories [52]. The interest in SUSY is due to the observation that measurements of the gauge coupling constants at LEP1 are in favour of the Grand Unification in a supersymmetric theory with superpartners of ordinary particles which are lighter than $O(1) \text{ TeV}$ [5]. Besides supersymmetric electroweak models offer the simplest solution of the gauge hierarchy problem [5]. In real life supersymmetry has to be broken and to solve the gauge hierarchy problem the masses of superparticles have to be lighter than $O(1) \text{ TeV}$. Supergravity provides natural explanation of the supersymmetry

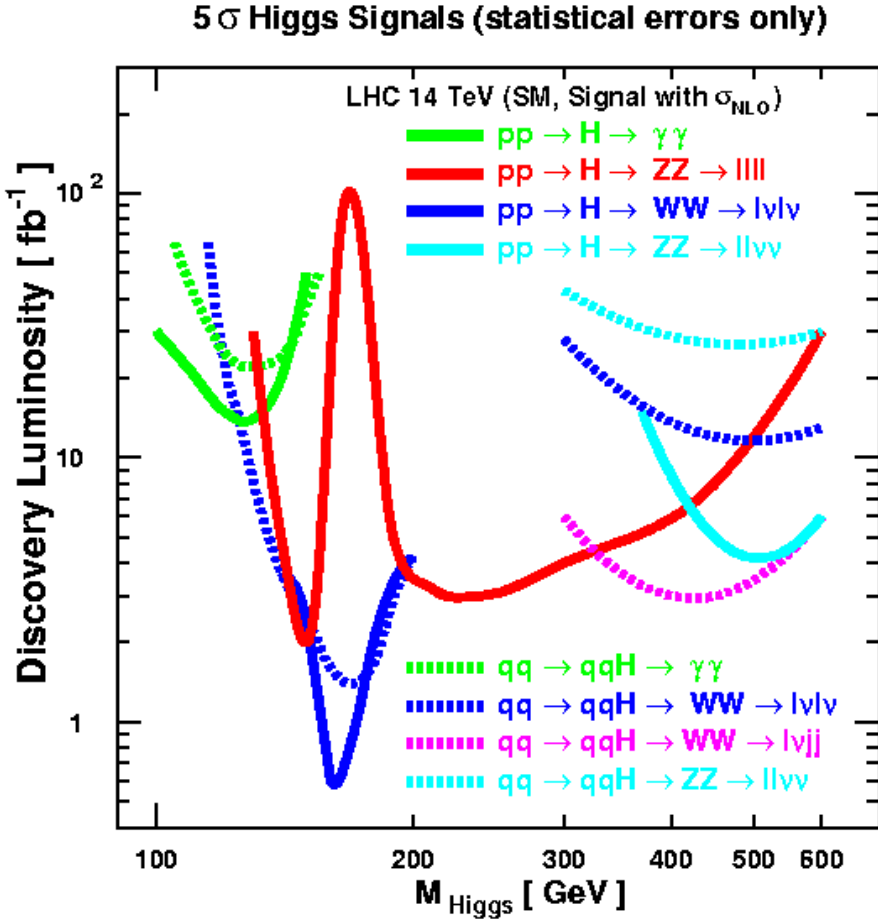


Figure 13: *The minimum luminosity to reach 5 σ discovery in CMS*

breaking [53], namely, an account of the supergravity breaking in hidden sector leads to soft supersymmetry breaking in observable sector.

An elegant formulation of supersymmetry can be achieved in the framework of superspace [50]. Two new Grassmannian (anticommuting) coordinates $\theta_\alpha, \bar{\theta}_{\dot{\alpha}}$ are introduced. Thus we extend our four dimensional space x_μ to superspace $(x_\mu, \theta_\alpha, \bar{\theta}_{\dot{\alpha}})$. There are two often used types of fields on a superfield: chiral superfield and vector superfield [50]. For the chiral superfield Grassmannian Taylor expansion has the form

$$\Phi(y, \theta) = A(y) + \sqrt{2}\theta\psi(y) + \theta\bar{\theta}F(y), \quad (53)$$

where $y = x + i\theta\sigma\bar{\theta}$. Chiral superfield $\Phi(y, \theta)$ has 2 bosonic (complex scalar field A) and 2 fermionic (Weyl spinor ψ) degrees of freedom. The component fields A and ψ are called

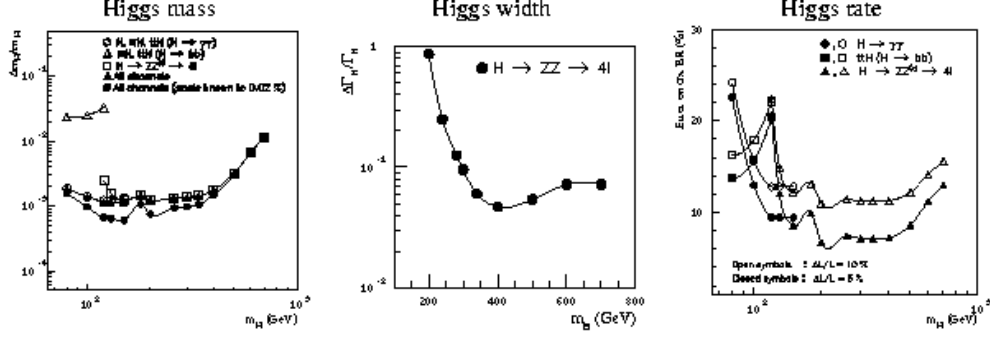


Figure 14: *The accuracy in measuring the SM Higgs boson mass, width and production rates in ATLAS*

superpartners. The field F is an auxiliary field and it has no physical meaning. One can get rid of the auxiliary field using the equations of motion. For any arbitrary function of chiral superfields one has

$$W(\Phi_i) = W(A_i + \sqrt{2}\theta\psi_i + \theta\theta F_i) = W(A_i) + \frac{\partial W}{\partial A_i} \sqrt{2}\theta\psi_i + \theta\theta \left(\frac{\partial W}{\partial A_i} F_i - \frac{1}{2} \frac{\partial^2 W}{\partial A_i \partial A_j} \psi_i \psi_j \right) \quad (54)$$

The W is usually referred to as a superpotential which replaces the usual potential for the scalar potentials. To construct the gauge invariant interactions, one needs a real vector superfield $V = V^+$. Under the abelian (super)gauge transformation the superfield V is transformed as

$$V \rightarrow V + \Phi + \Phi^+, \quad (55)$$

where Φ is chiral superfield. One can choose a gauge (the Wess-Zumino gauge) where

$$V = -\theta\sigma^\mu\bar{\theta}v_\mu(x) + i\theta\theta\bar{\theta}\bar{\lambda}(x) - i\bar{\theta}\bar{\theta}\theta\lambda(x) + \frac{1}{2}\theta\theta\bar{\theta}\bar{\theta}D(x). \quad (56)$$

The physical degrees of freedom corresponding to a real vector superfield V are the vector gauge field $v_\mu(x)$ and the Majorana spinor field $\lambda(x)$. The field $D(x)$ is an auxiliary field and can be eliminated with the help of equations of motion. One can also define a field strength tensor (an analog of $F_{\mu\nu}$ in gauge theories) as:

$$W_\alpha = -\frac{1}{4}\bar{D}^2 e^{gV} D_\alpha e^{-gV}, \quad (57)$$

$$\bar{W}_{\dot{\alpha}} = -\frac{1}{4} D^2 e^{gV} \bar{D}_{\dot{\alpha}} e^{-gV}. \quad (58)$$

The strength tensor is a chiral superfield and in the Wess-Zumino gauge it is a polynomial over component fields:

$$W_\alpha = T^a (-i\lambda_\alpha^a + \theta^\alpha D^a - \frac{i}{2} (\sigma^\mu \bar{\sigma}^\nu \theta)_\alpha F_{\mu\nu}^a + \theta^2 \sigma^\mu D_\mu \bar{\lambda}^a), \quad (59)$$

where

$$F_{\mu\nu}^a = \partial_\mu v_\nu^a - \partial_\nu v_\mu^a + g f^{abc} v_\mu^b v_\nu^c, \quad (60)$$

$$D_\mu \bar{\lambda}^a = \partial \bar{\lambda}^a + g f^{abc} v_\mu^b \bar{\lambda}^c. \quad (61)$$

Here T^a and f^{abc} are generators and structure constants of some group G . Supersymmetry invariant Lagrangians can be written in an elegant way in superspace if we use integration over the superspace according to the rules of Grassmannian integration [50]

$$\int d\theta_\alpha = 0, \int \theta_\alpha d\theta_\beta = \delta_{\alpha\beta}. \quad (62)$$

Let us start with the case of chiral superfields without local gauge invariance. The space-time Lagrangian density of the renormalizable Lagrangian is represented in the form [50]

$$L = \int d^2\theta d^2\bar{\theta} \Phi_i^+ \Phi_i + \left(\int d^2\theta W_3 + h.c. \right), \quad (63)$$

where

$$W_3 = \lambda_i \Phi_i + \frac{1}{2} m_{ij} \Phi_i \Phi_j + \frac{1}{3} h_{ijk} \Phi_i \Phi_j \Phi_k, \quad (64)$$

Performing explicit integration over the Grassmannian parameters one can find that

$$L = i\partial_\mu \bar{\psi}_i \bar{\sigma}^\mu \psi_i + \partial^\mu A_i^* \partial_\mu A_i + F_i^* F_i + [\lambda_i F_i + m_{ij} (A_i F_j - \frac{1}{2} \psi_i \psi_j) + h_{ijk} (A_i A_j F_k - \psi_i \psi_j A_k) + h.c.]. \quad (65)$$

Eliminating the auxiliary fields F_i and F_i^* using the equations of motion, one finally gets

$$L = i\partial_\mu \bar{\psi}_i \bar{\sigma}^\mu \psi_i + \partial^\mu A_i^* \partial_\mu A_i - \left(\frac{1}{2} m_{ij} \psi_i \psi_j + h_{ijk} \psi_i \psi_j A_k + h.c. \right) - |\lambda_k + m_{ik} A_i + h_{ijk} A_i A_j|^2. \quad (66)$$

Let us consider the case of gauge fields. The supersymmetric generalisation of the Yang-Mills Lagrangian has the form

$$L_{SYM} = \frac{1}{4} \int d^2\theta Tr(W^\alpha W_\alpha) + h.c. \quad (67)$$

In terms of component fields the Lagrangian (67) has the form

$$L_{SYM} = -\frac{1}{4} F_{\mu\nu}^a F^{a\mu\nu} - i\lambda^a \sigma^\mu D_\mu \bar{\lambda}^a + \frac{1}{2} D^a D^a. \quad (68)$$

A complete SUSY and gauge invariant renormalizable Lagrangian looks like

$$L_{SUSYYM} = \frac{1}{4} \left(\int d^2\theta Tr(W^\alpha W_\alpha) + h.c. \right) + \int d^2\theta d^2\bar{\theta} \Phi_{ia}^+(e^{gV})_b^a \Phi_i^b + \left(\int d^2\theta W_3(\Phi_i) + h.c. \right), \quad (69)$$

where $W_3(\Phi_i)$ is a gauge invariant superpotential. In terms of the component fields the above Lagrangian takes the form

$$\begin{aligned} L_{SYM} = & -\frac{1}{4} F_{\mu\nu}^a F^{a\mu\nu} - i\lambda^a \sigma^\mu D_\mu \bar{\lambda}^a + \frac{1}{2} D^a D^a \\ & + (\partial_\mu A_i - igv_\mu^a T^a A_i)^+ (\partial^\mu A_i - igv_\mu^a T^a A_i) \\ & - i\bar{\psi}_i \bar{\sigma}^\mu (\partial_\mu \psi_i - igv_\mu^a T^a \bar{\psi}_i) - g D^a A_i^+ T^a A_i - (i\sqrt{2} g A_i^+ T^a \lambda^a \psi_i + h.c.) \\ & + F_i^+ F_i + \left(\frac{\partial W}{\partial A_i} F_i - \frac{1}{2} \frac{\partial^2 W}{\partial A_i \partial A_j} \psi_i \psi_j + h.c. \right). \end{aligned} \quad (70)$$

Integrating out the auxiliary fields D^a and F_i one reproduces the usual Lagrangian.

The simplest supersymmetric generalisation of the SM is the Minimal Supersymmetric Standard Model (MSSM) [5], [51]. It is supersymmetric model based on standard $SU_c(3) \otimes SU_L(2) \otimes U(1)$ gauge group with electroweak symmetry spontaneously broken via vacuum expectation values of two different Higgs doublets. The MSSM consists of taking the SM and adding the corresponding supersymmetric partners. It should be stressed that the MSSM contains two hypercharges $Y = \pm 1$ Higgs doublets, which is the minimal structure for the Higgs sector of an anomaly-free supersymmetric extension of the SM. The supersymmetric electroweak models also require at least two Higgs doublets to generate masses for both “up”-type and “down”-type fermions.

The SUSY generalisation of the SM model Lagrangian can be presented in the form

$$L_{SUSY} = L_{Gauge,M} + L_{Yukawa}, \quad (71)$$

where

$$L_{Gauge,M} = \sum_{SU(3),SU(2),U(1)} \frac{1}{4} \left(\int d^2\theta Tr W^\alpha W_\alpha + h.c. \right) + \sum_{matter} \int d^2\theta d^2\bar{\theta} \Phi_i^+ e^{gV} \Phi_i , \quad (72)$$

$$L_{Yukawa} = \int d^2\theta (W_R + W_{NR}) + h.c. . \quad (73)$$

The renormalizable superpotential W_R of the MSSM determines the Yukawa interactions of quarks and leptons and preserves global $B - L$. Here B is the baryon number and L is the lepton number. It has the form

$$W_R = \epsilon_{ij} (h_{ab}^U Q_a^j U_b^c H_2^i + h_{ab}^D Q_a^j D_b^c H_1^i + h_{ab}^L L_a^j E_b^c H_1^i + \mu H_1^i H_2^j) , \quad (74)$$

where $i, j = 1, 2, 3$ are the $SU(2)$ and $a, b = 1, 2, 3$ are the generation indices; colour indices are omitted. The last term in the superpotential (74) describes the Higgs boson mixing. The most general expression for the superpotential W_{NR} has the form

$$W_{NR} = \epsilon_{ij} (\lambda_{abd}^L L_a^i L_b^j E_d^c + \lambda_{1abd}^L L_a^i Q_b^j D_d^c + \mu'_a L_a^i H_2^j) + \lambda_{abd}^B U_a^c D_b^c D_d^c \quad (75)$$

Note that the most general expression for the effective superpotential (75) contains renormalizable terms violating $B - L$ that can lead to the problems with proton decay. To get rid of such dangerous terms in the superpotential, R-parity conservation [54] is postulated. Here $R = (-1)^{3(B-L)+2S}$ for a particle with spin S . For ordinary particles $R = 1$, whereas for the corresponding supersymmetric partners $R = -1$. If we postulate R-parity conservation then the $W_{NR} = 0$. Experimental bounds on the R -parity violating coupling constants are rather strong [16], [55]

$$\lambda_{abc}^L < O(10^{-4}) , \quad (76)$$

$$\lambda_{1abc}^L < O(10^{-4}) , \quad (77)$$

$$\lambda_{abc}^B < O(10^{-9}) . \quad (78)$$

The R -parity conservation has a crucial impact on supersymmetric phenomenology. An important consequence of R -parity conservation is that the lightest supersymmetric particle (LSP) is stable. The cosmological constraints imply that the LSP is weakly-interacting

electrically neutral and colourless particle. Other important consequence of the R -parity conservation is that at supercolliders superparticles are produced in pairs, therefore at least two LSP have eventually to be produced at the end of the decays of heavy unstable supersymmetric particles. Being weakly interacting particle LSP escapes detector registration, therefore the classic signature for R -parity conserving supersymmetric models is the transverse missing energy due to the LSP-escape.

In real life supersymmetry has to be broken. At present the most popular scenario for producing low-energy supersymmetry breaking is called the hidden sector scenario [5], [53], [56]. According to this scenario, there exists two sectors: the usual matter belongs to the visible sector. The second hidden sector of the theory contains fields which lead to the supersymmetry breaking. These two sectors interact with each other by exchange of some fields which mediate SUSY breaking from the hidden to visible sector. At present there are two most elaborated scenario of SUSY breaking:

1. Gravity mediation (SUGRA) ,
2. Gauge mediation.

In SUGRA scenario [53], [5] visible and hidden sectors interact with each other via gravity. Some scalar fields in hidden sector develop nonzero vacuum expectation values for their F -components which lead to spontaneous SUSY breaking. Since in SUGRA theory supersymmetry is local, spontaneous SUSY breaking leads to Goldstone particle which is a Goldstone fermion. With the help of a super-Higgs effect this particle is absorbed into an additional component of a spin 3/2 particle -gravitino which becomes massive in close analogy with the standard Higgs mechanism. SUSY breaking is mediated to a visible sector via gravitational interactions leading to SUSY breaking scale $M_{SUSY} \sim m_{3/2}$, where $m_{3/2}$ is the gravitino mass. The effective low-energy Lagrangian contains explicit soft supersymmetry breaking terms

$$L_{soft} = - \sum_{i,j} m_{ij}^2 A_i A_j^* - \sum_i M_i (\lambda_i \lambda_i + \bar{\lambda}_i \bar{\lambda}_i) - (BW^{(2)}(A) + BW^{(3)}(A) + h.c.) . \quad (79)$$

Here $W^{(2)}$ and $W^{(3)}$ are the quadratic and cubic terms of the visible superpotential, respectively. The mass parameters in soft SUSY breaking Lagrangian (79) are proportional

to the gravitino mass $m_{3/2}$.

In gauge mediation mechanism [56] the SUSY breaking is mediated to the observable world via gauge interactions. The messengers are the gauge bosons or matter fields of the SM or of its GUT generalisation. In such scenario it is possible to have a renormalizable model with dynamic SUSY breaking where (in principle) all the parameters are calculated numbers. In gauge mediated scenario all soft SUSY breaking masses are correlated to the gauge couplings. Besides there is no problem with flavour violating couplings as well. In this scenario the lightest stable superparticle (LSP) is the gravitino. In general soft SUSY breaking mechanisms lead to the generation of soft SUSY breaking operators of the dimension ≤ 3 .

In the MSSM supersymmetry is softly broken at some high scale M by generic soft terms

$$\begin{aligned}
-L_{soft} = & m_0(A_{ij}^u U_i^c Q_j H_2 + A_{ij}^d D_i^c G_j H_1 + \\
& A_{ij}^l E_i^c L_j H_1 + h.c.) + (m_q^2)_{ij} Q_i^+ Q_j + (m_u^2)_{ij} (U_i^c)^+ U_j^c \\
& + (m_d^2)_{ij} (D_i^c)^+ D_j^c + (m_l^2)_{ij} (L_i^c)^+ L_j^c + (m_e^2)_{ij} (E_i^c)^+ \\
& E_j^c + m_1^2 H_1 H_1^+ + m_2^2 H_2 H_2^+ + (B m_0^2 H_1 H_2 + h.c.) + \left(\frac{1}{2} m_a (\lambda_a \lambda_a) + h.c.\right).
\end{aligned} \tag{80}$$

In general all soft SUSY breaking terms are arbitrary that complicates the analysis and spoils the predictive power of the theory. In MSUGRA model [5], [51] the universality of different soft parameters at GUT scale is postulated. Namely, all the spin 0 particle masses (squarks, sleptons, higgses) are postulated to be equal to the universal value m_0 at GUT scale. All gaugino particles masses are postulated to be equal to $m_{1/2}$ at GUT scale and all the cubic and quadratic terms proportional to A and B are postulated to repeat the structure of the Yukawa superpotential (74). It should be stressed that the MSUGRA model is not the general model and it could be considered as a “toy model” for concrete applications.

So, in MSUGRA model soft SUSY breaking masses and coupling constants are sup-

posed to be equal at M_{GUT} scale, namely:

$$A_{ij}^u(M_{GUT}) = Ah_{ij}^u(M_{GUT}), \quad A_{ij}^d(M_{GUT}) = Ah_{ij}^d(M_{GUT}), \quad A_{ij}^l(M_{GUT}) = Ah_{ij}^l(M_{GUT}), \quad (81)$$

$$(m_q^2)_{ij}(M_{GUT}) = (m_u^2)_{ij}(M_{GUT}) = (m_d^2)_{ij}(M_{GUT}) = (m_l^2)_{ij}(M_{GUT}) = \delta_{ij}m_1^2(M_{GUT}) = \delta_{ij}m_2^2(M_{GUT}) = \delta_{ij}m_0^2, \quad (82)$$

$$m_1(M_{GUT}) = m_2(M_{GUT}) = m_3(M_{GUT}) = m_{1/2}. \quad (83)$$

Note that it is more appropriate to impose boundary conditions not at GUT scale but at Planck scale $M_{PL} = 2.4 \cdot 10^{18} \text{ GeV}$. An account of the renormalization effects between Planck and GUT scales can drastically change the features of the spectrum. For instance, if we assume that the physics between Planck scale and GUT scale is described by SUSY $SU(5)$ model then an account of the evolution between Planck and GUT scales [58], [59] can change qualitatively the spectrum of sleptons for $m_0 \ll m_{1/2}$ [59]. The renormalization group equations for soft SUSY breaking parameters in neglection of all Yukawa coupling constants except top-quark Yukawa in one loop approximation read [57], [51]

$$\frac{d\tilde{m}_L^2}{dt} = (3\tilde{\alpha}_2 M_2^2 + \frac{3}{5}\tilde{\alpha}_1 M_1^2), \quad (84)$$

$$\frac{d\tilde{m}_E^2}{dt} = (\frac{12}{5}\tilde{\alpha}_1 M_1^2), \quad (85)$$

$$\frac{d\tilde{m}_Q^2}{dt} = (\frac{16}{3}\tilde{\alpha}_3 M_3^2 + 3\tilde{\alpha}_2 M_2^2 + \frac{1}{15}\tilde{\alpha}_1 M_1^2) - \delta_{i3} Y_t (\tilde{m}_Q^2 + \tilde{m}_U^2 + m_2^2 + A_t^2 m_0^2 - \mu^2), \quad (86)$$

$$\frac{d\tilde{m}_U^2}{dt} = (\frac{16}{3}\tilde{\alpha}_3 M_3^2 + \frac{16}{15}\tilde{\alpha}_1 M_1^2) - \delta_{i3} 2 Y_t (\tilde{m}_Q^2 + \tilde{m}_U^2 + m_2^2 + A_t^2 m_0^2 - \mu^2), \quad (87)$$

$$\frac{d\tilde{m}_D^2}{dt} = (\frac{16}{3}\tilde{\alpha}_3 M_3^2 + \frac{4}{15}\tilde{\alpha}_1 M_1^2), \quad (88)$$

$$\frac{d\mu^2}{dt} = 3(\tilde{\alpha}_2 + \frac{1}{5}\tilde{\alpha}_1 - Y_t)\mu^2, \quad (89)$$

$$\frac{dm_1^2}{dt} = 3(\tilde{\alpha}_2 M_2^2 + \frac{1}{5}\tilde{\alpha}_1 M_1^2) + 3(\tilde{\alpha}_2 + \frac{1}{5}\tilde{\alpha}_1 - Y_t)\mu^2, \quad (90)$$

$$\frac{dm_2^2}{dt} = 3(\tilde{\alpha}_2 M_2^2 + \frac{1}{5}\tilde{\alpha}_1 M_1^2) + 3(\tilde{\alpha}_2 + \frac{1}{5}\tilde{\alpha}_1)\mu^2 - 3Y_t (\tilde{m}_Q^2 + \tilde{m}_U^2 + m_2^2 + A_t^2 m_0^2), \quad (91)$$

$$\frac{dA_t}{dt} = -(\frac{16}{3}\tilde{\alpha}_3 \frac{M_3}{m_0} + 3\tilde{\alpha}_2 \frac{M_2}{m_0} + \frac{13}{15}\tilde{\alpha}_1 \frac{M_1}{m_0}) - 6Y_t A_t, \quad (92)$$

$$\frac{dB}{dt} = -3(\tilde{\alpha}_2 \frac{M_2}{m_0} + \frac{1}{5} \tilde{\alpha}_1 \frac{M_1}{m_0}) - 3Y_t A_t, \quad (93)$$

$$\frac{dM_i}{dt} = -b_i \tilde{\alpha}_i M_i, \quad (94)$$

$$b_1 = \frac{33}{5}, \quad b_2 = 1, \quad b_3 = -3. \quad (95)$$

Here \tilde{m}_U , \tilde{m}_D , \tilde{m}_E refer to the masses of the superpartner of the quark and lepton singlets, while \tilde{m}_Q and \tilde{m}_L refer to the masses of the isodoublet partners; m_1 , m_2 , m_3 and μ are the mass parameters in the Higgs potential, A and B are the coupling constants of the L_{soft} as defined before; M_i are gaugino masses before mixing. The renormalization group equation for the top Yukawa coupling constant has the form

$$\frac{dY_t}{dt} = Y_t \left(\frac{16}{3} \tilde{\alpha}_3 + 3\tilde{\alpha}_2 + \frac{13}{15} \tilde{\alpha}_1 \right) - 6Y_t^2, \quad (96)$$

while the RG equations for the gauge couplings are

$$\frac{d\tilde{\alpha}_i}{dt} = -b_i \tilde{\alpha}_i^2. \quad (97)$$

Here

$$\tilde{\alpha}_i = \frac{\alpha_i}{4\pi}, \quad Y_t = \frac{h_t^2}{16\pi^2}, \quad t = \ln \left(\frac{M_{GUT}^2}{Q^2} \right), \quad (98)$$

and the top Yukawa coupling h_t is related to the running top mass by the relation

$$m_t = h_t(m_t) \frac{v}{\sqrt{2}} \sin \beta. \quad (99)$$

The boundary conditions at $Q^2 = M_{GUT}^2$ are

$$\tilde{m}_Q^2 = \tilde{m}_U^2 = \tilde{m}_D^2 = \tilde{m}_E^2 = \tilde{m}_L^2 = m_0^2, \quad (100)$$

$$\mu = \mu_0; \quad m_1^2 = m_2^2 = \mu_0^2 + m_0^2; \quad m_3^2 = B\mu_0 m_0, \quad (101)$$

$$M_i = m_{1/2}, \quad \tilde{\alpha}_i(0) = \tilde{\alpha}_{GUT}; \quad i = 1, 2, 3. \quad (102)$$

For the gauginos of the $SU_L(2) \otimes U(1)$ gauge group one has to consider the mixings with the Higgsinos. The mass terms in the full Lagrangian are

$$L_{Gaugino-Higgsino} = -\frac{1}{2} M_3 \bar{\lambda}_3^a \lambda_3^a - \frac{1}{2} \bar{\chi} M^{(0)} \chi - (\bar{\psi} M^{(c)} \psi + h.c.), \quad (103)$$

where λ_3^a are the 8 Majorana gluino fields, and

$$\chi = \begin{pmatrix} \tilde{B}^0 \\ \tilde{W}^3 \\ \tilde{H}_1^0 \\ \tilde{H}_2^0 \end{pmatrix}, \quad (104)$$

$$\psi = \begin{pmatrix} \tilde{W}^+ \\ \tilde{H}^+ \end{pmatrix}, \quad (105)$$

are the Majorana neutralino and Dirac chargino fields. The mass matrices are:

$$M^{(0)} = \begin{pmatrix} M_1 & 0 & -A & B \\ 0 & M_2 & C & -D \\ -A & C & 0 & -\mu \\ B & -D & -\mu & 0 \end{pmatrix}, \quad (106)$$

$$M^{(c)} = \begin{pmatrix} M_2 & \sqrt{2}M_W \sin \beta \\ \sqrt{2}M_W \cos \beta & \mu \end{pmatrix}, \quad (107)$$

where:

$$A = M_Z \cos \beta \sin \theta_W, \quad B = M_Z \sin \beta \sin \theta_W, \quad (108)$$

$$C = M_Z \cos \beta \cos \theta_W, \quad D = M_Z \sin \beta \cos \theta_W. \quad (109)$$

After the solution of the corresponding renormalization group equations for $\alpha_{GUT} = \frac{1}{24.3}$, $M_{GUT} = 2.0 \cdot 10^{16}$ GeV, $\sin^2 \theta_W = 0.2324$, $\tan \beta = 1.65$ and $A_t(0) = 0$ one finds the numerical formulae for effective squark and slepton square masses at electroweak scale [51]

$$\tilde{m}_{E_L}^2(M_Z) = m_0^2 + 0.52m_{1/2}^2 - 0.27 \cos 2\beta M_Z^2, \quad (110)$$

$$\tilde{m}_{\nu_L}^2(M_Z) = m_0^2 + 0.52m_{1/2}^2 + 0.5 \cos 2\beta M_Z^2, \quad (111)$$

$$\tilde{m}_{E_R}^2(M_Z) = m_0^2 + 0.15m_{1/2}^2 - 0.23 \cos 2\beta M_Z^2, \quad (112)$$

$$\tilde{m}_{U_L}^2(M_Z) = m_0^2 + 6.5m_{1/2}^2 + 0.35 \cos 2\beta M_Z^2, \quad (113)$$

$$\tilde{m}_{D_L}^2(M_Z) = m_0^2 + 6.5m_{1/2}^2 - 0.42 \cos 2\beta M_Z^2, \quad (114)$$

$$\tilde{m}_{U_R}^2(M_Z) = m_0^2 + 6.1m_{1/2}^2 + 0.15 \cos 2\beta M_Z^2, \quad (115)$$

$$\tilde{m}_{D_R}^2(M_Z) = m_0^2 + 6.0m_{1/2}^2 - 0.07 \cos 2\beta M_Z^2, \quad (116)$$

$$\tilde{m}_{b_R}^2(M_Z) = \tilde{m}_{D_R}^2, \quad (117)$$

$$\tilde{m}_{b_L}^2(M_Z) = \tilde{m}_{D_L}^2 - 0.49m_0^2 - 1.21m_{1/2}^2, \quad (118)$$

$$\tilde{m}_{t_R}^2(M_Z) = \tilde{m}_{U_R}^2(M_Z) + m_t^2 - 0.99m_0^2 - 2.42m_{1/2}^2, \quad (119)$$

$$\tilde{m}_{t_L}^2(M_Z) = \tilde{m}_{U_L}^2(M_Z) + m_t^2 - 0.49m_0^2 - 1.21m_{1/2}^2. \quad (120)$$

After mixing the mass eigenstates of the stop matrix are:

$$\begin{aligned} \tilde{m}_{t_{1,2}}^2(M_Z) &\approx \frac{1}{2}[0.5m_0^2 + 9.1m_{1/2}^2 + 2m_t^2 + 0.5 \cos 2\beta M_Z^2] \\ &\mp \frac{1}{2}[(1.5m_{1/2}^2 + 0.5m_0^2 + 0.2 \cos(2\beta)M_Z^2)^2 + 4m_t^2(A_t m_o - \mu/\tan\beta)^2]^{1/2}. \end{aligned} \quad (121)$$

The gauginos and Higgsinos have similar quantum numbers which causes a mixing between the weak interaction eigenstates and the mass eigenstates. The two chargino eigenstates $\chi_{1,2}^\pm$ are:

$$M_{1,2}^2 = \frac{1}{2}[M_2^2 + \mu^2 + 2M_W^2] \mp \frac{1}{2}[(M_2^2 - \mu^2)^2 + 4M_W^4 \cos^2 2\beta + 4M_W^2(M_2^2 + \mu^2 + 2M_2\mu \sin 2\beta)]^{1/2}, \quad (122)$$

where at GUT scale the masses of gaugino fields of the $SU(3)$, $SU_L(2)$ and $U(1)$ groups are equal to $m_{1/2}$. The eigenvalues of the 4×4 neutralino mass matrix can be solved by a numerical diagonalization. If the parameter μ is much larger than M_1 and M_2 , the mass eigenstates become

$$\chi_i^0 = [\tilde{B}, \tilde{W}_3, \frac{1}{\sqrt{2}}(\tilde{H}_1 - \tilde{H}_2), \frac{1}{\sqrt{2}}(\tilde{H}_1 + \tilde{H}_2)] \quad (123)$$

with eigenvalues $|M_1|$, $|M_2|$, $|\mu|$ and $|\mu|$ respectively (the bino and neutral wino do not mix with each other and with the Higgsino eigenstates).

The tree level Higgs potential in MSSM has the form

$$V_0(H_1, H_2) = m_1^2|H_1|^2 + m_2^2|H_2|^2 - m_3^2(H_1 H_2 + h.c.) + \frac{g_2^2 + g_1^2}{8}(|H_1|^2 - |H_2|^2)^2 + \frac{g_2^2}{2}|H_1^+ H_2|^2. \quad (124)$$

The minimisation of the effective potential $V_0(H_1, H_2)$ leads to the equations:

$$v^2 = \frac{8(m_1^2 - m_2^2 \tan^2 \beta)}{(g_2^2 + g_1^2)(\tan^2 \beta - 1)}, \quad (125)$$

$$\sin 2\beta = \frac{2m_3^2}{m_1^2 + m_2^2}. \quad (126)$$

After the diagonalization of the corresponding mass matrices CP-odd neutral Higgs boson $A(x)$ acquires a mass $m_A^2 = m_1^2 + m_2^2$, charged Higgs boson $H^+(x)$ acquires a mass $m_{H^+}^2 = m_A^2 + M_W^2$ and CP-even Higgs bosons $H(x)$ and $h(x)$ have masses

$$m_{H,h}^2 = \frac{1}{2}[m_A^2 + M_Z^2 \pm \sqrt{(m_A^2 + M_Z^2)^2 - 4m_A^2 M_Z^2 \cos^2 2\beta}], \quad (127)$$

where $\langle H_1 \rangle = v_1 = \frac{v \cos \beta}{\sqrt{2}}$, $\langle H_2 \rangle = v_2 = \frac{v \sin \beta}{\sqrt{2}}$, $\tan \beta = \frac{v_2}{v_1}$. At tree level we have the following mass relations:

$$m_h^2 + m_H^2 = m_A^2 + M_Z^2, \quad (128)$$

$$m_h \leq m_A \leq m_H, \quad (129)$$

$$m_h \leq M_Z |\cos 2\beta| \leq M_Z. \quad (130)$$

Therefore at tree level the lightest Higgs boson is lighter than the Z-boson. However the radiative corrections due to big top quark Yukawa coupling constant increase the mass of the lightest Higgs boson in MSSM [21]. The upper limit on the Higgs boson mass in MSSM depends on the value of the top quark mass and on the value of stop quark masses. For $m_{t,pole} = 175$ Gev and stop quark masses lighter than 1 Tev the Higgs boson mass is lighter than 135 GeV [22].

After the solution of the corresponding equations for the determination of nontrivial electroweak potential the number of unknown parameters is decreased by 2. At present more or less standard choice of free parameters in MSSM includes m_0 , $m_{1/2}$, $\tan \beta$, A and $\text{sign}(\mu)$.

4.2 Superparticle cross sections.

At LHC sparticles can be produced via the following tree level reactions [102]:

- a. $gg, qq, qg \rightarrow \tilde{g}\tilde{g}, \tilde{g}\tilde{q}, \tilde{q}\tilde{q}$,

- b. $qq, gq \rightarrow \tilde{g}\tilde{\chi}_i^0, \tilde{g}\tilde{\chi}_i^\pm, \tilde{q}\tilde{\chi}_i^0, \tilde{q}\tilde{\chi}_i^\pm ,$
- c. $qq \rightarrow \tilde{\chi}_i^\pm \tilde{\chi}_j^\mp, \tilde{\chi}_i^\pm \tilde{\chi}_j^0, \tilde{\chi}_i^0 \tilde{\chi}_j^0 ,$
- d. $qq \rightarrow \tilde{l}\tilde{\nu}, \tilde{l}\tilde{l}, \tilde{\nu}\tilde{\nu} ,$

It is straightforward to calculate the elementary (tree level) cross sections for the production of superparticles in collisions of quarks and gluons. Here following ref.[102] we collect the main formulae for elementary cross sections.

The differential cross section of the production of two gauge fermions in quark-antiquark collisions is

$$\begin{aligned} \frac{d\sigma}{dt}(q\bar{q}' \rightarrow \text{gaugino1} + \text{gaugino2}) = & (131) \\ \frac{\pi}{s^2} [A_s \frac{(t-m_2^2)(t-m_1^2) + (u-m_1^2)(u-m_2^2) + 2sm_1m_2}{(s-M_s^2)^2} + A_t \frac{(t-m_1^2)(t-m_2^2)}{(t-M_t^2)^2} + \\ A_u \frac{(u-m_1^2)(u-m_2^2)}{(u-M_u^2)^2} + A_{st} \frac{(t-m_1^2)(t-m_2^2) + m_1m_2s}{(s-M_s^2)(t-M_t^2)} + \\ A_{tu} \frac{m_1m_2s}{(t-M_t^2)(u-M_u^2)} + A_{su} \frac{(u-m_1^2)(u-m_2^2) + m_1m_2s}{(s-M_s^2)(u-M_u^2)}], \end{aligned}$$

where m_1 and m_2 are the masses of the produced gauginos, M_s , M_t and M_u are the masses of the particles exchanged in the s,t, and u channels respectively. The coefficients A_x are given in ref. [102]. For instance, for the case of the gluino pair production in quark-antiquark collisions the coefficients A_x are [102]:

$$A_t = \frac{4}{9}A_s, A_u = A_t, A_{st} = A_s, A_{su} = A_{st}, A_{tu} = \frac{1}{9}A_s, A_s = \frac{8\alpha_s^2}{3}\delta_{qq'}$$

The differential cross section for the production of gluino pairs in gluon-gluon collisions is

$$\begin{aligned} \frac{d\sigma}{dt}(gg \rightarrow \tilde{g}\tilde{g}) = & (132) \\ \frac{9\pi\alpha_s^2}{4s^2} \left[\frac{2(t-m_{\tilde{g}}^2)(u-m_{\tilde{g}}^2)}{s^2} + \left[\left[\frac{(t-m_{\tilde{g}}^2)(u-m_{\tilde{g}}^2) - 2m_{\tilde{g}}^2(t+m_{\tilde{g}}^2)}{(t-m_{\tilde{g}}^2)^2} \right. \right. \right. & \\ \left. \left. \left. + \frac{(t-m_{\tilde{g}}^2)(u-m_{\tilde{g}}^2) + m_{\tilde{g}}^2(u-t)}{s(t-m_{\tilde{g}}^2)} \right] + (t \leftrightarrow u) \right] \\ + \frac{m_{\tilde{g}}^2(s-4m_{\tilde{g}}^2)}{(t-m_{\tilde{g}}^2)(u-m_{\tilde{g}}^2)} \right]. \end{aligned}$$

The total cross section has the form

$$\sigma(gg \rightarrow \tilde{g}\tilde{g}) = \frac{3\pi\alpha_s^2}{4s} \left[3 \left[1 + \frac{4m_{\tilde{g}}^2}{s} - \frac{4m_{\tilde{g}}^4}{s^2} \right] \ln \left[\frac{s+L}{s-L} \right] - \left[4 + \frac{17m_{\tilde{g}}^2}{s} \right] \frac{L}{s} \right], \quad (133)$$

where $L = [s^2 - 4m_{\tilde{g}}^2 s]^{1/2}$.

The differential cross section for the reaction $q_i q_j \rightarrow \tilde{q}_i \tilde{q}_j$ for the case of equal masses of right-handed and left-handed squarks is

$$\begin{aligned} \frac{d\sigma}{dt}(q_i q_j \rightarrow \tilde{q}_i \tilde{q}_j) = & \\ \frac{4\pi\alpha_s^2}{9s^2} & \left[-\frac{(t-m_i^2)(t-m_j^2) + st}{(t-m_{\tilde{g}}^2)^2} - \delta_{ij} \frac{(u-m_i^2)(u-m_j^2) + su}{(u-m_{\tilde{g}}^2)^2} + \right. \\ & \left. \frac{sm_{\tilde{g}}^2}{(t-m_{\tilde{g}}^2)^2} + \frac{sm_{\tilde{g}}^2}{(u-m_{\tilde{g}}^2)^2} \delta_{ij} - \frac{2sm_{\tilde{g}}^2}{3(t-m_{\tilde{g}}^2)(u-m_{\tilde{g}}^2)} \delta_{ij} \right], \end{aligned} \quad (134)$$

where m_i and m_j are the masses of produced squarks and $m_{\tilde{g}}$ is the gluino mass.

For the reaction $q_i \bar{q}_j \rightarrow \tilde{q}_i \tilde{q}_j^*$ the differential cross section has the form

$$\begin{aligned} \frac{d\sigma}{dt}(q_i \bar{q}_j \rightarrow \tilde{q}_i \tilde{q}_j^*) = & \\ \frac{4\pi\alpha_s^2}{9s^2} & \left[\left[\frac{ut - m_i^2 m_j^2}{s^2} \right] \left[\delta_{ij} \left[2 - \frac{2}{3} \frac{s}{(t-m_{\tilde{g}}^2)} \right] + \frac{s^2}{(t-m_{\tilde{g}}^2)^2} \right] + \frac{sm_{\tilde{g}}^2}{(t-m_{\tilde{g}}^2)^2} \right]. \end{aligned} \quad (135)$$

For the reaction $gg \rightarrow \tilde{q}_i \tilde{q}_i^*$ the differential cross section is

$$\begin{aligned} \frac{d\sigma}{dt}(gg \rightarrow \tilde{q}_i \tilde{q}_i^*) = & \\ \frac{\pi\alpha_s^2}{s^2} & \left[\frac{7}{48} + \frac{3(u-t)^2}{16s^2} \right] \left[1 + \frac{2m^2 t}{(t-m^2)^2} + \frac{2m^2 u}{(u-m^2)^2} + \frac{4m^4}{(t-m^2)(u-m^2)} \right]. \end{aligned} \quad (136)$$

Here m is the mass of the corresponding squark (we assume the left- and right-handed squarks are degenerated in mass).

The differential cross section for the reaction $gq_i \rightarrow gaugino + \tilde{q}_i$ has the form

$$\begin{aligned} \frac{d\sigma}{dt}(gq_i \rightarrow gaugino + \tilde{q}_i) = & \\ \frac{\pi}{s^2} & \left[B_s \frac{(\mu^2 - t)}{s} + B_t \frac{[(\mu^2 - t)s + 2\mu^2(m_i^2 - t)]}{(t - \mu^2)^2} + \right. \\ & B_u \frac{(u - \mu^2)(u + m_i^2)}{(u - m_i^2)^2} + B_{st} \frac{[(s - m_i^2 + \mu^2)(t - m_i^2) - \mu^2 s]}{s(t - \mu^2)} + \\ & B_{su} \frac{[s(u + \mu^2) + 2(m_i^2 - \mu^2)(\mu^2 - u)]}{s(u - m_i^2)} + \\ & \left. B_{tu} \frac{[(m_i^2 - t)(t + 2u + \mu^2) + (t - \mu^2)(s + 2t - 2m_i^2) + (u - \mu^2)(t + \mu^2 + 2m_i^2)]}{2(t - \mu^2)(u - m_i^2)} \right], \end{aligned} \quad (137)$$

where μ is the mass of the gauge fermion and m_i is the mass of the scalar quark. The coefficients B_x are contained in ref.[102]. For instance, for the case when $gaugino \equiv gluino$ the coefficients B_x are: $B_s = \frac{4\alpha_s^2}{9}\delta_{ij}$, $B_t = \frac{9}{4}B_s$, $B_u = B_s$, $B_{st} = -B_t$, $B_{su} = \frac{1}{8}B_s$, $B_{tu} = \frac{9}{8}B_s$.

Consider finally the production of sleptons. The differential cross section for the production of charged slepton-sneutrino pairs is

$$\frac{d\sigma}{dt}(d\bar{u} \rightarrow W^* \rightarrow \tilde{l}_L \bar{\tilde{\nu}}_L) = \frac{g_2^4 |D_W(s)|^2}{192\pi s^2} (tu - m_{\tilde{l}_L}^2 m_{\tilde{\nu}_L}^2). \quad (138)$$

For \tilde{l}_L pair production the differential cross section is

$$\begin{aligned} \frac{d\sigma}{dt}(q\bar{q} \rightarrow \gamma^*, Z^* \rightarrow \tilde{l}_L \bar{\tilde{l}}_L) = & \frac{2\pi\alpha^2}{3s^2} [tu - m_{\tilde{l}_L}^4] \left[\frac{q_l^2 q_q^2}{s^2} + \right. \\ & (\alpha_l - \beta_l)^2 (\alpha_q^2 + \beta_q^2) |D_Z(s)|^2 + \\ & \left. \frac{2q_l q_q \alpha_q (\alpha_l - \beta_l) (s - M_Z^2)}{s} |D_Z(s)|^2 \right], \end{aligned} \quad (139)$$

where $D_V(s) = 1/(s - M_V^2 + iM_V\Gamma_V)$, $q_l = -1$, $q_\nu = 0$, $q_u = 2/3$, $q_d = -1/3$, $\alpha_l = \frac{1}{4}(3t - c)$, $\alpha_\nu = \frac{1}{4}(c + t)$, $\alpha_u = -\frac{5}{12}t + \frac{1}{4}c$, $\alpha_d = -\frac{1}{4}c + \frac{1}{12}t$, $\beta_l = \frac{1}{4}(c + t)$, $\beta_\nu = -\frac{1}{4}(c + t)$, $\beta_u = -\frac{1}{4}(c + t)$, $\beta_d = \frac{1}{4}(c + t)$, $c = \cot \theta_W$, $t = \tan \theta_W$. The differential cross section for sneutrino pair production can be obtained by the replacement α_l , β_l , q_l and $m_{\tilde{l}}$ by α_ν , β_ν , 0 and $m_{\tilde{\nu}}$ respectively, whereas for \tilde{l}_R pair production one has substitute $\alpha_l - \beta_l \rightarrow \alpha_l + \beta_l$ and $m_{\tilde{l}_L} \rightarrow m_{\tilde{l}_R}$.

The QCD corrections to the squark and gluino tree level cross sections are essential [103]

4.3 Superparticle decays.

The decay widths of the superparticles depend rather strongly on the relations between superparticle masses. Here we outline the main decay channels only. The formulae for the decay widths are contained in refs.[60]. Consider at first the decays of gluino and squarks. For $m_{\tilde{g}} > m_{\tilde{q}}$ the main decays are the following:

$$\tilde{g} \rightarrow \tilde{q}_i \bar{q}_i, \tilde{\bar{q}}_k q_k, \quad (140)$$

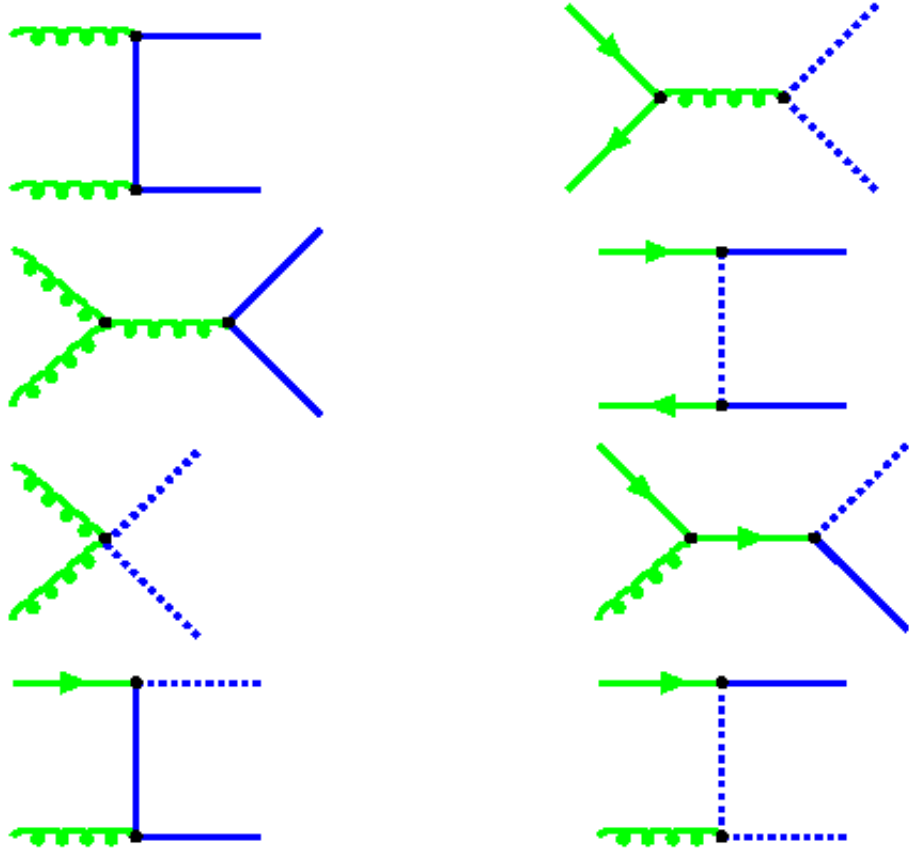


Figure 15: *Squark and gluino production diagrams*

$$\tilde{q}_k \rightarrow \tilde{\chi}_i^0 q_k , \quad (141)$$

$$\tilde{q}_k \rightarrow \tilde{\chi}_j^+ q_m, \tilde{\chi}_j^- q_l , \quad (142)$$

For $m_{\tilde{g}} < m_{\tilde{q}}$ the main decays are:

$$\tilde{q}_i \rightarrow \tilde{g} q_i , \quad (143)$$

$$\tilde{g} \rightarrow q \bar{q}' \tilde{\chi}_k^+ , \quad (144)$$

$$\tilde{g} \rightarrow q' \bar{q} \tilde{\chi}_k^- , \quad (145)$$

$$\tilde{g} \rightarrow q \bar{q} \tilde{\chi}_k^0 . \quad (146)$$

Charginos and neutralinos have a lot of decay modes. Especially interesting for the LHC SUSY discovery are their leptonic modes, for instance:

$$\tilde{\chi}_1^\pm \rightarrow \tilde{\chi}_1^0 l^\pm \nu, \quad (147)$$

$$\tilde{\chi}_1^\pm \rightarrow (\tilde{l}_L^\pm \rightarrow \tilde{\chi}_1^0 l^\pm) \nu, \quad (148)$$

$$\tilde{\chi}_1^\pm \rightarrow (\tilde{\nu} \rightarrow \tilde{\chi}_1^0 \nu) l^\pm, \quad (149)$$

$$\tilde{\chi}_1^\pm \rightarrow \tilde{\chi}_1^0 (W^\pm \rightarrow l^\pm \nu), \quad (150)$$

$$\tilde{\chi}_2^0 \rightarrow \tilde{\chi}_1^0 l^+ l^-, \quad (151)$$

$$\tilde{\chi}_2^0 \rightarrow (\tilde{\chi}_1^\pm \rightarrow \tilde{\chi}_1^0 l^\pm \nu) l^\mp \nu, \quad (152)$$

$$\tilde{\chi}_2^0 \rightarrow (\tilde{l}_{L,R}^\pm \rightarrow \tilde{\chi}_1^0 l^\pm) l^\mp. \quad (153)$$

Two-body decays of neutralinos and charginos into Higgs bosons are:

$$\tilde{\chi}_i^0 \rightarrow \tilde{\chi}_j^0 + h(H), \quad (154)$$

$$\tilde{\chi}_i^0 \rightarrow \tilde{\chi}_k^\pm + H^\mp, \quad (155)$$

$$\tilde{\chi}_i^\pm \rightarrow \tilde{\chi}_k^0 + H^\pm, \quad (156)$$

$$\tilde{\chi}_i^\pm \rightarrow \tilde{\chi}_j^\pm + h(H). \quad (157)$$

The left sleptons dominantly decay via gauge interactions into charginos or neutralinos via two body decays

$$\tilde{l}_L \rightarrow l + \tilde{\chi}_i^0, \quad (158)$$

$$\tilde{l}_L \rightarrow \nu_L + \tilde{\chi}_j^-, \quad (159)$$

$$\tilde{\nu}_L \rightarrow \nu_L + \tilde{\chi}_i^0, \quad (160)$$

$$\tilde{\nu}_L \rightarrow l + \tilde{\chi}_j^+. \quad (161)$$

For relatively light sleptons only the decays into the LSP are possible, so that light sneutrino decays are invisible. Heavier sleptons can decay via the chargino or other (non LSP) channels. These decays are important because they proceed via the larger $SU(2)$ gauge coupling constant and can dominate the direct decay to LSP. The $SU(2)$ singlet

charged sleptons \tilde{l}_R only decay via their $U(1)$ gauge interactions and in the limit of vanishing Yukawa coupling their decays to charginos are forbidden. Therefore the main decay mode of right-handed slepton is

$$\tilde{l}_R \rightarrow l + \tilde{\chi}_i^0. \quad (162)$$

In many cases the mode into LSP dominates.

4.4 Search for sparticles at LHC

Squarks and gluino. The gluino and squark production cross sections at LHC are the biggest ones compared to slepton or gaugino cross sections. Therefore gluinos and squarks production at LHC is the most interesting reaction from the SUSY discovery point of view with the cross sections around $1 pb$ for squark and gluino masses around $1 TeV$. The squark and gluino decays produce missing transverse energy from the LSP plus multiple jets and varying numbers of leptons from the intermediate gauginos [61].

It is natural to divide the signatures used for the squark and gluino detections into the following categories [61]:

- a. multi jets plus E_T^{miss} events,
- b. 1l plus jets plus E_T^{miss} events,
- c. 2l plus jets plus E_T^{miss} events,
- d. 3l plus jets plus E_T^{miss} events,
- e. 4l plus jets plus E_T^{miss} events,
- f. $\geq 5l$ plus jets plus E_T^{miss} events.

Multileptons arise as a result of the cascade decays of neutralinos and charginos into W- and Z-bosons with subsequent decays of W- and Z-bosons into leptonic modes. For instance, the same sign and opposite sign dilepton events arise as a result of the cascade decay

$$\tilde{g} \rightarrow q' \bar{q} \tilde{\chi}_i^\pm, \tilde{\chi}_i^\pm \rightarrow W^\pm \tilde{\chi}_1^0 \rightarrow l^\pm \nu \tilde{\chi}_1^0, \quad (163)$$

where l stands for both e and μ . Opposite sign dilepton events can arise also as a result

of cascade decay

$$\tilde{g} \rightarrow q\bar{q}\tilde{\chi}_i^0, \tilde{\chi}_i^0 \rightarrow Z\tilde{\chi}_1^0 \rightarrow l^+l^-\chi_1^0. \quad (164)$$

The main conclusion [62], [37] is that for the MSUGRA model LHC(CMS) will be able to discover SUSY with squark or gluino masses up to $(2 - 2.5) \text{ TeV}$ for $L_{tot} = 100 \text{ fb}^{-1}$. The most powerful signature for squark and gluino detection in MSUGRA model is the signature with multijets and the E_T^{miss} (signature a). It should be noted that for the case of the MSSM model with arbitrary squark and gaugino masses the LHC SUSY discovery potential depends rather strongly on the relation between the LSP, squark and gluino masses and it decreases with the increase of the LSP mass [63]. For the LSP mass close to the squark or gluino masses it is possible to discover SUSY with the squark or gluino masses up to $(1.2 - 1.5) \text{ TeV}$ [63].

Let us stress that multilepton supersymmetry signatures ($b - f$) arise as a result of decays of squarks or gluino into charginos or neutralinos different from LSP with subsequent decays of charginos or neutralinos into W-, Z-bosons plus LSP. Leptonic decays of W-, Z-bosons is the origin of leptons. However, for the case of nonuniversal gaugino masses it is possible to realize the situation when all charginos and neutralinos except LSP are heavier than gluino and squarks. Therefore, gluino and squarks will decay mainly into quarks or gluons plus LSP, so cascade decays and as a consequence multilepton events will be negligible.

Neutralino and chargino search. Chargino and neutralino pairs, produced through the Drell-Yan mechanism $pp \rightarrow \tilde{\chi}_1^\pm \tilde{\chi}_2^0$ may be detected through their leptonic decays $\tilde{\chi}_1^\pm \tilde{\chi}_2^0 \rightarrow lll + E_T^{miss}$. So, the signature is three isolated leptons with E_T^{miss} . The three-lepton signal is produced through the decays (148-153) and the undetected neutrino and χ_1^0 in decays (148-153) produce E_T^{miss} . The main backgrounds to the three lepton channel arise from WZ/ZZ , $t\bar{t}$, $Zb\bar{b}$ and $b\bar{b}$ production. There could be also SUSY background arising as a result of squark and gluino cascade decays into multileptonic modes.

Typical cuts are the following [62]:

- i. Three isolated leptons with $p_t^l > 15 \text{ GeV}$.

ii. Veto central jets with $E_t > 25$ GeV in $|\eta| < 3.5$.

iii. $m_{l\bar{l}} < 81$ GeV or $m_{l\bar{l}} \neq M_Z \pm \delta M_Z$.

The main conclusion is that neutralino and chargino could be detected provided their masses are lighter than 350 GeV [62]. Moreover, it is possible to determine the $M(\tilde{\chi}_2^0) - M(\tilde{\chi}_1^0)$ mass difference by the measurement of the distribution on l^+l^- invariant mass arising as a result of the decay $\tilde{\chi}_2^0 \rightarrow \tilde{\chi}_1^0 + l^+l^-$ [62].

Sleptons search. Slepton pairs, produced through the Drell-Yan mechanism $pp \rightarrow \gamma^*/Z^* \rightarrow \tilde{l}^+\tilde{l}^-$ can be detected through their leptonic decays $\tilde{l} \rightarrow l + \chi_1^0$. So the typical signature used for sleptons detection is the dilepton pair with missing energy and no hadronic jets [62]. For $L_t = 100 \text{ fb}^{-1}$ LHC(CMS) will be able to discover sleptons with the masses up to 400 GeV [62], [96].

The search for flavour lepton number violation in slepton decays. In supersymmetric models with explicit flavour lepton number violation due to soft supersymmetry breaking terms there could be detectable flavour lepton number violation in slepton decays [94]. For instance, for the case of nonzero mixing $\sin \phi \neq 0$ between right-handed selectrons and smuons we have flavour lepton number violation in slepton decays, namely [94]:

$$\Gamma(\tilde{\mu}_R \rightarrow \mu + LSP) = \Gamma \cos^2 \phi, \quad (165)$$

$$\Gamma(\tilde{\mu}_R \rightarrow e + LSP) = \Gamma \sin^2 \phi, \quad (166)$$

$$\Gamma(\tilde{e}_R \rightarrow e + LSP) = \Gamma \cos^2 \phi, \quad (167)$$

$$\Gamma(\tilde{e}_R \rightarrow \mu + LSP) = \Gamma \sin^2 \phi, \quad (168)$$

$$\Gamma = \frac{g_1^2}{8\pi} \left(1 - \frac{M_{LSP}^2}{M_{SL}^2}\right)^2. \quad (169)$$

The typical consequence of nonzero smuon-selectron mixing is the existence of accoplanar $e^\pm\mu^\mp$ signal events with missing energy arising as a result of the production of slepton pairs with their subsequent decays with flavour lepton number violation. The possibility to detect flavour lepton number violation in slepton decays at LHC has been discussed in

refs. [96]. The main conclusion is that for the most optimistic case of the maximal mixing $\sin \phi = \frac{1}{\sqrt{2}}$ between right-handed sleptons \tilde{e}_R and $\tilde{\mu}_R$ it would be possible to discover slepton mixing at LHC for slepton masses up to 275 GeV [96]. Other possibilities to detect the effects of flavour lepton number violation in slepton decays at LHC have been considered in refs. [97].

The measurement of sparticle masses. After the LHC SUSY discovery the main problem will be to separate many different channels produced by the SUSY cascade decays and to extract the values of SUSY parameters (squark, gluino, neutralino, chargino and slepton masses). In the MSSM model, the decay products of SUSY particles always contain an invisible LSP $\tilde{\chi}_1^0$, so SUSY particles can not be reconstructed directly. The most promising approach to determine sparticle masses is to use kinematical endpoints [64] in different distributions. For example, the l^+l^- distribution from $\tilde{\chi}_2^0 \rightarrow \tilde{\chi}_1^0 l^+ l^-$ decay has an endpoint that determines $M_{\tilde{\chi}_2^0} - M_{\tilde{\chi}_1^0}$. However, the distribution from the two-body decay $\tilde{\chi}_2^0 \rightarrow \tilde{l}^\pm l^\mp \rightarrow \tilde{\chi}_1^0 l^+ l^-$ has a sharp edge at the endpoint $\sqrt{\frac{(M_{\tilde{\chi}_2^0}^2 - M_l^2)(M_l^2 - M_{\tilde{\chi}_1^0}^2)}{M_l^2}}$. When a longer decay chain can be identified, more combinations of masses can be measured [37], [66]. Note also that as proposed in ref.[64] the “hardness” of an event is characterised by the scalar sum of transverse energies of the four hardest jets and the missing transverse energy:

$$E_T^{sum} = E_T^1 + E_T^2 + E_T^3 + E_T^4 + E_T^{miss} \quad (170)$$

The peak value of the E_T^{sum} spectrum for the inclusive SUSY signal provides a good estimate of the SUSY signal in MSUGRA model with the peak value $M_{peak} \equiv M_{SUSY} \approx \min(M_{\tilde{g}}, M_{\tilde{q}})$ [64], [65]. Here $M_{\tilde{q}}$ is the average mass of squarks from the first two generations. By the measurement of E_T^{sum} distribution it is possible to estimate the M_{SUSY} scale with (10-20) percent accuracy.

Gauge mediated supersymmetry breaking. In GMSM (Gauge Mediated Supersymmetry Breaking) models [92] the gravitino \tilde{G} is very light and the phenomenology depends on the type of the next lightest SUSY particle (NLSP), either the $\tilde{\chi}_1^0$ or a slep-

ton, and by its lifetime decay into \tilde{G} . If the NLSP is the $\tilde{\chi}_1^0$ and it decays mainly into $\tilde{\chi}_1^0 \rightarrow \tilde{G}\gamma$, then SUSY signature contains in addition two hard, isolated photons. If the NLSP is charged slepton and it is long-lived, then it penetrates the calorimeter like a muon but with $\beta < 1$. The slepton mass in this case can be measured directly using the muon chambers as a time-of-flight system [37], [35].

4.5 SUSY Higgs bosons search

The MSSM has three neutral and one charged Higgs bosons: h , H , A and H^\pm ⁴. As it has been mentioned before at tree level the lightest Higgs boson mass is predicted to be lighter than m_Z . However an account of radiative corrections [21] can increase the Higgs boson mass up to 135 GeV for stop masses less or equal to 1 TeV [22]. In MSUGRA the Higgs sector is described mainly by two parameters: the mass of A boson and $\tan(\beta)$ - the ratio of the vacuum expectation values of the Higgs fields that couple to up-type and down-type quarks. In the limit of large A boson mass, the couplings of h boson coincide with the corresponding couplings of the SM Higgs boson.

At high $\tan \beta$ the H , A decay mainly into $b\bar{b}$. However this mode is not very useful due to huge $b\bar{b}$ background. The decays of H and A to $\tau^+\tau^-$ and $\mu^+\mu^-$ are the most important for the A and H bosons detection [37], [68]. In the MSSM, the $H \rightarrow \tau^+\tau^-$ and $A \rightarrow \tau^+\tau^-$ rates are enhanced over the SM for large $\tan(\beta)$. The production of the heavy neutral MSSM Higgs bosons is mainly through $gg \rightarrow H_{SUSY}$ and $gg \rightarrow b\bar{b}H_{SUSY}$. The Higgs boson coupling to b -quarks is enhanced at high $\tan \beta$ and the associated $gg \rightarrow b\bar{b}H_{SUSY}$ production dominates ($\sim 90\%$ of the total rate) for $\tan \beta \geq 10$ and $M_H \geq 300\,GeV$. The gluon fusion cross section is determined by quark loops and can be significantly reduced in the case of large stop mixing and light stop mass [69]. Due to the dominance of the $gg \rightarrow b\bar{b}H_{SUSY}$ production mechanism at high $\tan \beta$ production rates for the heavy Higgs bosons H and A are not sensitive to the loop effects.

⁴LEP2 experiments give lower bounds 91.0 GeV and 91.9 GeV for light h and pseudoscalar A -bosons. Besides, the excluded $\tan \beta$ regions are $0.5 \leq \tan \beta \leq 2.4$ for the maximal mixing scenario and $0.7 \leq \tan \beta \leq 10.5$ for the no mixing scenario [17].

Light Higgs boson. For SUSY masses bigger than $O(300)$ Gev the decay widths and the production rates for the lightest Higgs boson h are approximately the same as for the SM Higgs boson (decoupling regime) and the most promising signature here is $h \rightarrow \gamma\gamma$. Also the signatures $pp \rightarrow t\bar{t}(h \rightarrow b\bar{b})$ and $pp \rightarrow qq$ ($h \rightarrow WW^* \rightarrow l^+l^-\nu\bar{\nu}$) are important. Note that in the case of large stop mixing and for light stop $m_{\tilde{t}_1} \leq 200$ GeV the rate $gg \rightarrow h \rightarrow \gamma\gamma$ could be significantly reduced due to the stop and top loops destructive interferences in $gg \rightarrow h$ which could lead to no discovery for this signature. For the most difficult region $m_h \sim m_A \sim m_H \sim 100$ GeV and high $\tan\beta$ the use of $gg \rightarrow b\bar{b}h \rightarrow b\bar{b}\mu^+\mu^-$ helps to detect the Higgs boson [33], [68], [72].

Heavy neutral bosons A and H . The $\tau\bar{\tau}$ final states can be searched for in a 2 lepton, lepton+ τ jet, 2 τ jet final states [33], [37]. For the one lepton plus one hadron final states, intermediate backgrounds are due to $Z, \gamma^* \rightarrow \tau\bar{\tau}; t\bar{t} \rightarrow \tau\bar{\tau} + X, \tau + X$ and $b\bar{b} \rightarrow \tau\bar{\tau} + X, \tau X$. Efficient τ -jet identification has been developed based on low energy multiplicity, narrowness and isolation of the τ -jet in $H, A \rightarrow \tau\tau$. This identification has been shown to provide a rejection factor ≥ 1000 per QCD jet. The Higgs boson can be reconstructed in the $H \rightarrow \tau\tau$ channel from the visible τ momenta (leptons or τ -jets) and E_t^{miss} using the collinearity approximation for the neutrinos from τ decays. Precision of the Higgs boson mass measurement is estimated to be $\leq 10\%$ for $A, H \rightarrow \tau\tau$ at high $\tan\beta$. The A, H bosons can be discovered using these $\tau\tau$ modes with the masses up to $(600 - 800)$ GeV [33], [68], [37] (see Fig.23).

In the MSSM the branching ratio for $A, H \rightarrow \mu\mu$ is small, $\sim 3 \cdot 10^{-4}$, however the associated $gg \rightarrow b\bar{b}H(A)$ production is enhanced at large $\tan\beta$. The Drell-Yan production $\gamma^*, Z^* \rightarrow \mu^+\mu^-$ is the dominant background and it is suppressed with b -tagging [33]. Precision of the Higgs boson mass measurement is estimated to be $0.1 - 1.5\%$ for this mode.

So the heavy H, A bosons are expected to be found at high $\tan\beta$ using $\tau\tau$ and $\mu\mu$ decay modes. LHC discovery range is $\tan\beta \geq 10$ for $m_A \leq 200$ GeV [33]. For $\tan\beta \leq 10$ the H, A decays to sparticles may be used. The channel $A, H \rightarrow \tilde{\chi}_2^0 \tilde{\chi}_2^0 \rightarrow 4l^\pm + X$ has been

found [71] to be the most promising one for heavy neutral Higgs bosons discovery, provided neutralinos and sleptons are light enough so that the $\tilde{\chi}_2^0 \rightarrow \tilde{l}l \rightarrow \tilde{\chi}_1^0 l^+ l^-$ branching ratio is significant. Using this channel it is possible to discover H, A bosons with the masses $(200 - 400) \text{ GeV}$ [68], [37].

Charged Higgs boson. Search for the charged Higgs boson at LHC is important for the understanding of the nature of the Higgs sector. Really, discovery of a charged Higgs boson at LHC would be a clear proof for physics beyond SM. For $m_{H^\pm} < m_{top}$ H^\pm decays mainly into $\tau\nu$. For $m_{H^\pm} > 200 \text{ GeV}$ the $H^\pm \rightarrow tb$ decay dominates but the $BR(H^\pm \rightarrow \nu\tau)$ approaches 0.1 for $m_{H^\pm} \geq 400 \text{ GeV}$. For light charged Higgs boson, $m_{H^\pm} < m_{top}$, the main H^\pm production mechanism is through the $t\bar{t}$ events followed by $t \rightarrow H^\pm b$. The use of the $H^\pm \rightarrow \tau\nu$ decay mode allows to discover H^\pm almost independently of $\tan\beta$ for light charged Higgs boson [68] [37]. The heavy charged Higgs boson, $m_{H^\pm} > m_{top}$, is mainly produced in association with the top quark through the processes $gb \rightarrow tH^\pm$ and $gg \rightarrow tbH^\pm$. Again in this case the decay mode $H^\pm \rightarrow \nu\tau$ is the most perspective for H^\pm detection. The use of the τ polarisation from $H^\pm \rightarrow \nu\tau$ decay [70] allows to suppress the backgrounds from $t\bar{t}, Wtb, W \rightarrow \tau\nu$ since due to spin correlations, the single pion from a one-prong τ decay is harder when it originates from an H^\pm than from a W . In purely hadronic final states in $gb \rightarrow t(H^\pm \rightarrow \nu\tau)$ with hadronic top quark decay the transverse mass reconstructed from the τ jet and the E_T^{miss} vector has a Jacobian peak structure with an endpoints at m_W for the backgrounds.. This allows to extract the H^\pm mass with the accuracy better than 10%. The discovery reach for this signature is shown in Fig.23.

The $H^\pm \rightarrow tb$ decay for the $gb \rightarrow tH^\pm$ production reaction has been studied requiring one isolated lepton from the decay of one of the top quarks [68], [37]. To extract the Higgs signature in these multijet events requires tagging of three b -jets, reconstruction of the leptonic and hadronic top quark decays and the Higgs boson mass reconstruction. The discovery reach for this signature is shown in Fig.23. Note also that the s-channel production of H^\pm in $q\bar{q}' \rightarrow H^\pm \rightarrow \tau\nu$ can be used for the H^\pm detection [73] but the reduction of huge $q\bar{q}' \rightarrow W \rightarrow \tau\nu$ background is rather difficult. A precision of $\sim (1-2)\%$

is expected for the charge Higgs boson mass measurement [33]. Moreover due to the $\sigma \sim \tan^2 \beta$ behaviour of the cross section it is possible to determine $\tan \beta$ with a precision better than 7% for $\tan \beta > 20$ and $m_{H^\pm} = 250 \text{ GeV}$ [33].

The main conclusion [33], [68], [37] concerning the situation with the search for MSSM Higgs bosons at LHC for different $(m_A, \tan(\beta))$ values is that almost the full $(m_A, \tan(\beta))$ -values can be explored with the $h \rightarrow \gamma\gamma$ $h \rightarrow b\bar{b}$ decay modes for total luminosity $L_t = 30 \text{ fb}^{-1}$. The heavy H, A bosons will be discovered for $\tan \beta \geq 10$ using the $H, A \rightarrow \tau\tau, \mu\mu$ decay modes with the A, H boson masses up to 800 GeV . For the search of the charged Higgs boson H^\pm , the $gb \rightarrow tH^\pm, H^\pm \rightarrow \tau\nu$ channel is the most important one with a discovery reach for $\tan \beta \geq 20$ up to $m_{H^\pm} \approx 400 \text{ GeV}$. The most difficult region with $110 \text{ GeV} \leq m_A \leq 200 \text{ GeV}$, $3 \leq \tan(\beta) \leq 10$ could be explored with the SUSY particle decay modes provided the neutralinos and sleptons are light enough.

5 Search for new physics beyond the SM and the MSSM

There are a lot of models different from the SM and the MSSM. Here we briefly describe some of them.

5.1 Extra dimensions

There is much theoretical interest in models that have extra space dimensions [75], [76], [77], [78], [79], [80], [81]. The main motivation is that models with big $R_c \geq O(1) \text{ TeV}^{-1}$ extra space dimensions can explain the hierarchy between the electroweak and Planck scale. In such models new physics can appear at a 1 TeV scale and therefore can be tested at the LHC.

In the ADD model [75] the metric looks like

$$ds^2 = g_{\mu\nu}(x)dx^\mu dx^\nu + \eta_{ab}(x, y)dy^a dy^b, \quad (171)$$

where $\nu, \nu = 0, 1, 2, 3$ and $a, b = 1, \dots, d$. All d additional dimensions are compactified with

a characteristic size R_c . The relation between a fundamental mass scale in $D = 4 + d$ dimensions, M_D , and 4-dimensional Planck scale M_{PL} has the form

$$M_{PL}^2 = V_d M_D^{2+d}, \quad (172)$$

where V_d is a volume of the compactified dimensions ($V_d = (2\pi R_c)^d$ for toroidal form of extra dimensions). In the ADD model there are 2 free parameters, the number d of additional dimensions and the fundamental scale M_D . From the requirement that $M_D \sim 1 \text{ TeV}$ one can find that the compactification radius R_c^{-1} ranges from 10^{-3} eV to 10 MeV if d runs from 2 to 6. In the ADD model all SM gauge and matter fields are to be confined to a 3-dimensional brane embedded into a $(3 + d)$ -dimensional space and only gravity lives in the bulk. It means that the energy-momentum tensor of matter has the form

$$T_{AB}(x, y) = \eta_A^\mu \eta_B^\nu T_{\mu\nu}(x) \delta(y), \quad (173)$$

with $A, B = 0, 1 \dots 3 + d$. The graviton interaction Lagrangian is

$$L_g = -\frac{1}{M_{PL}} G_{\mu\nu}^{(n)} T_{\mu\nu}, \quad (174)$$

where n labels the KK (Kaluza - Klein) excitation level and $\bar{M}_{PL} = M_{PL}/\sqrt{8\pi} = 2.4 \cdot 10^{18} \text{ GeV}$. From the Lagrangian (174) we see that the couplings of graviton excitations are universal and very small. The masses of the KK graviton excitations are

$$m_n = \frac{\sqrt{(n_a n^a)}}{R_c}, \quad (175)$$

where $n_a = (n_1, n_2 \dots n_d)$. A mass splitting $\Delta m \sim R_c^{-1}$ is extremely small and we have an almost continuous spectrum of the gravitons. The production cross section of the KK gravitons with masses $m_n \leq E$ is

$$\sigma_{KK} \sim \frac{E^d}{M_D^{d+2}}. \quad (176)$$

The lifetime of the massive graviton is [75]

$$\tau_n \sim \frac{1}{M_{PL}} \left(\frac{M_{PL}}{m_n} \right)^3. \quad (177)$$

Thus the KK gravitons behave like massive, almost stable non-interacting spin-2 particles. Their collider signature is an imbalance in missing mass of final states with a continuous mass distribution. The most promising signature of the graviton production at the LHC originates from the reaction $pp \rightarrow jet + E_T^{miss}$. Note that at parton level the subprocess $gq \rightarrow qG^{(n)}$ gives the largest contribution. The main background arises from the $Z + jet$, $Z \rightarrow \nu\bar{\nu}$ production. The use of this reaction allows to discover extra space dimensions at the LHC(ATLAS) with the inverse radius less than 9 TeV [37]. Very interesting signature for the direct production of the massive gravitons is the process $pp \rightarrow \gamma + E_T^{miss}$ which can be used as an independent test, although it has the much lower rate. The SM background comes mainly from $pp \rightarrow \gamma(Z \rightarrow \nu\bar{\nu})$. Another prediction of the ADD model is that the contribution of virtual massive graviton resonances to the matrix elements modifies the SM cross sections at large momentum transfer (for instance the Drell-Yan cross section). At tree level the contribution of virtual massive gravitons to a matrix element is proportional to

$$M \sim \frac{1}{\bar{M}_{PL}^2} \sum_n \frac{1}{s - m_n^2} \quad (178)$$

The sum in (178) diverges for $d \geq 2$, the cutoff M_c is to be calculated in full theory. The following very rough substitution $M \sim \frac{1}{M_c^4}$ is usually made to estimate lower bound on M_c which will be extracted from the LHC data. It appears that the diphoton and Drell-Yan productions at the LHC lead to sensitivity of M_c up to 7.4 TeV .

In RS (Randall-Sundrum) model [76] gravity lives in a 5-dimensional Anti-de Sitter space with a single extra dimension compactified to the orbifold S^1/Z_2 . The metric has the form

$$ds^2 = e^{-2k|y|} \eta_{\mu\nu} dx^\mu dx^\nu + dy^2, \quad (179)$$

where $y = r_c \theta$ ($0 \leq \theta \leq \pi$), r_c being a "radius" of the extra dimension. The parameter k defines the scalar curvature of the space. From the 5-dimensional action one can derive the relation

$$\bar{M}_{PL}^2 = \frac{M_5^3}{k} (1 - e^{-2kr_c\pi}), \quad (180)$$

which means that $k \sim \bar{M}_5 \sim \bar{M}_{PL}$. There are two 3-dimensional branes in the model with equal and opposite tension localised at the point $y = \pi r_c$ (so called the TeV brane) and at $y = 0$ (referred to as the Planck brane). All the SM fields are constrained to the TeV brane, while gravity propagates in the additional dimension. Using a linear expansion of the metric

$$g_{\mu\nu} = e^{-2ky}(\eta_{\mu\nu} + \frac{2}{M_5^{3/2}}h_{\mu\nu}) \quad (181)$$

one can obtain the interaction of the gravitons with the SM fields

$$L = -\frac{1}{\bar{M}_{PL}}T^{\mu\nu}h_{\mu\nu}^{(0)}(x) - \frac{1}{\Lambda_\pi}\sum_n T^{\mu\nu}h_{\mu\nu}^{(n)}(x), \quad (182)$$

where $\Lambda_\pi \sim \bar{M}_{PL}e^{-kr_c\pi}$. The couplings of massive states are suppressed by Λ_π^{-1} , while the zero mode couples with usual strength, \bar{M}_{PL}^{-1} . The physical scale on the *TeV* brane, Λ_π , is of the order of 1 *TeV* for $kr_c \sim 12$. The masses of the graviton KK excitations are given by

$$m_n = kx_n e^{-kr_c\pi}, \quad (183)$$

where x_n are the roots of the Bessel function $J_1(x)$. In RS model [76] the first graviton excitation has a mass $O(1)$ *TeV* and it decays into jets, leptons or photons. The most promising mode for the graviton resonance detection at the LHC is the use of the lepton decay modes. The signature $q\bar{q}, gg \rightarrow G_{res1} \rightarrow l^+l^-$ has been studied in refs.[86]. The signal is visible for $M_{G,res1} \leq 2$ *TeV*. Moreover, for $M_{G,res1} \leq 1.5$ *TeV* from the measurement of lepton angular distribution it is possible to confirm that the resonance is spin-2 particle.

Other nontrivial prediction of the RS model is the existence of relatively light scalar particle called radion and denoted as Φ . Radion is characterised by its mass m_Φ , some scale Λ_Φ and mixing parameter ζ with Higgs boson. The interactions of the radion with the SM particles are given by

$$L_{int} = \frac{\Phi}{\Lambda_\Phi}T_\mu^\mu(SM), \quad (184)$$

where $\Lambda_\Phi = <\Phi> \sim O(1)$ *TeV* and

$$T_\mu^\mu(SM) = \sum_f m_f \bar{f}f - 2m_W^2 W_\mu^+ W^\mu - m_Z^2 Z_\mu Z^\mu + m_H^2 H^2 + \dots \quad (185)$$

The radion interactions are very similar to those of the SM Higgs boson. Note that the radion has anomalous couplings from the trace anomaly to a pair of gluons(photons), in addition to the loop diagrams with the top-quark

$$T_\mu^\mu(SM)^{anom} = \sum_a \frac{\beta_a(g_a)}{2g_a} F_{\mu\nu}^a F^{a\mu\nu}, \quad (186)$$

where $\beta_{QCD}/2g_s = -\frac{\alpha_s}{8\pi}(11 - 2n_f/3)$ and $\beta_{QED}/2e = -\frac{11}{3}(\alpha/8\pi)$. Because of the anomalous coupling of the radion to gluons, the gluon fusion will be the most important production channel for the radion in hadronic collisions. In general the Higgs boson and radion should mix due to nonzero mixing term

$$S_\xi = \xi \int d^4x \sqrt{g_{vis}} R(g_{vis}) H^+ H, \quad (187)$$

where $R(g_{vis})$ is the Ricci tensor for the induced metric on the visible brane.

At the LHC the radion production subprocesses are $gg \rightarrow \Phi$ (the dominant channel), $qq' \rightarrow W\Phi, q\bar{q} \rightarrow Z\Phi, qq' \rightarrow qq'\Phi$ and $q\bar{q} \rightarrow t\bar{t}\Phi$. The most interesting radion decay modes which could be used for its discovery are: $\Phi \rightarrow \gamma\gamma, ZZ, hh$. For heavy radion ($m_\Phi \geq 2M_Z$) the cleanest signature is

$$gg \rightarrow \Phi \rightarrow ZZ \rightarrow 4l. \quad (188)$$

The radion LHC discovery limit depends on its mass and lies between $\Lambda_\Phi = 1 \text{ TeV}$ and $\Lambda_\Phi = 10 \text{ TeV}$ [37].

In the ADD and RS models all of the SM particles are confined to a brane while gravitons are free to move in the extra dimensions. However, there are no deep reasons why the SM particles have to be confined on a brane. In ref. [85] the scenario where all particles are free to move to all dimensions has been considered (braneless scenario)⁵. For the simplest case of one extra dimension the momentum conservation in the fifth dimension leads after the compactification to the conservation of the KK numbers. Because of the KK number conservation KK states are pair produced at the LHC in close analogy with the case of supersymmetry with R -parity conservation. Therefore the LHC phenomenology

⁵Similar model has been proposed in refs.[77],[82]

is determined by the pair production of KK quarks and KK gluons [77], [85]

$$qq' \rightarrow q^{(1)}q'^{(1)}, \quad (189)$$

$$q\bar{q} \rightarrow q^{(1)}\bar{q}^{(1)}, \quad (190)$$

$$gg \rightarrow g^{(1)}g^{(1)}, \quad (191)$$

$$gg, q\bar{q} \rightarrow q^{(1)}\bar{q}^{(1)}. \quad (192)$$

Each KK quark $q^{(1)}$ decays into jet and KK photon $\gamma^{(1)}$. Therefore the LHC signature will be jets with missing energy as in the case of supersymmetry. Also very interesting decay chain is $q^{(1)}$ decays into $W^{(1)}$ and $Z^{(1)}$ with the subsequent decays of $W^{(1)}, Z^{(1)}$ into leptons leading to the signature with isolated leptons, jets and missing energy again in close analogy with the supersymmetry case. The LHC will be able to discover KK quarks and gluons with the masses up to 1.5 TeV [85].

Note that there are mixed scenarios where some SM particles live on a brane while others can propagate in additional dimensions. For instance, in 5DSM-model [83] the 5-th dimension y is compactified on the orbifold S^1/Z_2 which has two fixed points at $y = 0$ and $y = \pi R_c$. The SM gauge fields propagate in the $5D$ bulk, while the chiral matter is localised on the $4D$ boundaries [83]. In this model the first excitation of the gauge bosons can be directly produced in Drell-Yan processes mediated by the first KK modes of the gauge bosons, $pp \rightarrow Z^{(1)} \rightarrow l^+l^-$. The LHC will be able to discover the KK gauge bosons with the masses up to 6 TeV [84].

In the ADD scenario the Planck scale at which the gravity becomes strong is $M_D \sim 1 \text{ TeV}$ for $d = 10$. In this scenario a production of black holes should be possible at $\sqrt{s} \gg 1 \text{ TeV}$. Black hole intermediate states are expected to dominate s -channel scattering since in the string theory the number of such states grows with black hole mass faster than the number of perturbative states [87]. The Schwartzchild radius of a $(4 + d)$ -dimensional black hole with the mass M_{BH} for spin $J = 0$ has the form [88]

$$R_S(M_{BH}) = \frac{1}{M_D} \left(\frac{M_{BH}}{M_D} \right)^{1/(1+d)} \quad (193)$$

The black hole production cross section of two partons a and b is taken in a simple geometrical form [87]

$$\sigma_{ab \rightarrow BH}(s) \approx \pi R_S^2(s) \quad (194)$$

The cross section (194) has no small coupling constant and it rises rapidly with an energy. With TeV scale gravity the production of the black holes should be dominant process at the LHC. The experimental consequences of the black hole decays in ADD model are very distinctive [81]:

- a. flavor-blind(thermal) decays,
- b. hard prompt charged leptons and photons (with energy $E \geq 100 \text{ GeV}$),
- c. the ratio of hadronic to leptonic activity is close to 5 : 1,
- d. complete cut-off of hadronic jets with $p_T > R_S^{-1}$,
- e. small missing energy.

These signatures have almost vanishing background. The LHC black hole discovery potential is maximal one in $e/\mu + X$ channel and the scales up to $M_D \leq 9 \text{ TeV}$ can be reached [89]. Note that the described scenario could be too crude and too optimistic (see refs. [90]). To our mind the situation with the possibility of black hole detection at the LHC is not very clear and a lot of further work is required.

5.2 Extra gauge bosons

Many string inspired supersymmetric electroweak models and grand unified models based on extended gauge groups ($SO(10), E_6, \dots$) predict the existence of new relatively light neutral Z' -bosons and charged W' -bosons [98]. The LHC Z' -boson discovery potential depends on the couplings of Z' -boson with quarks and leptons. The Lagrangian describing a single Z' and its interactions with the SM fields has the form [98]

$$L_{Z'} = -\frac{1}{4}F'_{\mu\nu}F'^{\mu\nu} - \frac{\sin\chi}{2}F'_{\mu\nu}F^{\mu\nu} + \frac{1}{2}M_{Z'}^2Z'_\mu Z'^\mu + \delta M^2 Z'_\mu Z^\mu - \frac{e}{2c_W s_W} \sum_i \bar{\psi}_i \gamma^\mu (f_V^i - g_A^i \gamma_5) \psi_i Z'_\mu, \quad (195)$$

where $c_W = \cos\theta_W$, $s_W = \sin\theta_W$, $F_{\mu\nu}$, $F'_{\mu\nu}$ are the field strength tensors for the hypercharge and the Z' boson respectively, ψ_i are the matter fields with the Z' vector and axial

charges f_V^i and f_A^i and Z_μ is the electroweak Z -boson. The mixing angle between Z - and Z' -bosons is

$$\xi \approx \frac{\delta M^2}{M_Z^2 - M_{Z'}^2} \quad (196)$$

If the Z' charges are generation-dependent, tree-level flavor-changing neutral currents will generally arise. There exist severe constraints in the first two generations coming from precision measurements such as the $K_L - K_S$ mass splitting and $Br(\mu \rightarrow 3e)$. If the Z' interactions commute with the SM gauge group, then per generation, there are 5 independent $Z' \bar{\psi} \psi$ couplings ; one can choose them in the form $f_V^u, f_A^u, f_V^d, f_V^e, f_A^e$.

Two Z' models are usually considered. In the first model an effective $SU_L(2) \otimes U_Y(1) \otimes U_{Y'}(1)$ gauge group originates from the breaking of the exceptional E_6 gauge group

$$E_6 \rightarrow SO(10) \otimes U(1)_\psi \rightarrow SU(5) \otimes U_\chi(1) \otimes U_\psi(1) \rightarrow SU_c(3) \otimes SU_L(2) \otimes U_Y(1) \otimes U_{Y'}(1)$$

The lightest new Z' -boson is defined as

$$Z' = Z_\chi \cos\beta + Z_\psi \sin\beta, \quad (197)$$

where β is the mixing parameter. In the second model new Z' boson arises in $SU_L(2) \otimes SU_R(2) \otimes U_{B-L}(1)$ left-right symmetric models. The Z' boson in such model couples to a linear combination of the right-handed and $B - L$ currents. Sometimes as a test example the non-realistic case of Z' boson with the same fermion couplings as the SM Z boson is considered.

The Z' decay width into a massless fermion-antifermion pair reads

$$\Gamma_{Z'}^f = N_c \frac{\alpha M_{Z'}}{12 c_W^2} [(f_V^i)^2 + (g_A^i)^2], \quad (198)$$

where N_c is the colour factor and α is the effective electromagnetic coupling constant to be evaluated at the scale $M_{Z'}$ leading to $\alpha \sim 1/128$. Typically in the considered models Z' boson is rather narrow [98] with the total decay width $\Gamma_t(Z') \sim O(10^{-2})M_{Z'}$ and with $Br(Z' \rightarrow e^+ e^-) \sim 0.05$.

The main mechanism for the production of such new neutral vector bosons is the quark-antiquark fusion. The cross section is given by the standard formula

$$\sigma(pp \rightarrow Z' + \dots) = \sum_i \frac{12\pi^2 \Gamma(Z' \rightarrow \bar{q}_i q_i)}{9s M_{Z'}} \int_{M_{Z'}^2/s}^1 \frac{dx}{x} \quad (199)$$

$$[\bar{q}_{pi}(x, \mu)q_{pi}(x^{-1}M_{Z'}^2s^{-1}, \mu) + q_{pi}(x, \mu)\bar{q}_{pi}(x^{-1}M_{Z'}^2s^{-1}, \mu)]$$

Here $\bar{q}_{pi}(x, \mu)$ and $q_{pi}(x, \mu)$ are the parton distributions of the antiquark \bar{q}_i and quark q_i in the proton at the normalisation point $\mu \sim M_{Z'}$ and $\Gamma(Z' \rightarrow \bar{q}_i q_i)$ is the hadronic decay width of the Z' boson into quark-antiquark pair with a flavour i .

The best way to detect Z' -bosons is to use the $Z' \rightarrow e^+e^-, \mu^+\mu^-, jet\ jet$ decay modes. The study of the angular distribution of lepton pairs allows to obtain nontrivial information on Z' -boson coupling constants with quarks and leptons and confirm that Z' -boson is spin-1 particle. For considered Z' -boson models new Z' bosons can be observed in the reaction $pp \rightarrow Z' \rightarrow l^+l^-$, up to masses about $5\ TeV$ for an integrated luminosity of $100\ fb^{-1}$ [8], [37], [99]. The measurements of the forward-backward lepton charge asymmetry, both on Z' peak and in the interference region plus the measurement of the Z' rapidity distribution allow to discriminate between different Z' models for Z' masses up to $2 - 2.5\ TeV$ for total luminosity $L_t = 100\ fb^{-1}$ [99].

The most attractive candidate for W' is the W_R gauge boson associated with the left-right symmetric models [100]. These models provide a spontaneous origin for parity violation in weak interactions. The gauge group of left-right symmetric model is $SU_c(3) \otimes SU_L(2) \otimes SU_R(2) \otimes U(1)_{B-L}$ with the SM hypercharge identified as $Y = T_{3R} + \frac{1}{2}(B - L)$, T_{3R} being the third component of $SU_R(2)$. The fermions transform under the gauge group as $q_L(3, 2, 1, 1/3) + q_R(3, 1, 2, 1/3)$ for quarks and $l_L(1, 2, 1, -1) + l_R(1, 1, 2, -1)$ for leptons. The model requires the introduction of right-handed neutrino ν_R which is the essential ingredient for the see-saw mechanism for explaining the smallness of the ordinary neutrino masses. A Higgs bidoublet $\Phi(1, 2, 3, 0)$ is usually introduced to generate fermion masses.

The main production mechanism for the W' -boson is the quark-antiquark fusion similar to the case of Z' -boson production. If right-handed neutrino ν_R is heavier than W_R the decay mode $W_R \rightarrow \nu_R + l$ is forbidden kinematically and the dominant decay of W_R will be into dijets. If ν_R is lighter than W_R the decay $W_R \rightarrow l_R \nu_R$ is allowed. The decay of $\nu_R \rightarrow e_R q \bar{q}'$ leads to the $e\ e\ jet\ jet$ signature. The use of the signature $pp \rightarrow W_R \rightarrow e\nu_R \rightarrow ee q\bar{q}$ allows to discover W_R boson up to masses of $4.6\ TeV$ for

$L_t = 30 \text{ fb}^{-1}$ and $m_{\nu_R} \leq 2.8 \text{ TeV}$ [37].

For the W' boson with coupling constants to the SM fermions equal to the ordinary W -boson coupling constants the best way to look for W' -boson is through its leptonic decay mode $W' \rightarrow l\nu$. For such model it would be possible to discover the W' -boson through its leptonic mode with a mass up to 6 TeV [37], [8]. By the measurement of the W' -boson transverse mass distribution it is possible to determine its mass with the accuracy $(50 - 100) \text{ GeV}$ [37].

5.3 Heavy neutrino

Left-right symmetric models [100] based on $SU_c(3) \otimes SU_L(2) \otimes SU_R(2) \otimes U(1)$ gauge group predict the existence of heavy Majorana neutrinos $\nu_{R,e,\mu,\tau}$. For $m_{\nu_R} < M_{W_R}$ it is possible to look for heavy Majorana neutrinos in heavy right-handed W_R -boson decay using the signature

$$pp \rightarrow W_R + \dots \rightarrow l(\nu_{R,l} \rightarrow ljj) + \dots$$

Due to Majorana nature of neutrino half of events will be with the same sign leptons plus ≥ 2 jets from $\nu_{R,l} \rightarrow ljj$ decay that makes the signature with the same sign leptons the most promising one for both the ATLAS [37] and CMS [74]. For $L_t = 30 \text{ fb}^{-1}$ it is possible to detect heavy neutrino with a mass up to 2.8 TeV .

5.4 Sgoldstinos

It is well known, that exist models of supergravity breaking with relatively light sgoldstinos (scalar S and pseudoscalar P particles — superpartners of goldstino ψ). Such pattern emerges in a number of non-minimal supergravity models [106] and also in gauge mediation models if supersymmetry is broken via non-trivial superpotential (see, Ref. [107] and references therein). To the leading order in $1/F$, where F is the parameter of supersymmetry breaking, and to zero order in MSSM gauge and Yukawa coupling constants, the interactions between the component fields of goldstino supermultiplet and MSSM fields have been derived in Ref. [108]. They correspond to the most attractive for collider studies

processes where only one of these *new* particles appears in a final state. In this case light gravitino behaves exactly as goldstino. For sgoldstinos, as they are R-even, only sgoldstino couplings to goldstino and sgoldstino couplings to SM fields have been included as the most interesting phenomenologically.

All relevant sgoldstino coupling constants presented in Ref. [108] are completely determined by the MSSM soft terms and the parameter of supersymmetry breaking F , but sgoldstino masses (m_S, m_P) remain free. If sgoldstino masses are of the order of electroweak scale and $\sqrt{F} \sim 1$ TeV — sgoldstino may be detected in collisions of high energy particles at supercolliders [109, 110].

There are flavor-conserving and flavor-violating interactions of sgoldstino fields. As concerns flavor-conserving interactions, the strongest bounds arise from astrophysics and cosmology, that is $\sqrt{F} \geq 10^6$ GeV [111, 112], or $m_{3/2} > 600$ eV, for models with $m_{S(P)} < 10$ keV and MSSM soft flavor-conserving terms being of the order of electroweak scale. For the intermediate sgoldstino masses (up to a few MeV) constraints from the study of SN explosions and reactor experiments lead to $\sqrt{F} \geq 300$ TeV [112]. For heavier sgoldstinos, low energy processes (such as rare decays of mesons) provide limits at the level of $\sqrt{F} \geq 500$ GeV [112].

The collider experiments exhibit the same level of sensitivity to light sgoldstinos as rare meson decays. Indeed the studies [113, 114, 115, 116] of the light sgoldstino ($m_{S,P} \leq a \text{ few MeV}$) phenomenology based on the effective low-energy Lagrangian derived from N=1 linear supergravity yield the bounds: $\sqrt{F} \geq 500$ GeV (combined bound on $Z \rightarrow S\bar{f}f, P\bar{f}f$ [115]; combined bound on $e^+e^- \rightarrow \gamma S, \gamma P$ [114]) at $M_{soft} \sim 100$ GeV, $\sqrt{F} \geq 1$ TeV [116] (combined bound on $p\bar{p} \rightarrow gS, gP$) at gluino mass $M_3 \sim 500$ GeV. Searches for heavier sgoldstinos at colliders, though exploiting another technique, results in similar bounds on the scale of supersymmetry breaking. Most powerful among the operating machines, LEP and Tevatron, give a constraint of the order of 1 TeV on supersymmetry breaking scale in models with light sgoldstinos. Indeed, the analysis carried out by DELPHI Collaboration [117] yields the limit $\sqrt{F} > 500 \div 200$ GeV at sgoldstino masses $m_{S,P} = 10 \div 150$ GeV and $M_{soft} \sim 100$ GeV. The constraint depends on the MSSM soft

breaking parameters. In particular, it is stronger by about a hundred GeV in the model with degenerate gauginos. At Tevatron, a few events in $p\bar{p} \rightarrow S\gamma(Z)$ channel, and about 10^4 events in $p\bar{p} \rightarrow S$ channel would be produced at $\sqrt{F} = 1$ TeV and $M_{soft} \sim 100$ GeV for integrated luminosity $\mathcal{L} = 100$ pb $^{-1}$ and sgoldstino mass of the order of 100 GeV [110]. This gives rise to a possibility to detect sgoldstino, if it decays inside the detector into photons and \sqrt{F} is not larger than $1.5 \div 2$ TeV.

In terms of $SU(3)_c \times SU(2)_L \times U(1)_Y$ fields the sgoldstino effective Lagrangian reads [108]:

$$L_S = - \sum_{\substack{\text{all gauge} \\ \text{fields}}} \frac{M_\alpha}{2\sqrt{2}F} S \cdot F_a^\alpha{}_{\mu\nu} F_a^{\alpha\mu\nu} - \frac{\mathcal{A}_{ab}^L}{\sqrt{2}F} y_{ab}^L \cdot S \\ (\epsilon_{ij} l_a^j e_b^c h_D^i + h.c.) - \frac{\mathcal{A}_{ab}^D}{\sqrt{2}F} y_{ab}^D \cdot S (\epsilon_{ij} q_a^j d_b^c h_D^i + h.c.) \\ - \frac{\mathcal{A}_{ab}^U}{\sqrt{2}F} y_{ab}^U \cdot S (\epsilon_{ij} q_a^j u_b^c h_U^i + h.c.) , \quad (200)$$

$$L_P = \sum_{\substack{\text{all gauge} \\ \text{fields}}} \frac{M_\alpha}{4\sqrt{2}F} P \cdot F_a^\alpha{}_{\mu\nu} \epsilon^{\mu\nu\lambda\rho} F_a^\alpha{}_{\lambda\rho} \\ - i \frac{\mathcal{A}_{ab}^L}{\sqrt{2}F} y_{ab}^L \cdot P (\epsilon_{ij} l_a^j e_b^c h_D^i - h.c.) - i \frac{\mathcal{A}_{ab}^D}{\sqrt{2}F} y_{ab}^D \cdot P \\ (\epsilon_{ij} q_a^j d_b^c h_D^i - h.c.) - i \frac{\mathcal{A}_{ab}^U}{\sqrt{2}F} y_{ab}^U \cdot P (\epsilon_{ij} q_a^j u_b^c h_U^i - h.c.) . \quad (201)$$

$$L_{\psi, S, P} = i\partial_\mu \bar{\psi} \bar{\sigma}^\mu \psi + \partial_\mu S \partial^\mu S \\ - \frac{1}{2} m_S^2 S^2 + \partial_\mu P \partial^\mu P - \frac{1}{2} m_P^2 P^2 \\ + \frac{m_S^2}{2\sqrt{2}F} S (\psi\psi + \bar{\psi}\bar{\psi}) - i \frac{m_S^2 2}{\sqrt{2}F} P (\psi\psi - \bar{\psi}\bar{\psi}) . \quad (202)$$

where M_α are gaugino masses and $A_{\alpha\beta}$, $y_{\alpha\beta}$ are soft trilinear coupling constants. Usually the case when $\mathcal{A}_{ab} = A$ and Yukawas $y_{ab} \propto \delta_{ab}$ is considered for numerical estimates.

At hadron colliders sgoldstinos will be produced mostly by gluon resonant scattering $gg \rightarrow S(P)$ [110]. The associated production $gg \rightarrow S(P)g$ has several times smaller cross section than resonant production and the corresponding discovery potential (in analogy

with SM Higgs boson case) is expected to be weaker than the discovery potential for the resonant mode $gg \rightarrow S(P)$.

One has to consider the subsequent decay of the sgoldstino inside the detector. Indeed, for the range of parameters that are relevant for this study, sgoldstinos are expected to decay inside the detector, not far from the collision point. Then, assuming that the supersymmetric partners (others than the gravitino \tilde{G}) are too heavy to be relevant for the sgoldstino decays, the main decay channels are:

$$S(P) \rightarrow gg, \gamma\gamma, \tilde{G}\tilde{G}, f\bar{f}, \gamma Z, WW, ZZ.$$

The corresponding widths have been calculated in Refs. [109, 110].

For sgoldstinos decaying into pairs of massless gauge bosons, one has

$$\Gamma(S(P) \rightarrow \gamma\gamma) = \frac{M_{\gamma\gamma}^2 m_{S(P)}^3}{32\pi F^2}, \quad \Gamma(S(P) \rightarrow gg) = \frac{M_3^2 m_{S(P)}^3}{4\pi F^2},$$

where $M_{\gamma\gamma} = M_1 \cos^2 \theta_W + M_2 \sin^2 \theta_W$, and θ_W is the electroweak mixing angle. Note that for $M_{\gamma\gamma} \sim M_3$ gluonic mode dominates over the photonic one due to the color factor enhancement.

For the values of \sqrt{F} which are interesting, gravitino is very light, with mass in the range $m_{\tilde{G}} = \sqrt{8\pi/3} F/M_{Pl} \simeq 10^{-3} \div 10^{-1}$ eV. Then, the sgoldstinos decay rates into two gravitinos are given by

$$\Gamma(S(P) \rightarrow \tilde{G}\tilde{G}) = \frac{m_{S(P)}^5}{32\pi F^2},$$

and become comparable with the rate into two photons for heavy sgoldstinos, such that $m_{S(P)} \sim M_{\gamma\gamma}$.

Model	M_1	M_2	M_3	A
I	100 GeV	300 GeV	500 GeV	300 GeV
II	300 GeV	300 GeV	300 GeV	300 GeV

Table 1: The sets of parameters which the LHC sensitivity is presented for.

In ref. [91] the LHC sgoldstino discovery potential has been studied. Two sets of the MSSM soft SUSY breaking parameters have been considered (see table 1). The most reliable signatures with $\gamma\gamma$ and ZZ in a final state have been studied. The main result is that it would be possible to discover sgoldstino at the LHC with $\sqrt{F} \leq (2 - 8) \text{ TeV}$ (see Figs. 28, 29).

5.5 Scalar leptoquarks

Scalar leptoquarks (LQ) are particles having both lepton and baryon numbers different from zero. They are predicted by many models [105] with gauge symmetry larger than $SU_c(3) \otimes SU_L(2) \otimes U(1)$ of the SM. Leptoquarks decay mainly into quark and lepton. At LHC both pair and single leptoquark production mechanisms are possible:

$$q + g \rightarrow LQ + l \rightarrow 2l + j, \quad (203)$$

$$g + g \rightarrow LQ + LQ \rightarrow 2l + 2j. \quad (204)$$

Single leptoquark production cross section depends on unknown Yukawa coupling constant of leptoquark with quark and lepton. Pair leptoquark production cross section depends mainly on leptoquark mass. Leptoquark pair production mechanism has been studied in refs. [93], [37] for leptoquark detection at LHC. The main signature here are the events with 2 jets and 2 isolated leptons arising from leptoquark decays with the invariant jet-lepton mass equal to leptoquark mass. For the first and second generation leptoquarks it would be possible to discover them with the masses up to 1.6 TeV at the LHC for $L_t = 100 \text{ fb}^{-1}$ [93], [37].

5.6 Compositeness

In the SM quarks and leptons are the fundamental point-like particles. But the proliferation of quarks and leptons has inspired the speculations that they are composite structures, bound states of more fundamental constituents often called preons. If quarks have substructure, it will be revealed in the deviation of the jet cross-section from that

predicted by QCD. The deviation can be parametrised by an interaction of the form

$$\delta L = \frac{4\pi}{\Lambda^2} \bar{q} \gamma^\mu q \bar{q} \gamma_\mu q \quad (205)$$

which is strong at a scale Λ . Comparing the QCD predictions for the jet cross section at high p_T with data it would be possible to restrict the value of Λ . The main conclusion is that the LHC(ATLAS) at full luminosity 300 fb^{-1} will be able to probe the compositeness with $\Lambda \leq 20 \text{ TeV}$ provided the systematic uncertainties are smaller than the statistical ones [37].

In ref.[101] the possibility to search for quark-lepton contact interaction

$$\delta L = \frac{4\pi}{\Lambda_{ql}^2} \bar{l} \gamma^\mu l \bar{q} \gamma_\mu q \quad (206)$$

at LHC(CMS) has been studied. The Drell-Yan process $pp \rightarrow q\bar{q} \rightarrow \gamma^*/Z^* \rightarrow l^+l^-$ has been considered. The interaction (206) modifies SM predictions for Drell-Yan cross section in the high dielectron mass region. The main conclusion is that for $L_t = 100 \text{ fb}^{-1}$ LHC(CMS) will be able to obtain lower bound $\Lambda_{ql} \geq 35 \text{ TeV}$ at 95 % *C.L.* level.

5.7 *R*-parity violation

Most of supersymmetric phenomenology assumes the MSSM which conserves R-parity. As a consequence of R-parity conservation supersymmetric particles can only be produced in pairs and a supersymmetric state cannot decay into conventional states. This has untrivial consequence for the search for supersymmetric particles at supercolliders; in particular most of experimental searches of SUSY rely on pair production and on missing transverse momentum p_T^{miss} as a signal for the production of the LSP, which must be stable and electrically neutral. However, at present there are no deep theoretical motivations in favour of R-parity conservation. The phenomenology of the models with explicit R-parity violation at hadron colliders has been studied in refs. [95]. The terms in the superpotential (75) violate baryon and lepton number and, if present in the Lagrangian of the MSSM, they generate an unacceptably large amplitude for proton decay suppressed only by the inverse squark mass squared. The R-parity prohibits the dangerous terms (75). However,

R-parity conservation is not the single way to construct a minimal supersymmetric extension of the SM. It is easy to write down alternative to R-parity symmetries which allow for a different set of couplings. For example, under the transformation

$$(Q, \bar{U}, \bar{D}) \rightarrow -(Q, \bar{U}, \bar{D}), \quad (L, \bar{E}, H_{1,2}) \rightarrow +(L, \bar{E}, H_{1,2}), \quad (207)$$

only the quark superfields change sign. If the superpotential (75) is invariant under transformations (207) then only the last, baryon number violating term $\bar{U}\bar{D}\bar{D}$ is forbidden. This gives a new model in which a single supersymmetric state can couple to standard model states breaking R-parity. Similarly, there are analogous transformations forbidding the lepton number violating terms.

In the direct search for supersymmetric particles the phenomenology is altered considerably when including R-parity violating terms in the superpotential. In general both the production mechanisms and the decay patterns can change. Other than the standard supersymmetric pair production of particles there is now the possibility of production of R-odd final states as well. Also, if all supersymmetric particles decay in the detector, we will no longer have the standard p_t^{miss} signal and the decay patterns will all be altered. In particular, the LSP will decay mainly into three-body final states [95]. However, except for LSP, which now decays, all particles predominantly decay as in the MSSM. Consider the case when LSP decays within the detector. If lepton number is violated, the SUSY signal will contain multiple leptons from $\tilde{\chi}_1^0 \rightarrow l^+l^-\nu, lq\bar{q}$ [95]. If baryon number is conserved, the LSP will decay into jets, $\tilde{\chi}_1^0 \rightarrow qqq$, giving events with high jet multiplicity and without missing transverse energy. It is not easy to extract such signal since the QCD background is huge. It is possible to detect SUSY events using cascade decays involving leptons, for instance, $\tilde{\chi}_2^0 \rightarrow \tilde{l}^\pm l^\mp \rightarrow qqq l^+l^-$.

Note that it is possible to construct a model [104] with supersmall *R*-parity violation and with relatively long-lived $t \sim (10^{-1} - 10^{-9})$ sec charged $\tilde{\tau}_R$ slepton playing the role of the LSP. The phenomenology of such model is the similar to the GMSB (gauge mediated supersymmetry breaking) model [92] phenomenology with the NLSP $\tilde{\tau}$.⁶

⁶Remember that in GMSB model gravitino \tilde{G} becomes LSP (lightest stable superparticle). Neutralino

5.8 Additional Higgs bosons with big Yukawa coupling constants

Many Higgs doublet model where each Higgs doublet couples with its own quark with relatively big Yukawa coupling constant has been considered in ref. [118]. For non small Yukawa coupling constants the main reaction for the production of the Higgs doublets corresponding to the first and the second generations is quark-antiquark fusion. The phenomenology of the Higgs doublets corresponding to the third generation is very similar to the phenomenology of the model with two Higgs doublets. The cross section for the quark-antiquark fusion in quark-parton model in the approximation of the infinitely narrow resonances is given by the standard formula

$$\sigma(AB \rightarrow H_{q_i q_j} + X) = \frac{4\pi^2 \Gamma(H_{q_i q_j} \rightarrow \bar{q}_i q_j)}{9s M_H} \int_{\frac{M_H^2}{s}}^1 \frac{dx}{x} [\bar{q}_{Ai}(x, \mu) q_{Bj}(x^{-1} M_H^2 s^{-1}, \mu) + q_{Aj}(x, \mu) \bar{q}_{Bj}(x^{-1} M_H^2 s^{-1}, \mu)]. \quad (208)$$

Here $\bar{q}_{Ai}(x, \mu)$ and $q_{Aj}(x, \mu)$ are parton distributions of the antiquark \bar{q}_i and quark q_j in hadron A at the normalisation point $\mu \sim M_H$ and the $\Gamma(H_{q_i q_j} \rightarrow \bar{q}_i q_j)$ is the hadronic decay width of the Higgs boson into quark-antiquark pair. For the Yukawa Lagrangian

$$L_Y = h_{q_i q_j} \bar{q}_{Li} q_{Rj} H_{q_i q_j} + h.c., \quad (209)$$

the hadronic decay width for massless quarks is

$$\Gamma(H_{q_i q_j} \rightarrow \bar{q}_i q_j) = \frac{3M_H h_{q_i q_j}^2}{16\pi}. \quad (210)$$

The value of the renormalization point μ has been chosen equal to the mass M_H of the corresponding Higgs boson. The variation of the renormalization point μ in the interval $0.5M_H - 2M_H$ leads to the variation of cross section less than 50 percent. In considered model there are Higgs bosons which couple both with down quarks and leptons so the best signature is the search for electrically neutral Higgs boson decays into $e^+ e^-$ or $\mu^+ \mu^-$ χ_1^0 or stau $\tilde{\tau}$ can be the “Next to LSP” and it can be stable or long lived. Such $\tilde{\tau}$ would look like a “heavy muon” traversing detector with velocity significantly lower than the velocity of light. One can measure its time of flight and hence calculate the mass $m_{\tilde{\tau}}$ [35], [37].

pairs. For charged Higgs bosons the best way to detect them is to look for their decays into charged leptons and neutrino. The Higgs doublets which couple with up quarks in model with massless neutrino do not couple with leptons so the only way to detect them is the search for the resonance type structure in the distribution of the dijet cross section on the dijet invariant mass as in the case of all Higgs bosons, since in the considered models all Higgs bosons decay mainly into quark-antiquark pairs that leads at the hadron level to additional dijet events. However, the accuracy of the determination of the dijet invariant mass is $O(10)$ percent, so it would be not so easy to find stringent bound on the Higgs boson mass by the measurement of dijet differential cross section at LHC. In considered model, due to the smallness of the vacuum expectation values of the Higgs doublets corresponding to the u, d, s and c quarks, after electroweak symmetry breaking the mass splitting inside the Higgs doublets is small, so in such models the search for neutral Higgs boson decaying into lepton pair is in fact the search for the corresponding Higgs isodoublet. The main background in the search for neutral Higgs bosons through their decays into lepton pair is the Drell-Yan process which is under control. The main conclusion of the ref.[118] is that at LHC for $L_t = 100 \text{ fb}^{-1}$ and for the Yukawa coupling constant $h_Y = 1$ it would be possible to detect such Higgs bosons with the masses up to $4.5 - 5 \text{ TeV}$.

5.9 Astroparticle applications

Let us briefly mention interesting proposal for astroparticle physics application of the CMS detector⁷. One of the main design features of the CMS detector is the presence of a large volume of high magnetic field instrumented all around its surface with the electromagnetic calorimeter (ECAL) and surrounded by almost 4π hermetic hadronic calorimeter (HCAL). This feature provides unique opportunity for the most sensitive search for cosmic scalar or pseudoscalar particles (e.g. such as axion) with two-photon interaction vertex in the energy region from several GeV up to ultra-high values, which might be relevant to the

⁷S.N.Gninenko, private communication, to be published

GZK cutoff. New particles, if they exist, would penetrate the CMS HCAL detector, used as efficient VETO against cosmic ray interactions, and would be observed in the CMS ECAL through the Primakoff effect, i.e. through their conversion into real high energy photons in the process of interactions with the virtual photons from the magnetic field of the CMS superconducting solenoid. For high energies, axion-photon conversion is coherent throughout the CMS detector volume, thus enhancing the signal and allowing a substantial increase in the sensitivity to axion masses up to $0 \leq m_a \leq 32 \times \sqrt{E_a[\text{GeV}]}$, where m_a is the axion mass in eV. A preliminary constraint on the product of the coupling to two photons and integral flux of particle through the detector $\Phi_a \times g_{a\gamma\gamma}$ could be set in the case of zero signal.

6 Conclusion

There are no doubts that at present the supergoal number one of the experimental high energy physics is the search for the Higgs boson - the last non discovered cornerstone of the Standard Model. The LHC will be able to discover the Higgs boson and to check its basic properties. The experimental Higgs boson discovery will be the triumph of the idea of the renormalizability (in some sense it will be the “experimental proof” of the renormalizability of the electroweak interactions). The LHC will be able also to discover the low energy broken supersymmetry with the squark and gluino masses up to 2.5 TeV. Also there is nonzero probability to find something new beyond the SM or the MSSM (extra dimensions, Z' -bosons, W' -bosons, compositeness, ...). At any rate after the LHC we will know the mechanism of the electroweak symmetry breaking (the Higgs boson or something more exotic?) and the basic elements of the matter structure at TeV scale.

We thank our colleagues from INR theoretical department for useful discussions. The work of N.V.Krasnikov has been supported by RFFI grant No 03-02-16933.

References

- [1] S.L.Glashow, Nucl.Phys.**22**(1961)579;
S.Weinberg, Phys.Rev.Lett.**19**(1967)1264;
A.Salam, Elementary Particle Theory (ed. N.Svartholm) Almquist and Wiksells, Stockholm, 1964;
H.D.Politzer, Phys.Rev.Lett.**30**(1973)1346;
D.J.Gross and F.E.Wilczek, Phys.Rev.Lett.**30**(1973)1343.
- [2] N.N.Bogolyubov and D.V.Shirkov, Introduction to the Theory of Quantized Fields (3rd ed.) (John Wiley Inc., New York, 1980).
- [3] Y.Fukuda et. al., Phys.Rev.Lett.**81**(1998)1562;
K.Eguchi et. al., Phys.Rev.Lett.**90**(2003)021802;
M.H.Ahn al., Phys.Rev.Lett.**90**(2003)041803.
- [4] Y.A.Goldfand and E.P.Likhtmann, JETP Letters **13**(1971)452;
D.V.Volkov and V.P.Akulov, JETP Letters **16**(1972)621;
J.Wess and B.Zumino, Phys.Lett.**B49**(1974)52.
- [5] Reviews and original references can be found in:
R.Barbieri, Riv.Nuovo Cim.**11**(1988)1; A.B.Lahanus and
D.V.Nanopoulos, Phys.Rep.**145**(1987)1; H.E.Haber and G.L.Lane,
Phys.Rep. **117**(1985)75; H.P.Nilles, Phys.Rep.**110**(1984)1.
- [6] S.Weinberg, Phys.Rev.**D19**(1979)1277;
L.Susskind, Phys.Rev.**D20**(1979)2619;
S.Dimopoulos and L.Susskind, Nucl.Phys.**B155**(1979)237;
E.Eichten and K.Lane, Phys.Lett.**B90**(1980)125.
- [7] The Large Hadron Collider, CERN/AC/95-05.
- [8] CMS, Technical Proposal, CERN/LHCC/94-38.

- [9] ATLAS, Technical Proposal, CERN/LHCC/94-43.
- [10] ALICE Technical Proposal, CERN/LHCC/95-71.
- [11] LHC-B, Technical Proposal, CERN/LHCC/95-XX.
- [12] See, for example:
 N.V.Krasnikov and V.A.Matveev, Phys.Part.Nucl.**28** (1997)441;
 hep-ph/9703204; N.V.Krasnikov and V.A.Matveev,
 Theoretical and Mathematical Physics **132**(2002)349.
- [13] P.Higgs, Phys.Lett.**12**(1964)132; F.Englert and R.Brout,
 Phys.Rev.Lett.**13**(1964)321.
- [14] The LEP working group for Higgs boson searches: CERN-EP/2001-055.
- [15] As a review, see for example:
 L.B.Okun, Leptons and Quarks, (North Holland) Pub. Comp. 1982);
 Ta-Pei Cheng and Ling-Fong-Li, Gauge Theory of Elementary Particle
 Physics(Oxford University Press, Oxford, 1984);
 Stefan Pokorsky, Gauge Field Theories (Cambridge University Press, Cambridge,
 1987);
 D.Bailin and A.Love, Introduction to Gauge Field Theory
 (Adam Hilger, Bristol, 1986);
 V.I.Borodulin, R.N.Rogalyov and S.R.Slabospitsky,
 COmpendium of RElations, IHEP Preprint 95-50;
 J.F.Gunion, H.E.Haber, G.Kane and S.Dawson,
 The Higgs Hunter's Guide(Addison-Wesley Publishing
 Company, Redwood City, CA)1990.
- [16] Review of Particle Physics, Phys.Rev.**D66**(2002)010001-1.
- [17] The LEP working group for Higgs boson searches: CERN-EP/2001-055.

- [18] M.W.Grnewald, Electroweak Physics, Talk at 31 st High Energy Physics Conference, 2002; hep-ex/0210003.
- [19] N.Cabibbo, L.Maiani, G.Parisi and R.Petronzio, Nucl.Phys. **B158**(1979)295; M.Lindner, Z.Phys. **C31**(1986)295.
- [20] N.V.Krasnikov, Sov.J.Nucl.Phys. **28**(1978)549; P.Q.Hung, Phys.Rev.Lett. **42**(1979)873; H.D.Politzer and S.Wolfram, Phys.Lett. **B82**(1979)242; A.A.Anselm, JETP Lett. **29** (1979)590; M.Lindner, M.Sher and M.Zaglauer, Phys.Lett. **B228**(1989)139.
- [21] J.Ellis, G.Ridolfi and F.Zwirner, Phys.Lett. **B257**(1991)83; H.Haber and R.Hempfling, Phys.Rev.Lett. **66**(1991)1815; A.Yamada, Phys.Lett. **B263**(1991)233; R.Barbieri, M.Frigeni and F.Caravaglis, Phys.Lett. **B258**(1991)233; P.M.Chanowski, S.Pokorski and J.Rosick, Phys.Lett. **B275**(1992)191.
- [22] G.Degrassi, S.Heinemeyer, W.Holik, P.Slavich and G.Weiglin, Eur.Phys.J. **C28**(2003)133.
- [23] N.V.Krasnikov and S.Pokorski, Phys.Lett. **B288**(1992)184; M.A.Diaz, T.A. ter Veldhuis and T.J.Weiler, Phys.Rev.Lett. **74**(1995)2876 and Phys.Rev. **D54**(1996)5855.
- [24] N.Cray, D.J.Broadhurst, W.Grafe and K.Schilcher, Z.Phys. **C48**(1990)673.
- [25] See, for example: N.V.Krasnikov and V.A.Matveev, Phys.Part.Nucl. **31**(1999)255; hep-ph/9909490.
- [26] M.Spira, Fortsch.Phys. **43**(1998)203.
- [27] J.Ellis, M.K.Gaillard and D.V.Nanopoulos, Nucl.Phys. **B106**(1976)292.

- [28] A.Djouadi, D.Graudenz, M.Spira and P.Zervas, Nucl.Phys.**B452**(1995)17;
T.Inami, T.Kubotta and Y.Okada, Z.Phys.**C18**(1983)69.
- [29] K.G.Chetyrkin, B.A.Kniehl and M.Steinhauser, Phys.Rev.Lett.**79**(1997)353.
- [30] R.N.Cahn and S.Dawson, Phys.Lett.**B136**(1984)196;
K.Hikasa, Phys.Lett.**B164**(1985)341;
G.Altarelli, B.Mele and F.Pitoli, Nucl.Phys.**B287**(1987)205;
T.Han, G.Valensia and S.Willenbrock, Phys.Rev.Lett.**69**(1992)3274.
- [31] S.L.Glashow, D.V.Nanopoulos and A.Yildiz, Phys.Rev.**D18**(1978)1724.
- [32] Z.Kunszt, Nucl.Phys.**B247**(1984)339;
J.F.Gunion, Phys.Lett.**B253**(1991)269;
W.J.Marciano and F.E.Paige, Phys.Rev.Lett.**66**(1991)2433.
- [33] As a review of the Higgs boson physics at LHC, see:
R.Kinnunen, Higgs Physics at LHC, CMS CR 2002/020;
K.Lassila-Perini, Higgs Physics at the LHC, CMS CR 2001/018.
- [34] Claudia-Elisabeth Wulz, CMS Physics Overview, CMS CR 2001/016.
- [35] G.Wrochna, Physics at LHC, CMS CR 2002/015.
- [36] J.G.Branson et. al., High Transverse Momentum Physics at the Large Hadron Col-
lider, hep-ph/0110021
- [37] ATLAS Collaboration, ATLAS Detector and Physics Performance
Technical Design Report, CERN/LHCC/99-14.
- [38] S.I.Bityukov and N.V.Krasnikov, Mod.Phys.Lett.**A13**(1998)3235;
hep-ph/9908402; CMS IN Note 1999/027.
- [39] M.N.Dubinin, V.A.Ilyin and V.I.Savrin, CMS Note 1997/101.

- [40] M.Dittmar and H.Dreiner, Phys.Rev.**D55**(1997)167 [hep-ph/9608317];
LHC Higgs Search with $l^+\nu l^-\bar{\nu}$ final states, CMS Note 1997/083.
- [41] D.Green et al., Search for the Standard Model Higgs Boson with $M_H \approx 170 \text{ GeV}/c^2$ in W^+W^- Decay Mode, CMS Note 1998/089.
- [42] D.Rainwatwer and D.Zeppenfeld, **JHEP**(1997)9712:005.
- [43] D.Rainwater and D.Zeppenfeld, Phys.Rev.**D59**(1999)014037.
- [44] D.Rainwater, K.Hagiwara and D.Zeppenfeld, Searching for $H \rightarrow \tau\tau$ in weak boson fusion, hep-ph/9808468(1998).
- [45] R.N.Cahn et al., Phys.Rev.**D35**(1987)1626;
R.Kleiss and W.J.Stirling, Phys.Lett.**200B**(1988)193.
- [46] M.N.Dubinin, CMS Note 2001/022.
- [47] N.Akchurin et. al., CMS Note 2002/016.
- [48] L.Poggiali, ATLAS Internal Note, PHYS-No-066(1995).
- [49] M.Dittmar, Pramana **55**(2000)151.
- [50] See for example:
J.Wess and J.Bagger, Supersymmetry and Supergravity, Princeton Univ. Press, 1983;
P.West, Introduction to Supersymmetry and Supergravity, World Scientific, 1986.
- [51] See, for example:
D.I.Kazakov, Beyond the standard model, hep-ph/0012288.
- [52] See for example:
M.B.Green, J.H.Schwarz and E.Witten, Superstring theory, Cambridge Press, 1987.
- [53] H.P.Nilles, Phys.Lett.**B115**(1982)193;
R.Barbieri, S.Ferrara and C.A.Savoy, Phys.Lett.**B119**(1982)343;
E.Cremmer, P.Fayet and L.Girardello, Phys.Lett.**B122**(1983)41;

L.Ibanez, Phys.Lett.**B118**(1982)73;
 A.H.Chamseddine, R.Arnowitt and P.Nath, Phys.Rev.Lett.**49**(1982)970.

[54] P.Fayet, Phys.Lett.**B69**(1977)489;
 A.Salam and J.Strathdee, Nucl.Phys.**B87**(1975)85.

[55] H.Dreiner and G.G.Ross, Nucl.Phys.**B365**(1991)597;
 K.Enqvist, A.Masiero and A.Riotto, Nucl.Phys.**B373**(1992)95;
 V.Barger, M.S.Berger, R.J.N.Philips and T.Wohrmann, Phys.Rev.**D53**(1996)6407.

[56] M.Dine and A.E.Nelson, Phys.Rev.**D48**(1993)1277;
 M.Dine, A.E.Nelson and Y.Shirman, Phys.Rev.**D51**(1995)1362;
 M.Dine, A.E.Nelson, Y.Nir and Y.Shirman, Phys.Rev.**D53**(1996)2658.

[57] L.E.Ibanez, C.Lopez and C.Munoz, Nucl.Phys.**B256**(1985)218.

[58] N.Polonsky and A.Pomarol, Phys.Rev.Lett.**73**(1994)2292.

[59] N.V.Krasnikov and V.V.Popov, hep-ph/9511298.

[60] H.Baer et al., Phys.Lett.**B161**(1985)175;
 G.Gamberini, Z.Phys.**C30**(1986)605; H.Baer et al., Phys.Rev.
D36(1987)96; G.Gamberini et al., Phys.Lett.**B203**(1988)
 453; R.M.Barnett, J.Gunion and H.Haber, Phys.Rev.**D37**(1988)
 1892; A.Bartl et al., Z.Phys.**C52**(1991)477.

[61] See for example:
 H.Baer et al., Mod.Phys.**A4**(1989)4111.

[62] S.Abdullin et. al., CMS Note 1998/006.

[63] S.I.Bityukov and N.V.Krasnikov, Phys.Lett.**B469**(1999)149;
 S.I.Bityukov and N.V.Krasnikov, Phys.Atom.Nucl.**65**(2002)1441; S.I.Bityukov and
 N.V.Krasnikov, hep-ph/0210269.

[64] I.Hinchliffe et. al., Phys.Rev.**D55**(1997)5520.

- [65] D.R.Tovey, Phys.Lett.**B498**(2001)1.
- [66] A.Alessia, Sparticle Searches with CMS at LHC, CMS CR 2002/022.
- [67] M.Kazana, G.Wrochna and P.Zalewski, CMS CR 1999/019.
- [68] D.Denegri et. al., Summary of the CMS Discovery Potential for the MSSM SUSY Higgses, CMS Note 2001/032.
- [69] A.Djouadi, Phys.Lett.**B435**(1998)101.
- [70] D.P.Roy, Phys.Lett.**B459**(1999)607.
- [71] S.Abdullin, D.Denegri and F.Moortgat, Observability of MSSM Higgs bosons via sparticle decay modes in CMS, CMS NOTE-2001/042.
- [72] E.Boos, A.Djouadi and A.Nikitenko, hep-ph/0307079.
- [73] S.Slabospitsky, CMS NOTE 2002/010; hep-ph/0203094.
- [74] S.N.Gninenko, M.M.Kiryanov, N.V.Krasnikov and V.A.Matveev, hep-ph/0301140.
- [75] N.Arkani-Hamed, S.Dimopoulos and G.R.Dvali, Phys.Lett.**B429**(1998)263; Phys.Rev.**D59**(1999)086004.
- [76] L.Randall and R.Sundrum, Phys.Rev.Lett.**83**(1999)3370; ibid. **83**(1999)4690.
- [77] I.Antoniadis, Phys.Lett.**B246**(1990)377; I.Antoniadis and K.Benakli, Phys.Lett.**B326**(1994)69; I.Antoniadis, K.Benakli and M.Quiros, Phys.Lett.**B331**(1994)313; I.Antoniadis et al., Phys.Lett.**B436**(1998)257.
- [78] N.V.Krasnikov, Phys.Lett.**B273**(1991)246.
- [79] G.F.Guidice, R.Rattazzi and J.D.Wells, Nucl.Phys.**B544**(1999)3.
- [80] V.A.Rubakov, Usp.Fiz.Nauk**171**(2001)913.

- [81] As a recent review, see for example: J.Hewett and M.Spiropoulu, hep-ph/0205106; A.Kisselev, hep-ph/0303090; K.Cheung, hep-ph/0305003.
- [82] T.Appelquist, H.Cheng and B.Dobresku, Phys.Rev.**D64**(2001)035002.
- [83] A.Pomarol and M.Quiros, Phys.Lett.**B438**(1998)255; M.Masip and A.Pomarol, Phys.Rev.**D60**(1999)096005.
- [84] T.G.Rizzo, Phys.Rev.**D61**(2000)055005; I.Antoniadis,K.Benakli and M.Quiros, Phys.Lett.**B460**(1999)176.
- [85] H.-C.Cheng, K.Matchev and M.Schmaltz, Phys.Rev.**D66**(2002)036005; ibid**D66**(2002)056006.
- [86] P.Traczyk and G.Wrochna, Search for Randall-Sundrum Graviton Excitations in the CMS experiment, CMS IN 2002/061; M.-C.Lemaire and J.-P.Pansart, Search for Randall-Sundrum Graviton decaying into a pair of electrons or photons, CMS IN 2002/63.
- [87] S.B.Giddings and S.Thomas, Phys.Rev.**D65**(2002)056010.
- [88] R.C.Myers and M.J.Perry, Ann.Phys.**172**(1986)304.
- [89] S.Dimopoulos and G.Landsberg, Phys.Rev.Lett.**87**(2001)161602.
- [90] T.Han, G.D.Kribs and B.McElrath, Phys.Rev.Lett.**90**(2002)031601; A.V.Kotwal and C.Hays, Phys.Rev.**D66**(2002)116005; P.Argyres, S.Dimopoulos and J.March-Russel, Phys.Lett.**B441**(1998)96; R.Casadio and B.Harms, Int.J.Mod.Phys.**A17**(2002)4635. M.Cavaglia, S.Das and R.Maartens, Will we obserbe black holes at LHC?, hep-ph/0305223.
- [91] D.S.Gorbunov and N.V.Krasnikov, JHEP**0207**(2002)043; hep-ph/020307.
- [92] See for example: G.F.Guidice and R.Rattazzi, Phys.Rept.**322**(1999)419; S.L.Dubovsky, D.S.Gorbunov and S.V.Troitsky, Phys.Usp.**42**(1999)62.

[93] G.Wrochna, First look at leptoquarks in CMS, CMS CR-1996/003 and the proceedings of “New Directions for High Energy Snowmass”, Colorado, June 1996; S.Abdullin, F.Charles and F.Luckel, CMS NOTE-1999/027.

[94] N.V.Krasnikov, Mod.Phys.Lett.**A9**(1994)791; N.V.Krasnikov, Phys.Lett.**B388**(1996)783; N.Arkani-Hamed et al., Phys.Rev.Lett.**77**(1996)1937.

[95] S.Dimopoulos et al., Phys.Rev.**D41**(1990)2099; S.Dawson, Nucl.Phys.**B261**91985)297; G.G.Ross and H.Dreiner, Nucl.Phys.**B365**91988)397; R.Barbieri et al., hep-ph/9810232.

[96] N.V.Krasnikov, Zhetp.Lett.**65**(1997)139;hep-ph/9611282; S.I.Bityukov and N.V.Krasnikov, Yad.Phys.**62**(1999)1288; hep-ph/9806504.

[97] K.Agashe and M.Graesser, Phys.Rev.**D61**(2000)075008; I.Hinchliffe and F.E.Paige, Phys.Rev.**D63**(2001)115006; J.Hisano, R.Kitano and M.N.Nojiri, hep-ph/02022129; W.Porod and W.Majerotto, hep-ph/0210326; J.Kalinowski, hep-ph/020751.

[98] For a review. see:
J.Hewett and T.Rizzo, Phys.Rep.**183**(1989)193;
A.Leike, Phys.Rep.**D56**(1999)143.

[99] A.Djouadi, M.Dittmar and A.Nicollerat, Z' studies at the LHC: an update, hep-ph/0307020.

[100] J.C.Pati and A.Salam, Phys.Rev.**D10**(1974)275;
R.N.Mohapatra and J.C.Pati, Phys.Rev.**D11**(1975)566;
G.Senjanovic and R.N.Mohapatra, Phys.Rev.**D12**(1975)1502.

[101] A.K.Gupta, S.Jain and N.K.Mondal, CMS NOTE 1999/075.

[102] E.Eichten, I.Hinchliffe, K.Lane and C.Quigg,
Review of Modern Physics **56**(1984)231.

[103] W.Beenakker et al., Phys.Rev.Lett.**74**(1995)2905,
Z.Phys.**C69**(1995)163, Nucl.Phys.**B492**(1995)51.

[104] N.V.Krasnikov, Phys.Lett.**B386**(1996)161.

[105] J.C.Pati and A.Salam, Phys.Rev.**D10**(1974)275;
W.Buchmuller, R.Ruckl and D.Wyler, Phys.Lett.**B191**(1987)442;
L.E.Abbott and E.Farhi, Phys.Lett.**B101**(1981)69.

[106] J. R. Ellis, K. Enqvist and D. V. Nanopoulos, Phys.Lett.**B147**(1984)99; J. R. Ellis,
K. Enqvist and D. V. Nanopoulos, Phys.Lett.**B151**(1985)357.

[107] G. F. Giudice and R. Rattazzi, Phys. Rept.**322**(1999)419; S. L. Dubovsky, D. S. Gor-
bunov and S. V. Troitsky, Phys.Usp.**42**(1999)623.

[108] D. S. Gorbunov and A. V. Semenov, LAPTH-884/01.

[109] E. Perazzi, G. Ridolfi and F. Zwirner, Nucl.Phys.**B574**(2000)3.

[110] E. Perazzi, G. Ridolfi and F. Zwirner, Nucl.Phys.**B590**(2000)287.

[111] M. Nowakowski and S. D. Rindani, Phys.Lett.**B348**(1995).

[112] D. S. Gorbunov, Nucl.Phys.**B602**(2001)213.

[113] D. A. Dicus, S. Nandi and J. Woodside, Phys.Rev.**D41**(1990)2347.

[114] D. A. Dicus and P. Roy, Phys.Rev.**D42**(1990)938.

[115] D. A. Dicus, S. Nandi and J. Woodside, Phys. Rev.**D43**(1991)2951.

[116] D. A. Dicus and S. Nandi, Phys.Rev.**D56**(1997)4166.

[117] P. Abreu *et al.* [DELPHI Collaboration], Phys.Lett.**B494**(2000)20.

[118] N.V.Krasnikov, Mod.Phys.Lett.**A10**(1995)2675.

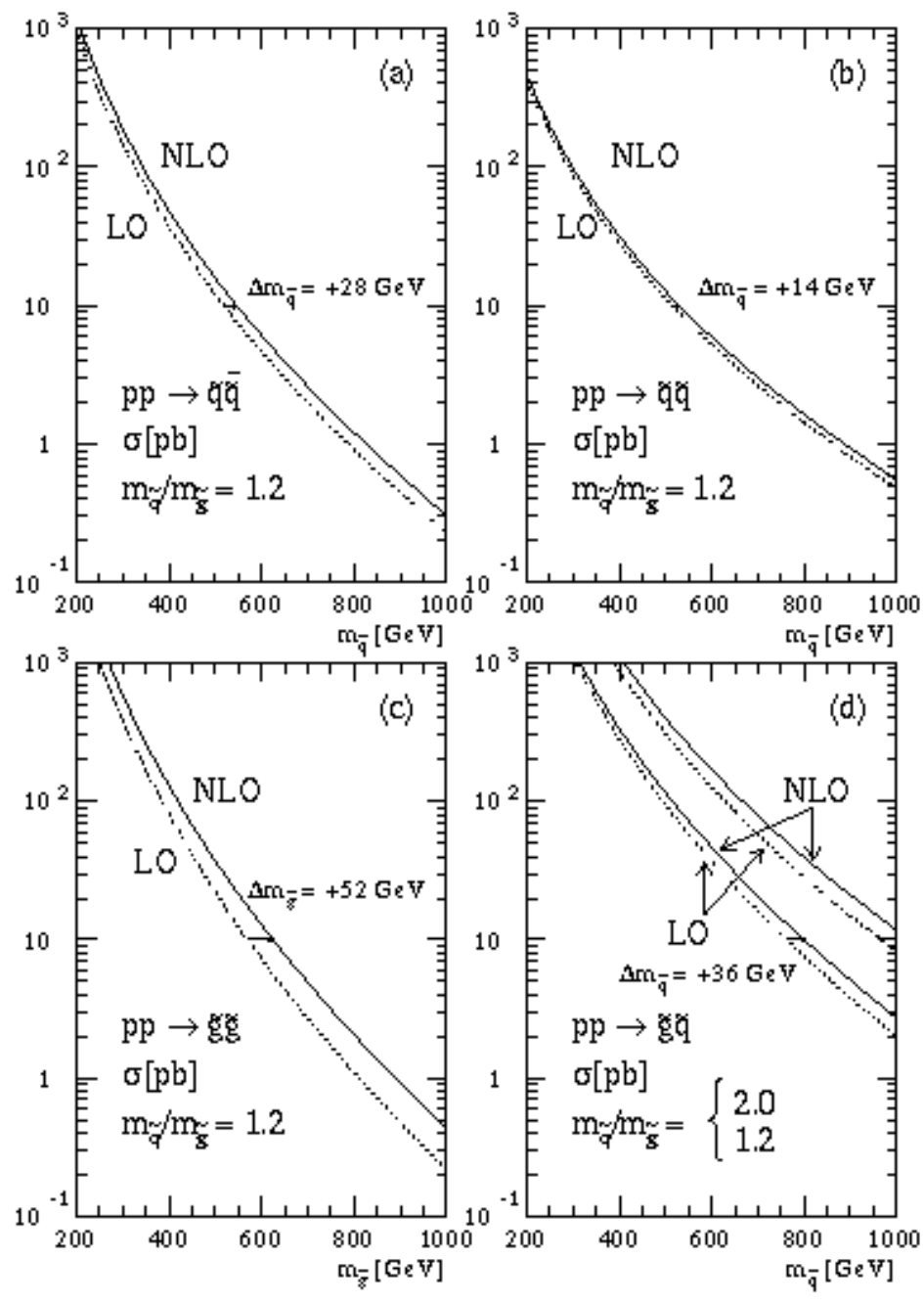


Figure 16: The total SUSY cross sections for the LHC

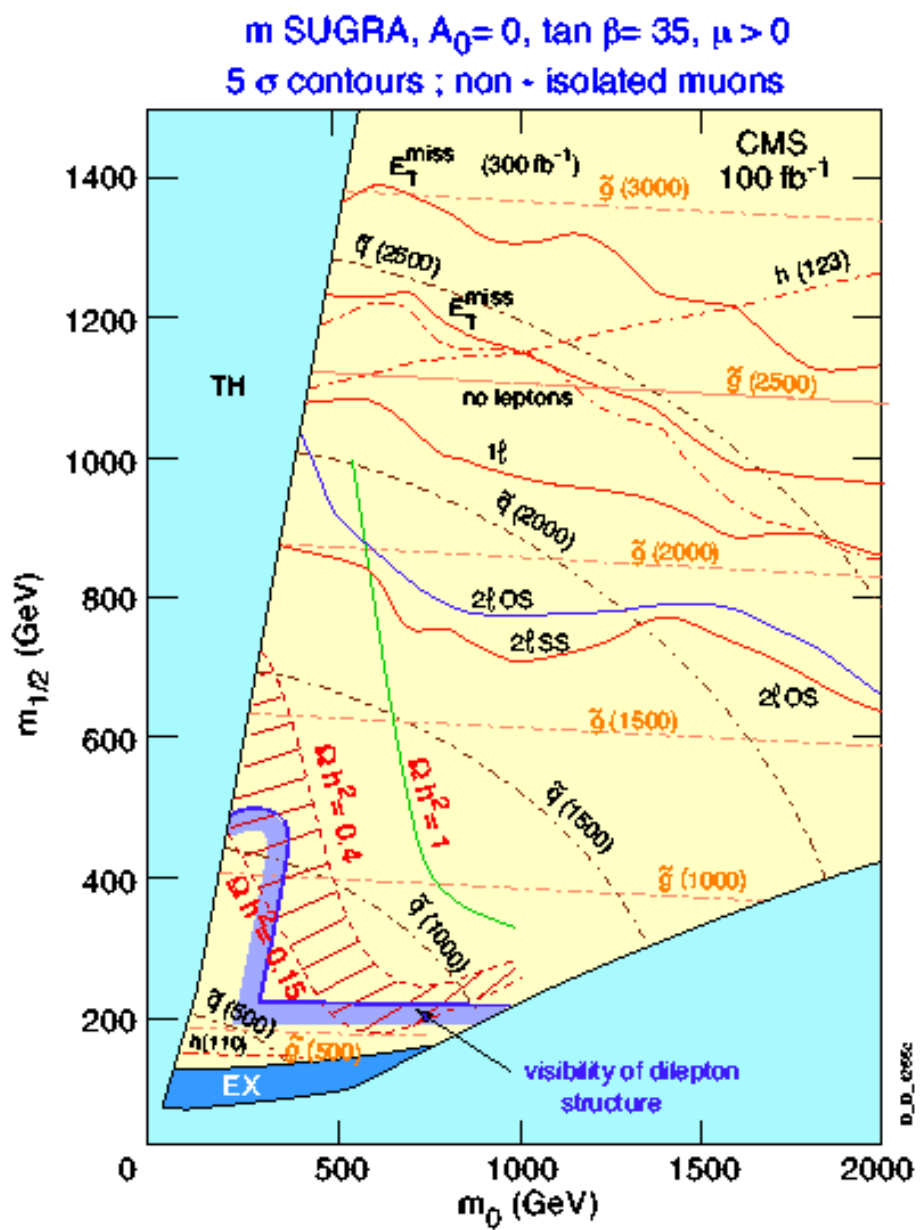


Figure 17: *Discovery potential in MSUGRA model for $\tan \beta = 35$ and $\mu = +$*

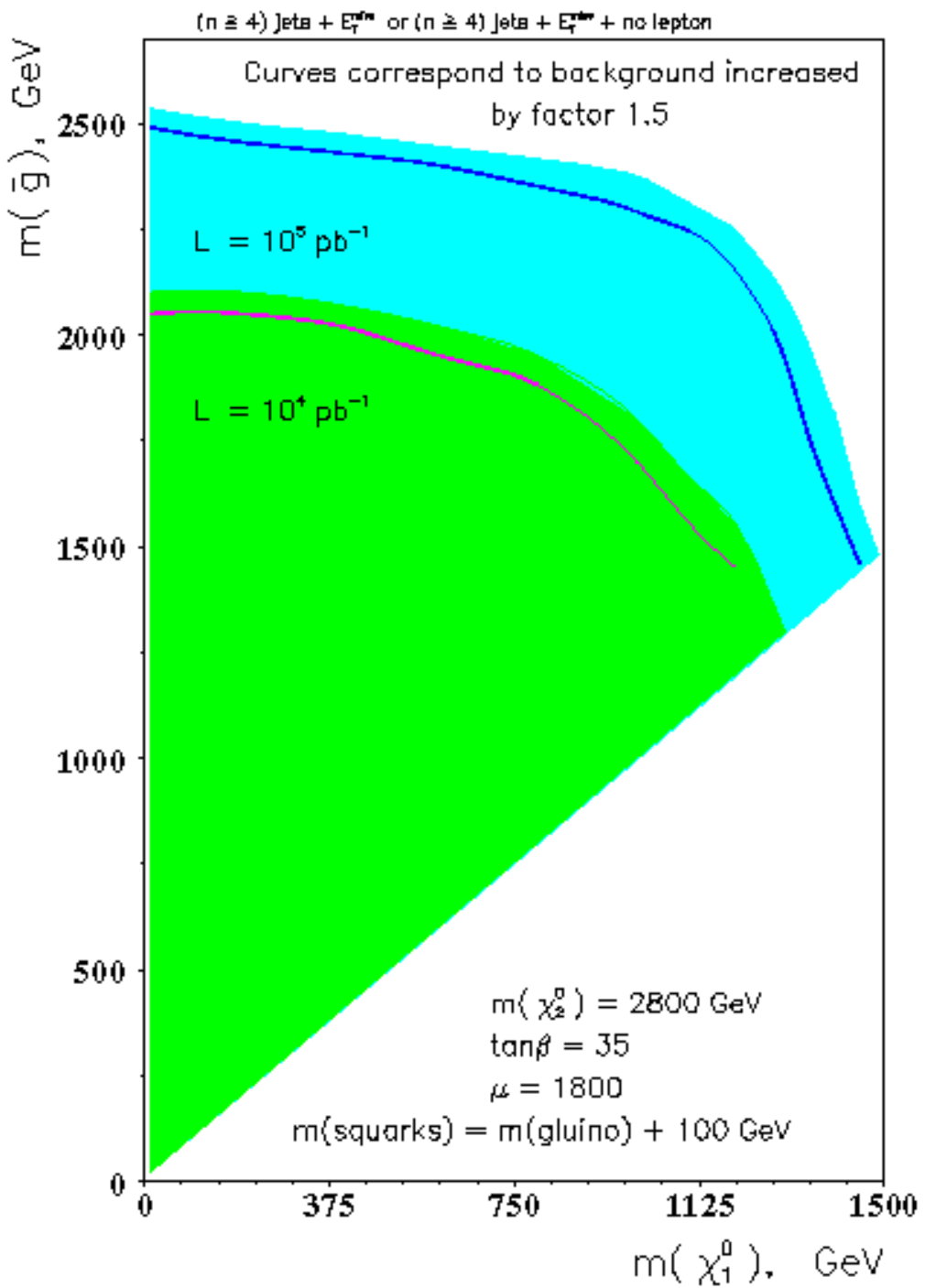


Figure 18: The CMS discovery potential at 100 fb^{-1} for different values of $m_{\tilde{\chi}_1^0}$ and $m_{\tilde{g}}$ in the case $m_{\tilde{q}} = m_{\tilde{g}} + 100 \text{ GeV}$

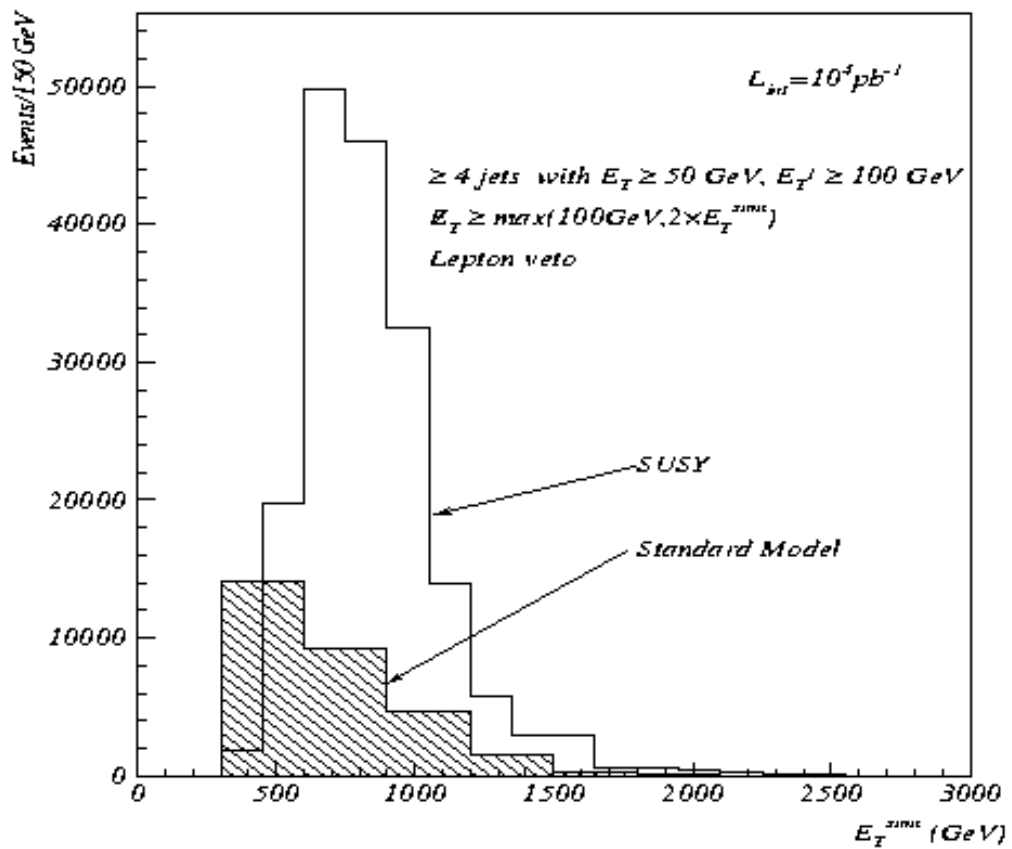


Figure 19: E_T^{sum} distribution for both the inclusive SUSY and the SM backgrounds after event selection cuts have been applied

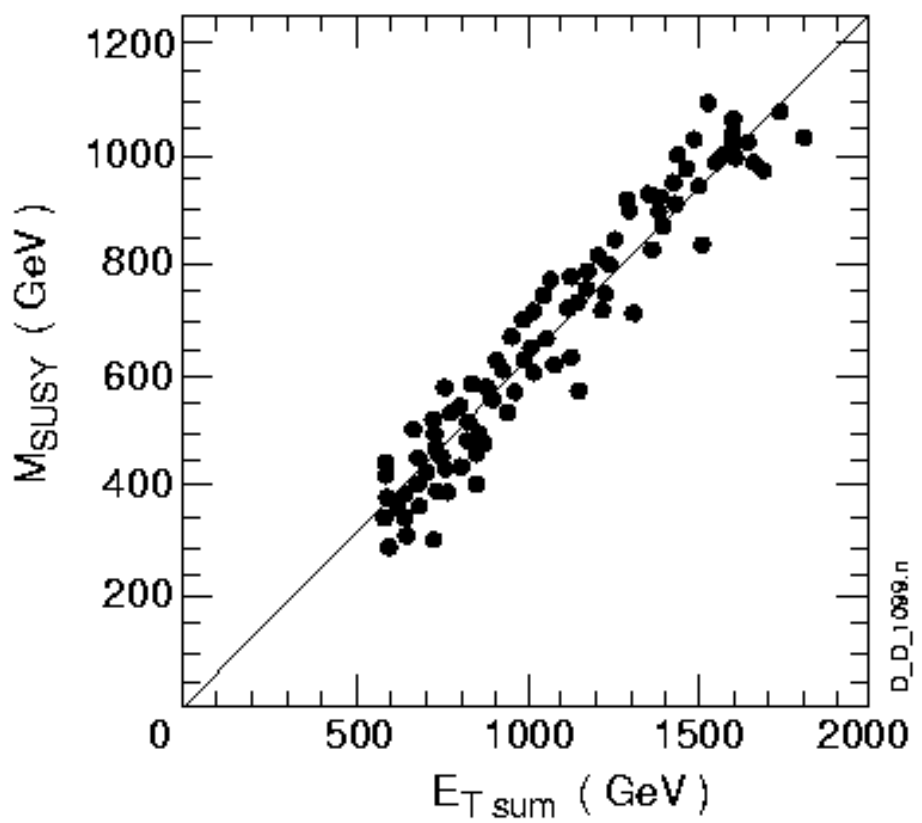


Figure 20: *The relation between the peak value of the E_T^{miss} distribution and the M_{SUSY} value*

$\tilde{\chi}_1^0$ mass determination in $3\ell^\pm + \text{no jets} + E_T^{\text{miss}}$
 final state from $\tilde{\chi}_1^\pm \tilde{\chi}_2^0$ production

$m_0 = 200 \text{ GeV}$, $m_{1/2} = 100 \text{ GeV}$, $\tan\beta = 2$, $A_0 = 0$, $\mu < 0$
 $M(\tilde{\chi}_2^0) - M(\tilde{\chi}_1^0) \approx M(\tilde{\chi}_1^0) \approx 52 \text{ GeV}$

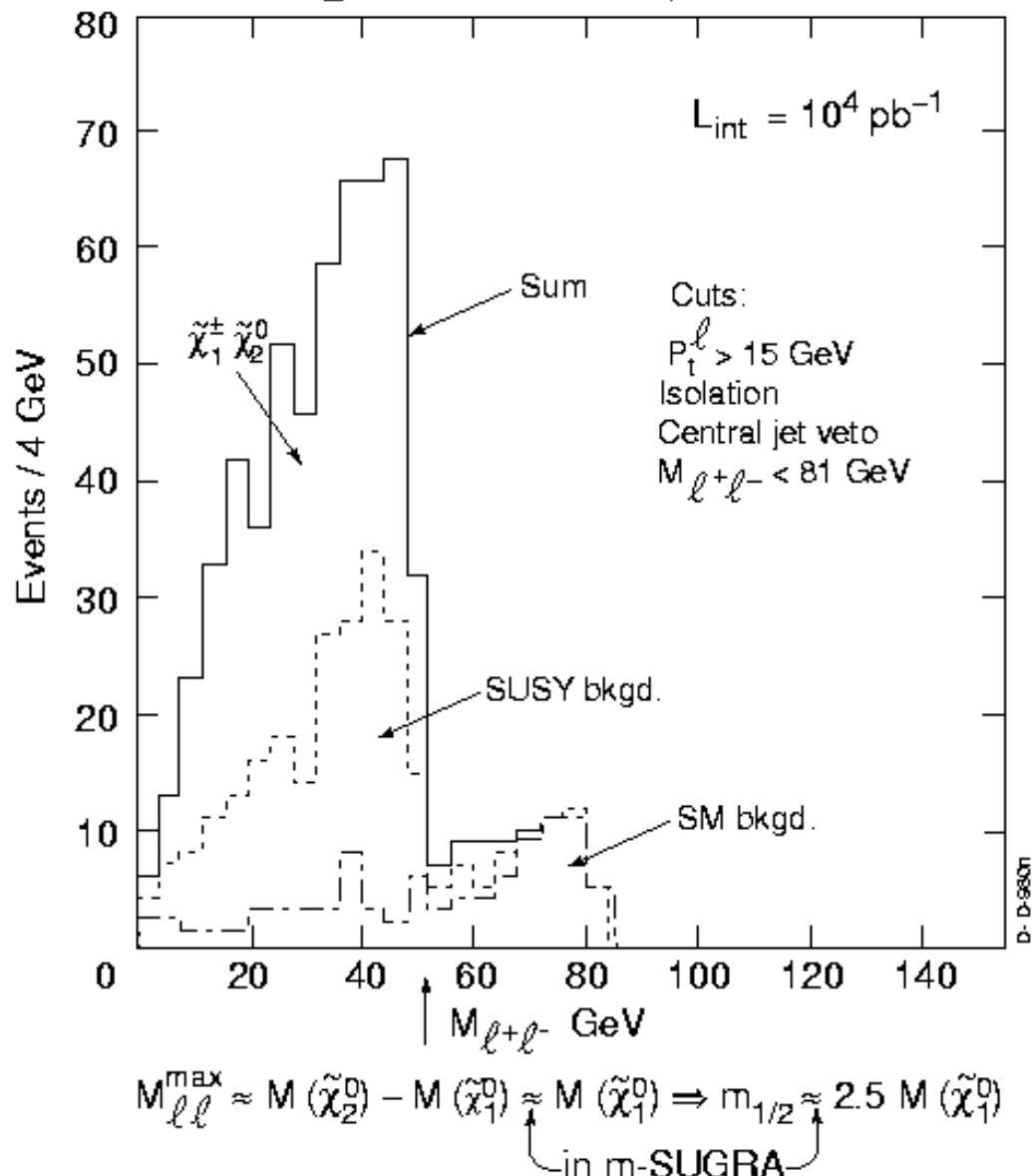


Figure 21: Dilepton invariant masses distribution for MSUGRA point ($m_0 = 200 \text{ GeV}$, $m_{1/2} = 100 \text{ GeV}$ in the $3l + \text{no jets} + E_T^{\text{miss}}$ events. Contribution from SM and SUSY backgrounds are also shown

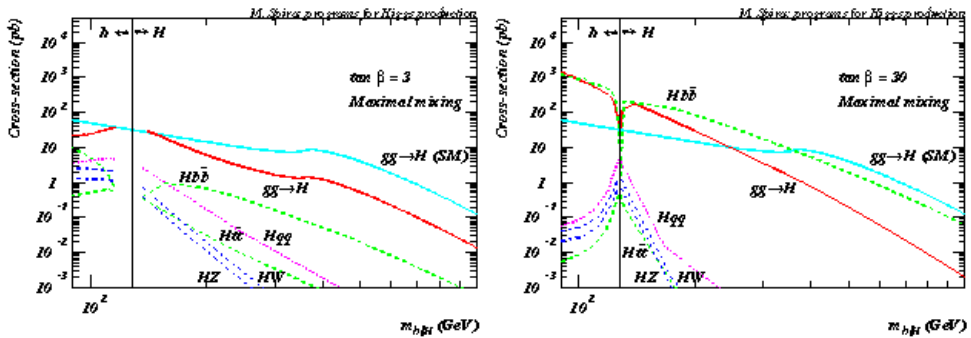


Figure 22: The branching ratios of light h and heavy H as a function of their masses

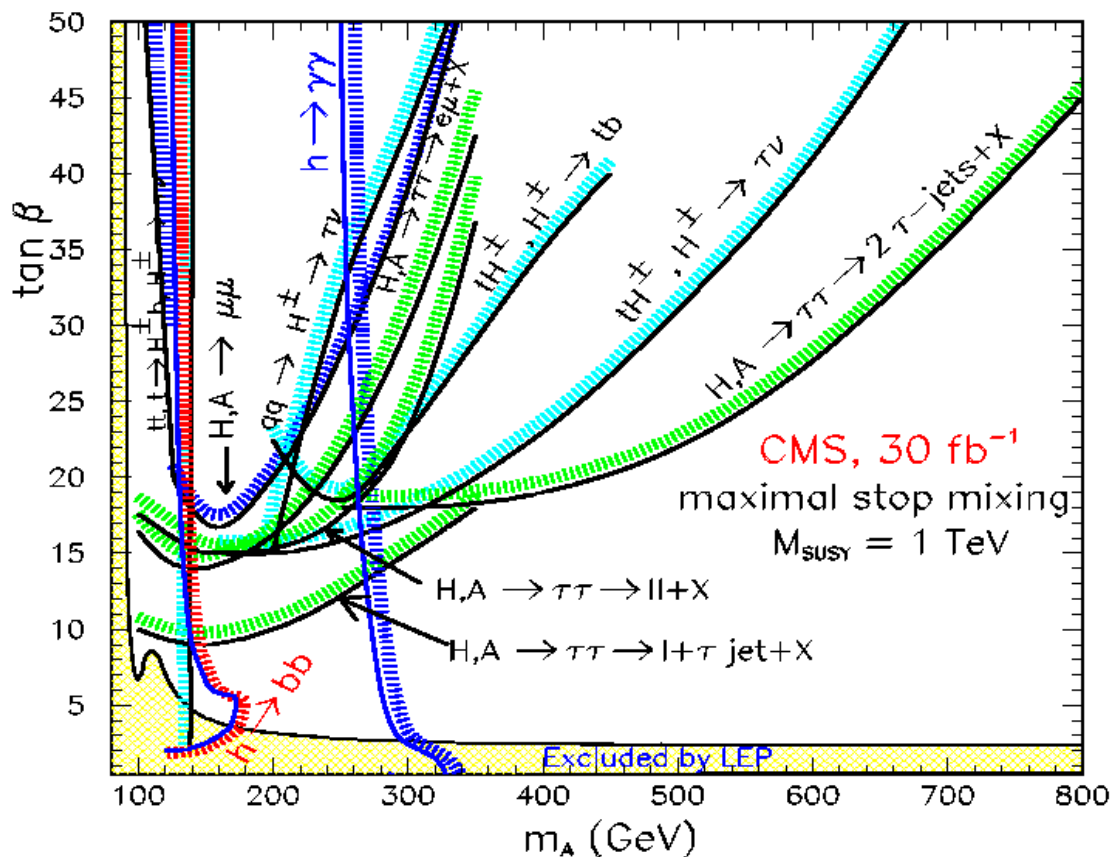


Figure 23: Expected 5σ discovery range for the MSSM Higgs bosons with maximal stop mixing in the CMS detector for 30 fb^{-1}

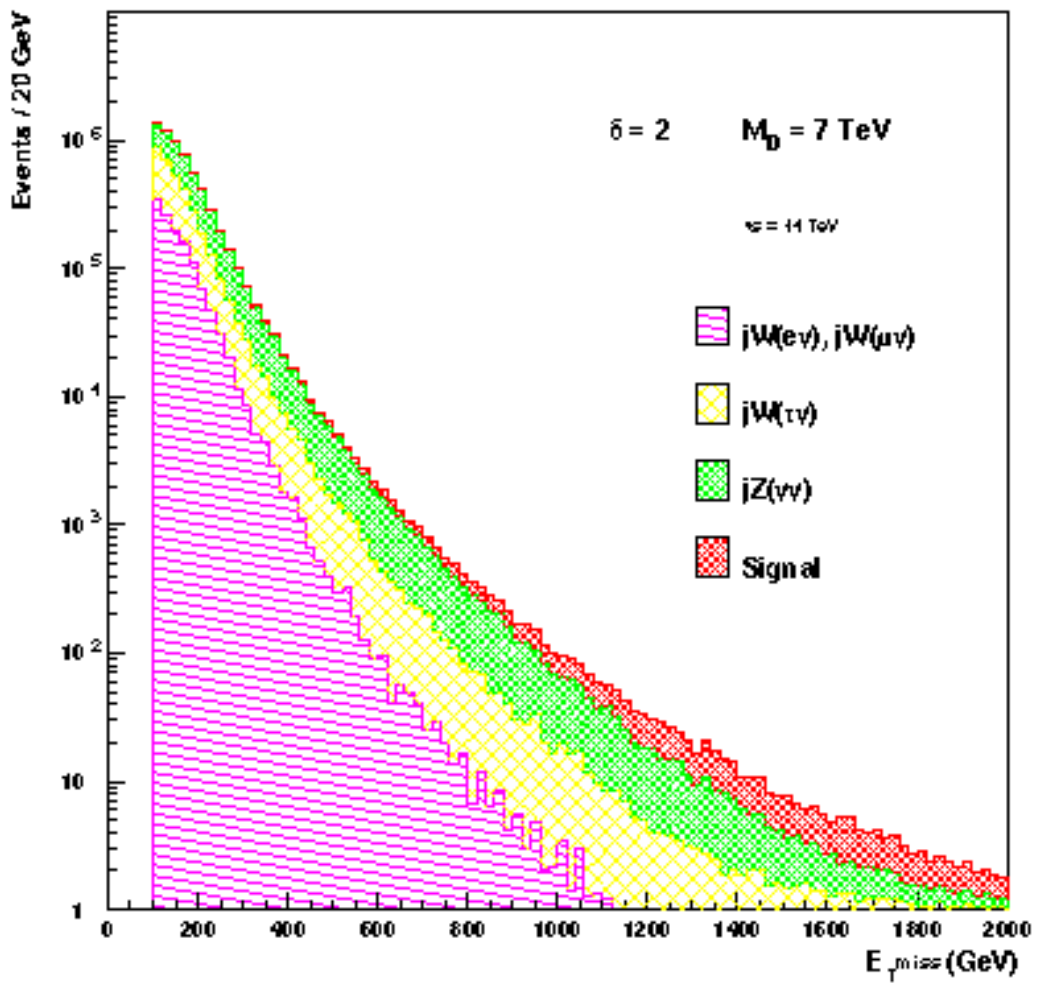


Figure 24: *Distributions of the missing transverse energy in extra dimensions signal and background events after the selection and for 100 fb^{-1} . $d = 2$, $M_d = 7 \text{ TeV}$ is shown for signal*

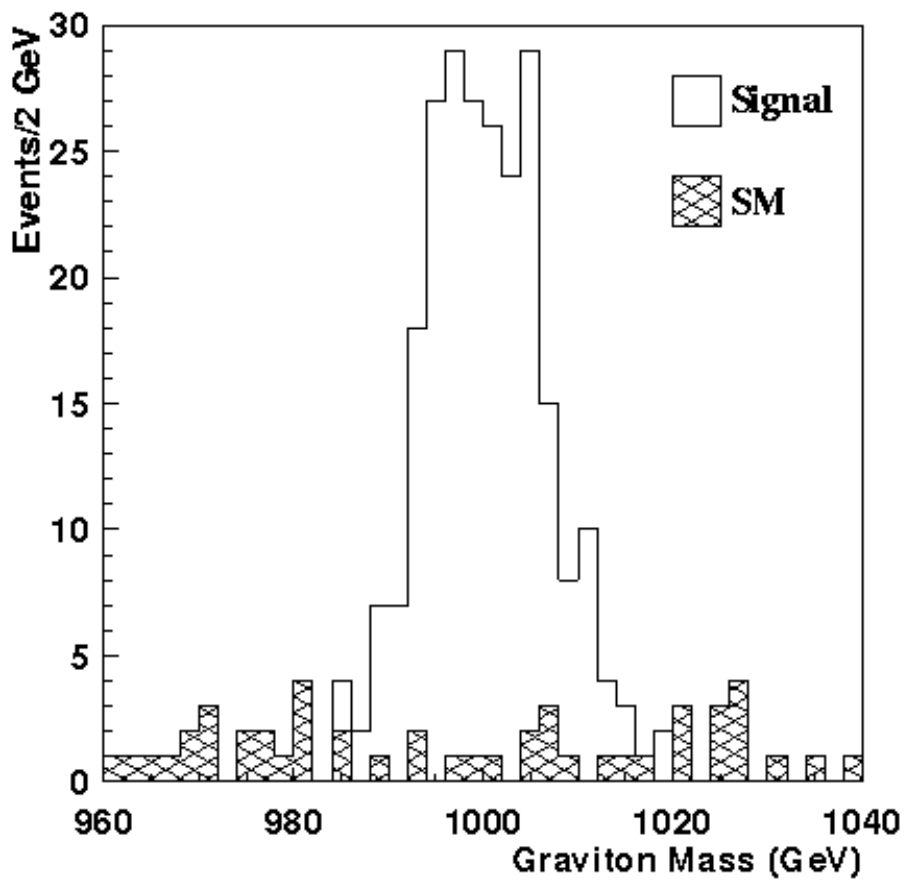


Figure 25: *Distributions of the e^+e^- invariant mass in signal from a graviton resonance of mass 1 TeV and in background after event selection for $L_t = 100 \text{ fb}^{-1}$*

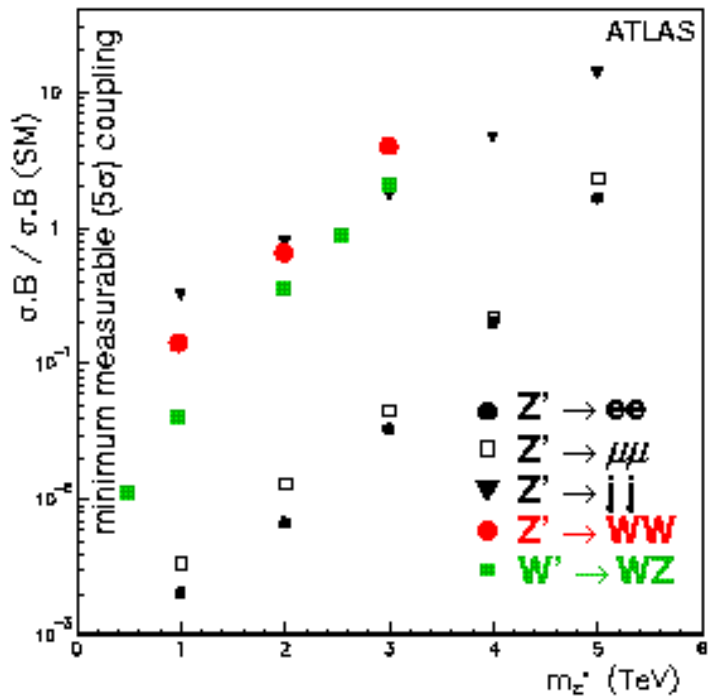


Figure 26: 5σ limits on W' and Z' coupling for fermionic (100 fb^{-1}) and bosonic (300 fb^{-1}) modes

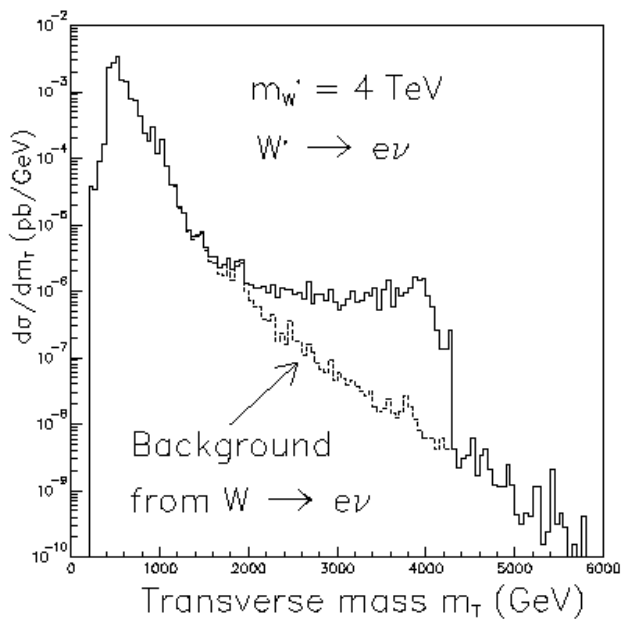


Figure 27: Expected electron-neutrino transverse mass distribution in ATLAS for $W' \rightarrow e\nu$ decays

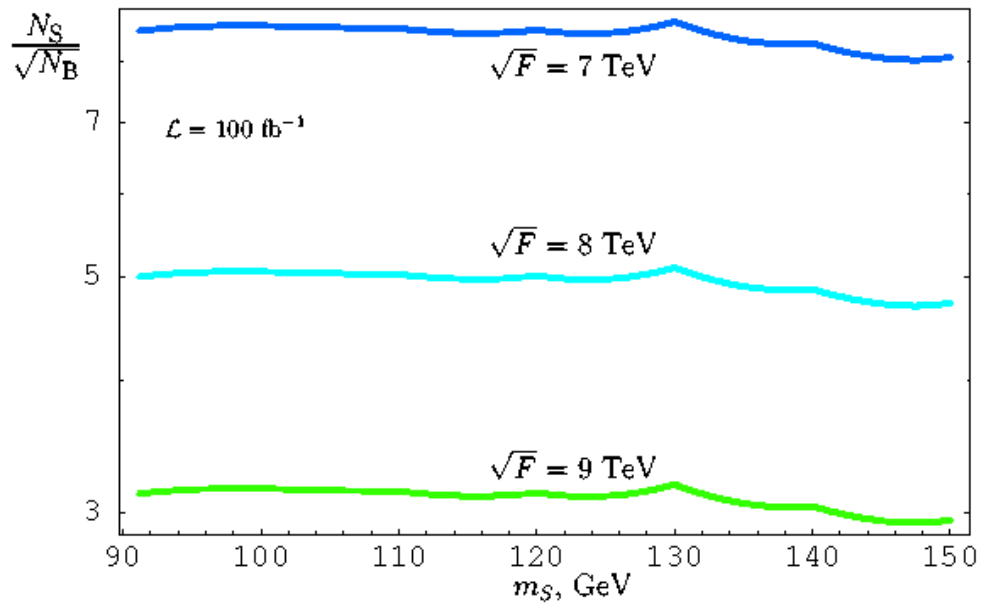


Figure 28: *Signal significance of $\gamma\gamma$ channel as a function of sgoldstino mass m_S for the model II.*

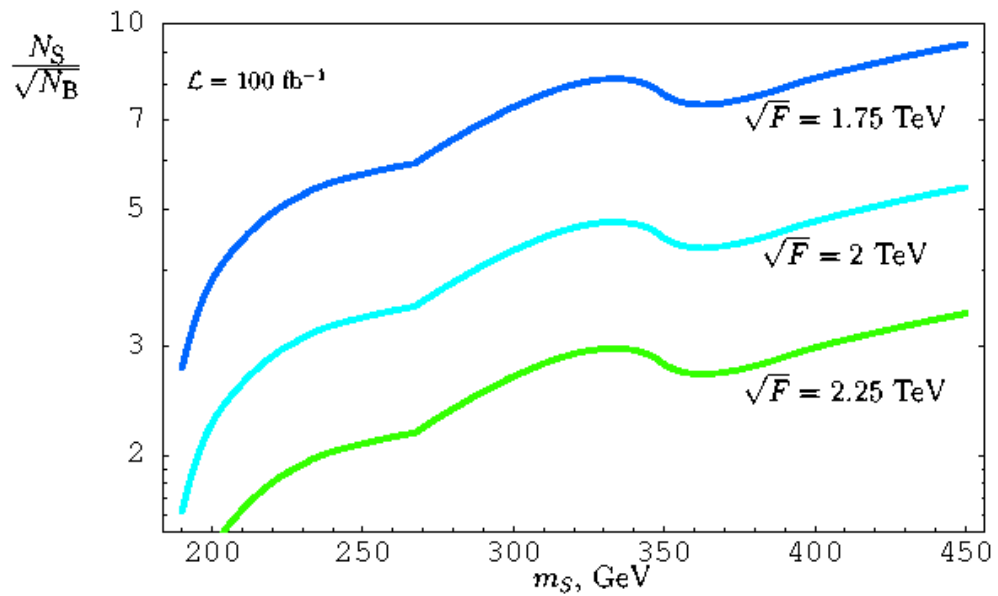


Figure 29: *Signal significance of ZZ channel as a function of sgoldstino mass m_S for the model I.*

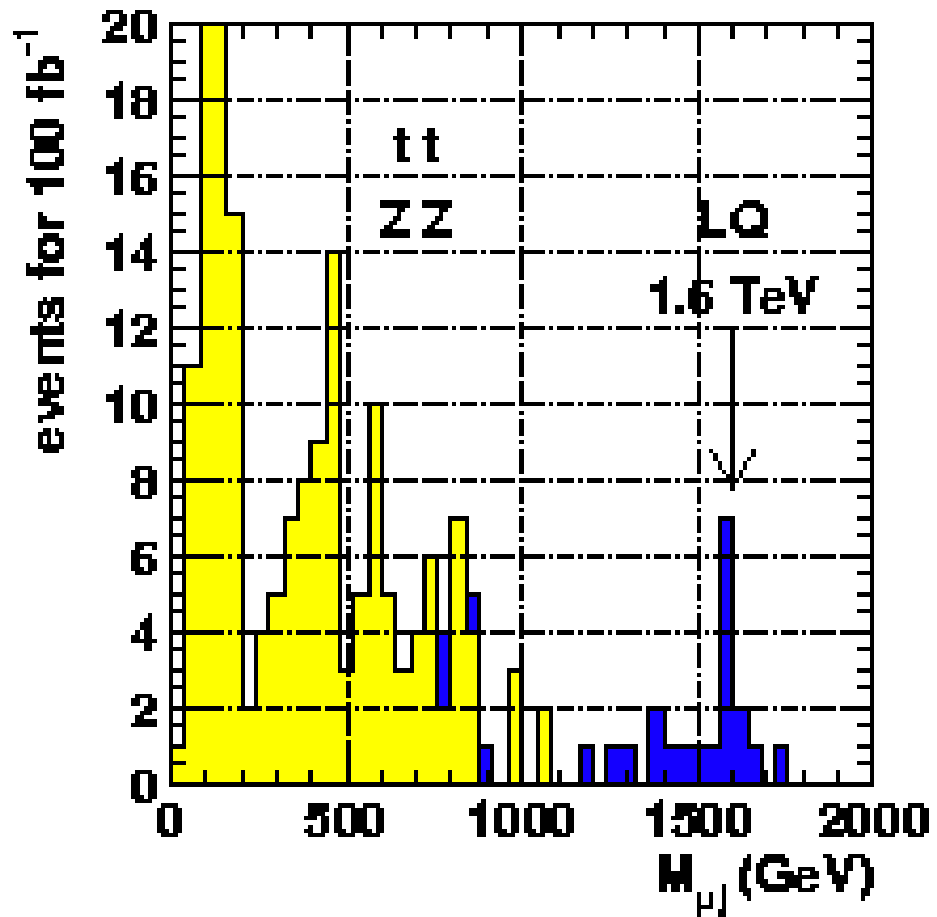


Figure 30: *Mass distribution for scalar, 2nd generation leptoquarks with $M_{LQ2} = 1.6 \text{ TeV}$ produced in pairs*

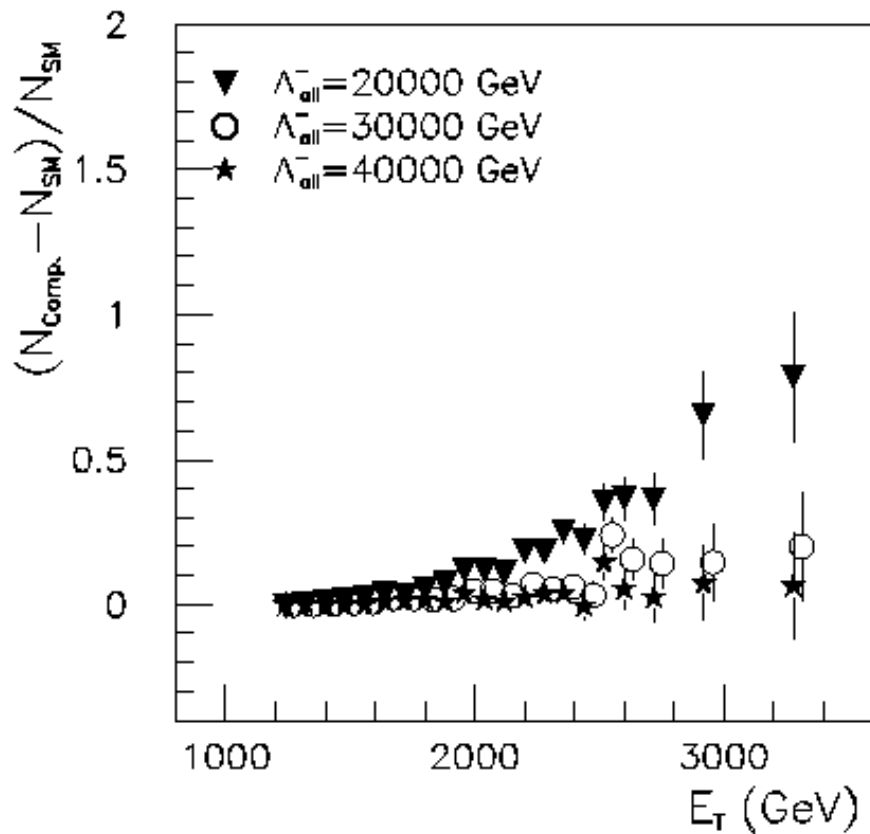


Figure 31: *Difference of the SM prediction and the effect of compositeness on the jet E_T distribution, normalised to the SM rate. The errors correspond to $L_t = 300 \text{ fb}^{-1}$ for various values of the compositeness scale Λ*